



Errata

P 37

Figure 27 should be **Figure 28**

P 38

Figure 27: Diagram of furnace should read

Figure 28: Diagram of furnace

UNIVERSITEIT VAN PRETORIA



2101656

Evaluation of the REAS test for blast furnace charge materials

By

Wilhelmina Fredrika van der Vyver

Dissertation submitted in partial fulfillment of the requirements of the degree MSc in the
Department of Metallurgical Engineering

Faculty of Engineering
University of Pretoria

30 October 1998

EVALUATION OF THE REAS TEST FOR BLAST FURNACE CHARGE MATERIALS

By

Wilhelmina Fredrika van der Vyver

Supervisor:

Prof PC Pistorius

Department of Metallurgical Engineering

University of Pretoria

MSc

Synopsis

During the past two decades many efforts have been made to increase the control of blast furnace conditions to ensure a homogeneous product. The dissections on blast furnaces by various iron and steel companies in Japan in the early 70s provided valuable information on the high temperature properties of charging material

Standard tests (ISO) to determine ore, sinter and pellet qualities only provide information of up to 1100°C . By using the REAS apparatus – a high temperature reduction vessel that simulates the blast furnace process from stockline to melting - the high temperature properties of burden materials have been investigated. The REAS process not only provides an insight into the reactions occurring during the softening and melting process but a range of indices with which to judge the blast furnace performance.

Keywords: Blast furnace, REAS, Softening, Melting, Fayalite, Slag, Iron ore, Pressure drop, Direct reduction.

Since 1993 new developments started and a test method for Iscor blast furnaces was specifically developed. Although certain indices have been established, uncertainties around the melting mechanisms still existed. These uncertainties include:

- Why does the maximum pressure over the sample bed vary extensively between different samples?
- Why does a temperature decrease occur only in certain samples and what determines the extent of the temperature decrease?
- Which low melting phase forms that causes the initial rise in pressure drop over the sample bed?

Four tests were performed on a mixture of Sishen and Thabazimbi ore to determine the phase changes in the test sample. During the reduction of the iron ore, five distinct phases are present. Above 1200°C two liquid phases, an alkali rich phase and a liquid phase with a fayalite composition is present. The rest of the iron reports at different stages in various forms of metallic iron and wustite. Small amounts of a high melting oxide phase, hercynite, also occurs.

Softening of the sample is said to occur when the ΔP over the sample bed increases by more than 200 mm H₂O. For the specific tests evaluated, this occurred at 1200°C. At this temperature, the liquid with a fayalite composition as well as the alkali rich liquid are present. The formation of the low melting fayalite phase with a high viscosity appears to cause the sudden rise in ΔP . A temperature arrest occurs at the same time supporting the suggestion that liquid formation is responsible for the pressure increase.

The results indicate that the mechanisms responsible for the observed pressure drop (decreased gas permeability) and dripping may well be different from those given in the literature. The literature mechanisms emphasise the importance of the amount of FeO available to act as flux for the silica which is present as gangue; hence a greater degree of (indirect) reduction below the melting point of fayalite gives

poorer fluxing of silica since less FeO is available. However, the charge materials considered in this study appear to be of substantially higher grade than those used in the previous work. For this reason, there does not appear to be any shortage of FeO to act as flux. This abundance of FeO, and the observation that the peak in pressure drop is not associated with any great change in the amount of liquid, together imply that the literature mechanism regarding changes in the amount and composition of the liquid (i.e. becoming more SiO₂-rich and viscous as the FeO is reduced) cannot explain the pressure fluctuations observed here. Rather, the increase in pressure appears to be a joint effect of liquid being present (giving the first increase in pressure) and compaction of the sample. Loss of voidage in the sample by this substantial amount of compaction appears the likely cause of the pressure increase. The subsequent decrease in the pressure drop is probably associated with lower viscosity as the sample temperature increases.

The importance of compaction means that the amount of indirect reduction does play a role in the development of the pressure drop, but not for the reasons cited in the literature. Pure iron is more malleable than the oxides, and reduction gives a porous iron structure which is more easily compacted. For both these reasons, the metallic product of indirect reduction favours compaction (and hence the pressure increase). The sharp increase in reduction rate close to the peak pressure presumably results from better contact between the remaining iron oxide (in the fayalite-based liquid, and wustite) with the coke reductant, so favouring direct reduction; this increased reduction (endothermic because of the Boudouard reaction) results in one of the noticeable temperature arrests on the sample temperature curve.

The correspondence between the temperature arrests and the changes within the sample do imply that these arrests can be used to gain some information on the reduction mechanisms. However, the reliability of the temperature arrests as indicators of the state of the sample and the reaction conditions within the sample must be tested by further work.

EVALUERING VAN DIE REAS TOETS VIR HOOGOOND VOER MATERIALE

Deur

Wilhelmina Fredrika van der Vyver

Studieleier:

Prof PC Pistorius

Departement van Metallurgiese Ingenieurswese

Universiteit van Pretoria

MSc

Synopsis

Die afgelope twee dekades is verskeie pogings aangewend om beter beheer oor die hoogoond bedryfstoestande te verkry om 'n meer homogene produk te verseker. Die ontledings van hoogoonde deur verskeie yster en staal maatskappye in Japan het waardevolle inligting verskaf ten opsigte van die hoë temperatuur eienskappe van grondstowwe vir hoogoondbedryf.

Standaard toetse (ISO) om die kwaliteit van erts, sinters en ertskorrels te bepaal, verskaf slegs inligting tot en met 1100°C. Deur gebruik te maak van die REAS-toetsapparaat – 'n hoë temperatuur reduksie oond wat die hoogoondproses van die laaiproses tot en met smelting naboots – kan die hoëtemperatuureienskappe van grondstowwe vir hoogoondgebruik bepaal word. Die REAS-toetsapparaat verskaf inligting ten opsigte van die reaksies wat tydens versagting en smelting voorkom, sowel as indekse wat gebruik word om die hoogoondprestasie te evalueer.

Sleutelwoorde: Hoogoond, REAS, Versagting, Smelting, Fajaliet, Slak, Ystererts, Drukval, Direkte reduksie.

Sedert 1993 is met nuwe ontwikkelings begin om 'n spesiale toets metode vir Iscor-hooggoonde te ontwikkel. Ten spyte daarvan dat sekere indekse bepaal is, het daar steeds onsekerheid rondom die smeltmeganisme bestaan. Hierdie onsekerhede sluit onder andere in:

- Waarom wissel die maksimum drukval oor die monster so sterk tussen verskillende ladings?
- Waarom kom 'n temperatuur afname slegs in sekere monsters voor en wat bepaal die grootte van die temperatuur afname?
- Watter laagsmeltende fases vorm wat verantwoordelik is vir die aanvanklike toename in drukval oor die monster?

Vier eksperimente is uitgevoer op 'n mengsel van Sishen en Thabazimbi erts om die faseverandering in die monster te bepaal. Tydens die reduksie van die ystererts het vyf fases voorgekom. Bokant 1200°C was twee vloeistof fases teenwoordig, naamlik 'n vloeistof fase met 'n fajaliet samestelling en 'n alkali-ryke fase. Die res van die yster kom op verskillende stadiums in verskillende vorms van metalliese yster en wustiet voor. Klein hoeveelhede van 'n hoogsmeltende fase, herseniet, is ook teenwoordig.

Versagting van die monster word gedefinieer as die punt waar die drukverskil oor die monster bed met meer as 200 mm H_2O toeneem. Vir die spesifieke toetse wat uitgevoer is, het dit voorgekom by 1200°C . By hierdie temperatuur is die fase met 'n fajaliet samestelling en die alkali-ryke fase in 'n vloeistof toestand. Die vorming van die laagsmeltende fajaliet fase met 'n hoë viskositeit lei skynbaar tot die skielike toename in differensiële druk. Terselfde tyd kom 'n afplatting in die temperatuur kromme voor wat ook 'n aanduiding is dat vloeistof vorming verantwoordelik is vir die toename in differensiële druk.

Die resultate toon dat die meganismes wat verantwoordelik is vir die waargenome toename in druk val (afname in gas deurlaatbaarheid) en die metaal drup verskil van dié in literatuur. In die literatuur word die hoeveelheid beskikbare FeO wat optree as 'n vloeimiddel vir die silika, wat teenwoordig in die ganggesteentes, beklemtoon;

‘n hoër mate van (indirekte) reduksie onder die smeltpunt van fajaliet gee aanleiding tot ‘n meer viskose slak weens die tekort aan FeO om as vloeimiddel op te tree. ‘n Hoër graad voer materiaal is egter tydens hierdie studie gebruik en geen tekort aan FeO kom tydens die ondersoek voor nie. Die oormaat FeO beskikbaar, sowel as die waarneming dat die persentasie vloeistof redelik konstant bly waar die piek in die differensiële kromme voorkom dui aan dat die meganismes wat in die literatuur gebruik word om die fluktuasies in die differensiële druk kromme te verklaar, naamlik ‘n toename in die hoeveelheid vloeistof en ‘n verandering in samestelling van die vloeistof, nie in die geval geldig is nie. Dit blyk eerder dat die rede vir die toename in drukval ‘n kombinasie is van die vloeistof wat teenwoordig is (verantwoordlik vir die aanvanklike toename in differensiële druk) en die kompaktering van die monster. Die skielike kompaktering van die monster lei tot ‘n afname in die deurlaatbaarheid van die monster wat verder lei tot die toename in drukval. Soos wat die temperatuur toeneem, verlaag die viskositeit van die slak wat aanleiding gee tot die afname in die differensiële druk kromme.

Die invloed wat kompaktering het op die drukval dui aan dat die hoeveelheid indirekte reduksie wel ‘n rol speel in die ontwikkeling van die differensiële druk kromme, maar nie vir dieselfde redes wat aangevoer word in die literatuur nie. Suiwer yster is meer vervormbaar as die okiedes, en reduksie lei tot ‘n poreuse yster struktuur wat makliker gekompakteer kan word. Beide die redes toon aan dat die metalliese produk van indirekte reduksie kompaktering bevoordeel (wat lei tot ‘n toename in drukval). Die skerp toename in die reduksie tempo by die maksimum druk is waarskynlik die gevolg van beter kontak tussen die oorblywende ysterokied (in die fajalietagtige vloeistof en wustiet) met die kooks wat direkte reduksie bevoordeel. Hierdie toename in reduksie (endotermies weens die Boudouard reaksie) lei tot een van die waargenome afplattings in die monster temperatuur krommes.

Die ooreenkomste tussen die afplattings in die temperatuur krommes en die veranderinge wat in die monster voorkom dui aan dat hierdie afplattings gebruik kan word om meer inligting ten opsigte van die reduksie meganismes te bekom. Die

herhaalbaarheid van die temperatuur afplattings as indikators van die toestand waarin die monster is, sal egter verder ondersoek moet word.

TABLE OF CONTENT	P
1. INTRODUCTION	1
2. BLAST FURNACE BACKGROUND	3
2.1. REACTIONS IN THE LOWER ZONE (MELTING/PROCESSING)	3
2.2. REACTIONS IN THE MIDDLE ZONE (ISOTHERMAL/THERMAL RESERVE)²	6
2.3. REACTIONS IN THE UPPER ZONE (PREHEATING/PREPARATION)	7
3. THE DEVELOPMENT OF A FURNACE AND TEST PROCEDURES	8
3.1. TEST APPARATUS	8
3.1.1. FURNACE WITH REACTOR	8
3.1.2. COMPUTERISED CONTROL SYSTEM	9
3.2. TEST PARAMETERS	11
3.2.1. TIME DURATION	11
3.2.2. TEMPERATURE CYCLE	11
3.2.3. GAS COMPOSITION AND FLOW	11
3.2.4. LOAD	12
3.2.5. SAMPLE COMPOSITION AND MASS	12
3.2.6. PARTICLE SIZE	12

3.3. INDICES	13
3.3.1. PERCENTAGE REDUCTION	13
3.3.2. MAXIMUM PRESSURE DROP OVER THE SAMPLE BED (ΔP_{MAX})	14
3.3.3. SOFTENING TEMPERATURE (ST)	14
3.3.4. MELTING TEMPERATURE (MT)	14
3.3.5. DRIPPING TEMPERATURE (DP)	14
3.3.6. RELATIVE DRIPPING MASS	14
3.3.7. COHESIVE AND SOFTENING ZONE	14
3.3.8. VISCOSITY	14
3.3.9. COMPACTION	15
3.3.10. CARBON LOSS	15
3.4. CURRENT TESTWORK AND DEVELOPMENTS	16
3.4.1. HIGH TEMPERATURE REDUCIBILITY.	16
3.4.2. SOFTENING PROPERTIES (SOFTENING (ST) AND MELTING TEMPERATURES (MT) AND THE EFFECT THESE HAVE ON THE PERMEABILITY OF THE CHARGE.	16
3.4.3. DRIPPING PROPERTIES	19
3.4.4. MAXIMUM PRESSURE OVER THE SAMPLE BED	20
3.4.5. VISCOSITY (S)	20

4.	TESTWORK AND RESULTS	21
4.1.	DETERMINATION OF THE VARIOUS PHASES OF FE (DEGREE OF REDUCTION) DURING THE TEST	21
4.2.	EVALUATION OF THE HEAT TRANSFER RATE DURING THE TEST	36
4.2.1.	ENTHALPY OF THE BURDEN	36
4.2.2.	HEAT TRANSFER IN THE FURNACE	37
5.	DISCUSSION	40
5.1.	DETERMINATION OF THE VARIOUS PHASES OF IRON (DEGREE OF REDUCTION) DURING THE TEST	40
5.1.1.	TEST NO. 1 (SOFTENING OF SAMPLE STARTED)	40
5.1.2.	TEST NO. 2 ($\Delta P = \text{MMH}_2\text{O}$)	40
5.1.3.	TEST NO. 3 ($\epsilon_{\text{P MAX}}$ REACHED – MATERIAL STARTS FLOWING)	42
5.1.4.	TEST NO. 4 (COMPLETE TEST)	42
5.2.	EVALUATION OF THE HEAT TRANSFER RATE DURING THE TEST	47
6.	CONCLUSION	51
7.	REFERENCES	53

**APPENDIX 1:
DERIVATION OF THE WORKING EQUATION FOR REDUCTION RATE
DETERMINATION OF THE COKE CONSUMPTION DURING THE TEST**

**APPENDIX 2:
REAS TEST RESULTS – TEST 4**

**APPENDIX 3:
FeO-SiO₂-Al₂O₃ – PHASE DIAGRAM**

**APPENDIX 4:
MOLE PERCENTAGES OF THE DIFFERENT PHASES**

1. INTRODUCTION

Before the work presented here was started, a test was developed that simulated the blast furnace process from loading to melting. The initial furnace and test method purchased by Iscor were designed and developed by SGA in Germany - the so-called REAS-furnace (Reduktion, Erweichung und Abschmelzen, that means reduction, softening and melting). Since 1985 Iscor Research & Development tested various ores, sinters and pellets in the REAS to determine the repeatability of the REAS test method and certain test parameters. Since 1993 new developments started and a test method for Iscor blast furnaces was specifically developed. Although certain indices have been established, uncertainties around the melting mechanisms still existed. These uncertainties include:

- Why does the maximum pressure over the sample bed vary extensively between different samples?
- Why does a drop or arrest in temperature occur only in certain samples and what determines the extent of the arrest?
- Which low melting phase forms that causes the initial rise in pressure drop over the sample bed?

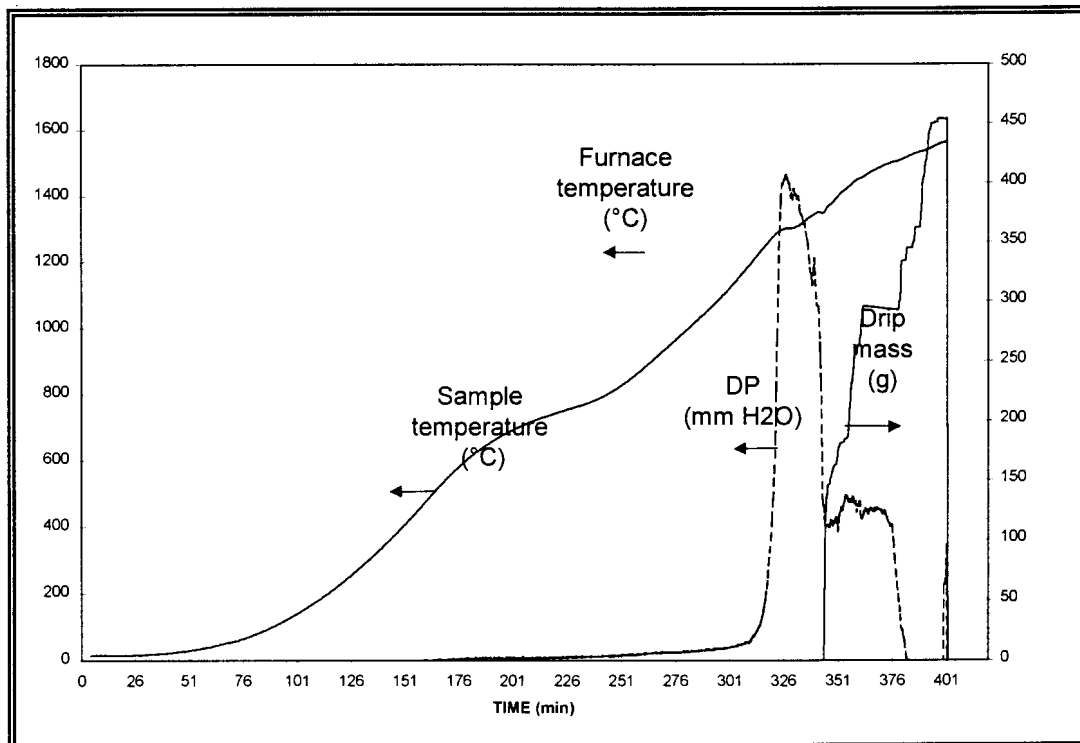


Figure 1a: Typical REAS test results.

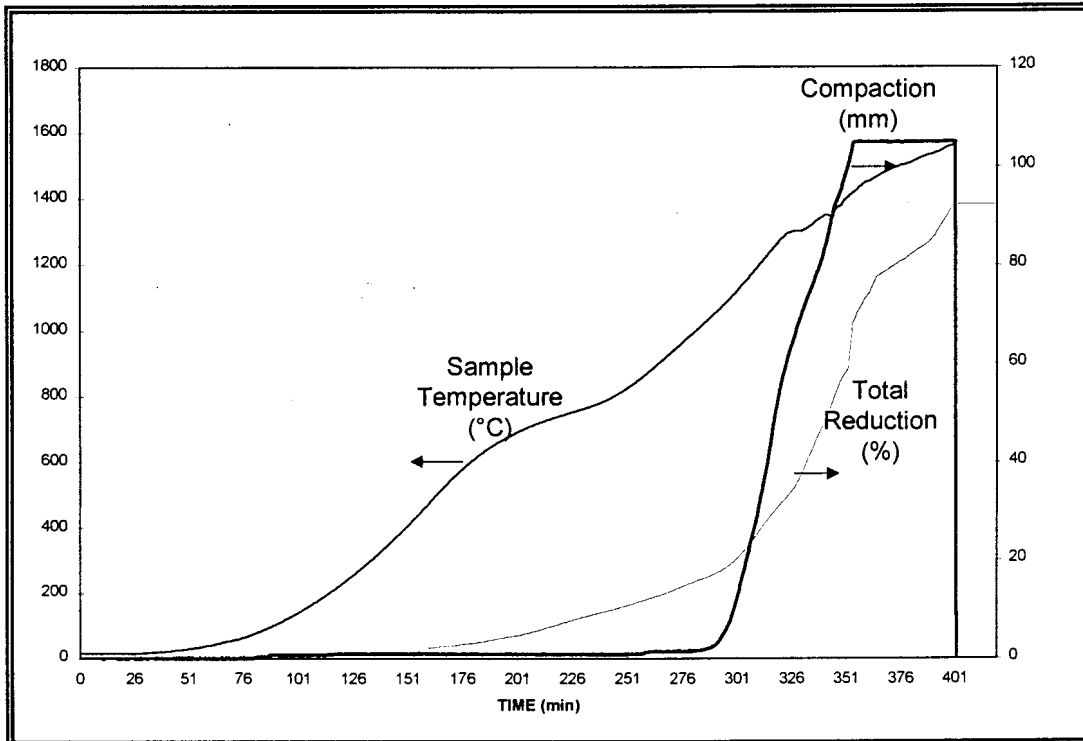


Figure 1b: Typical REAS test results (continues).

The goal of fully understanding the mechanisms during the REAS test led to the intensive investigation of Vanderbijlpark ore. The aim of the study is to determine

1. the different phases that form during the reduction of the ore.
2. the heats of the different reactions that occur during reduction.
3. the possible influence of the different phases on the pressure over the sample bed.
4. what influences the extent of the temperature arrest during the test.

Due to the extent of a full investigation, no attention was given to the viscosity of the sample.

2. BLAST FURNACE BACKGROUND

During the past two decades many efforts have been made to increase the control of the blast furnace conditions to ensure a homogeneous product. The dissections on blast furnaces by various iron and steel companies in Japan in the early 70s provided valuable information on the high temperature properties of charging material¹. A section of the blast furnace is shown in **Figure 2**².

During the dissections three distinct temperature zones, as indicated by **Figure 3** were identified in the blast furnace^{2,3}. The ascending gases in the lower and upper zones supply the total heat requirement, the middle one being almost isothermal. This hot gas rises through the active coke bed to the bosh, belly and the shaft and reduces the iron oxides. Indirect or gaseous reduction of iron ores takes place according to **Equations 1-3**. The reaction product is CO₂ and the overall **Equations 1-3** are mildly exothermic. If any wustite remains unreduced in a zone where temperatures are higher than 1000°C, the CO₂ produced by **Equation 3** is rapidly reduced by carbon according to **Equation 4** (also known as the Boudouard reaction).



Combining **Equations 3 and 4**,



Equation 4 is highly endothermic and also deteriorates CO utilisation. CO utilisation is determined by the conversion of CO to CO₂, *i.e.* a higher CO₂ fraction in the outgoing gas means that less C is necessary for reduction, which increases the CO utilisation. **Equation 5** is called direct reduction and is endothermic.

2.1. REACTIONS IN THE LOWER ZONE (MELTING/PROCESSING)²

This zone extends from the tuyere level to 3-5m above. The temperature of the molten materials varies between 1400-1450°C and the gases cool down to 800-1000°C. The more important chemical reactions occurring in this zone are:

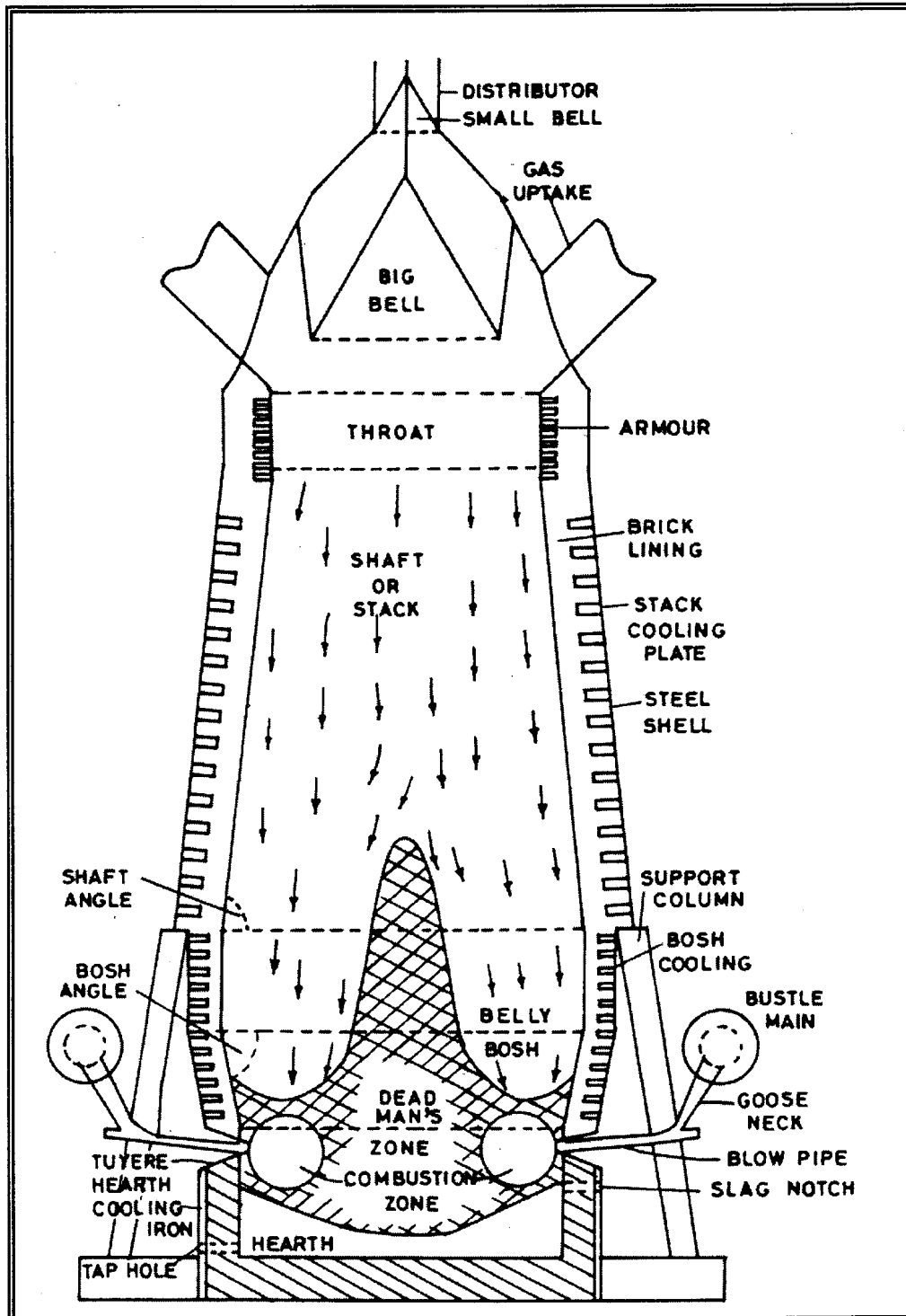


Figure 2: Blast furnace section.²

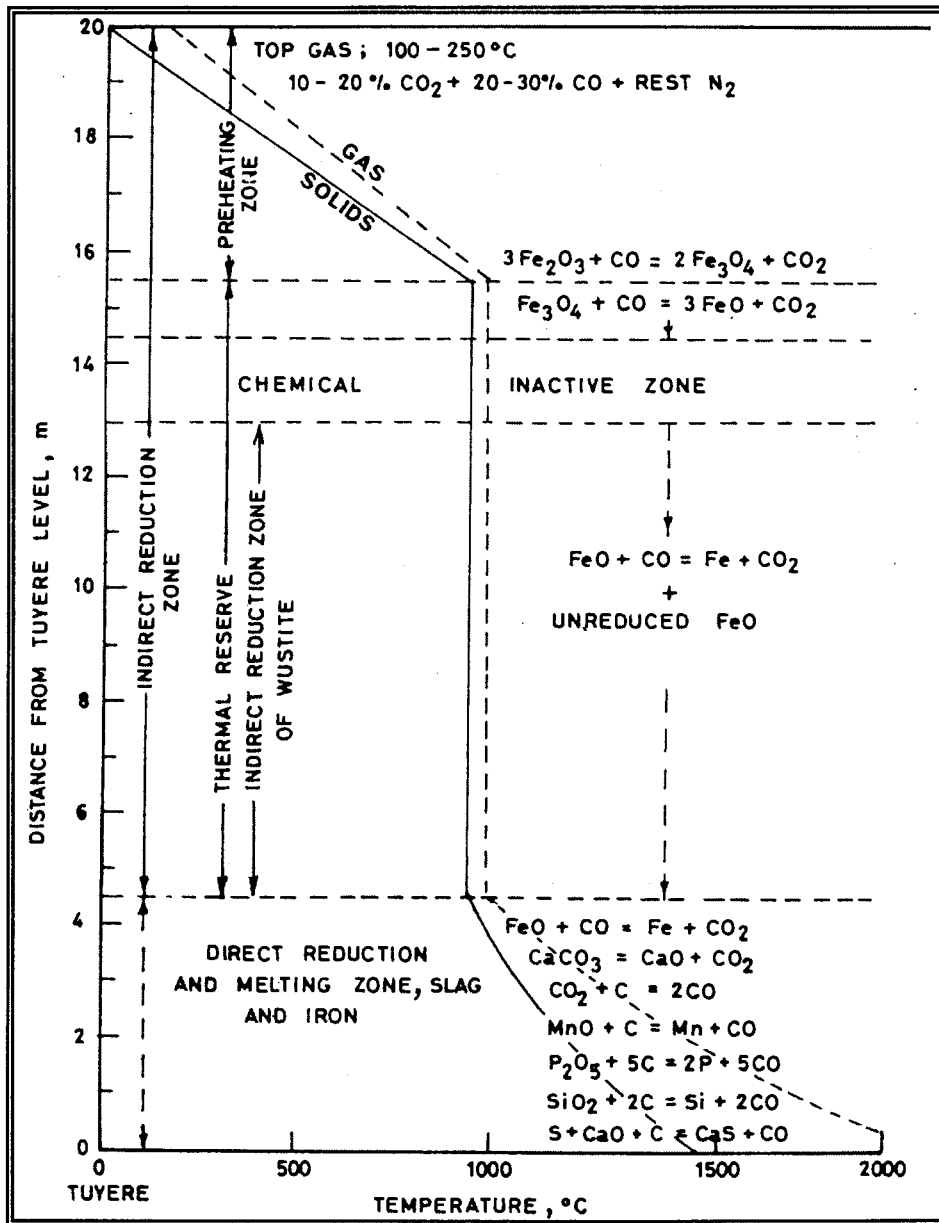


Figure 3: Temperature zones in blast furnace.²

- The endothermic calcination of limestone.

$$\text{CaCO}_3 \Leftrightarrow \text{CaO} + \text{CO}_2$$
- The endothermic direct reduction of wustite.

$$\text{FeO} + \text{C} \Leftrightarrow \text{Fe} + \text{CO}$$
- The endothermic direct reduction of SiO_2

$$\text{SiO}_2 + 2\text{C} \Leftrightarrow \text{Si} + 2\text{CO}$$
- The endothermic direct reduction of MnO .

$$\text{MnO} + \text{C} \Leftrightarrow \text{Mn} + \text{CO}$$
- The endothermic direct reduction of P_2O_5 .

$$\text{P}_2\text{O}_5 + 5\text{C} \Leftrightarrow 2\text{P} + 5\text{CO}$$
- The endothermic removal of sulphur

$$\text{FeS} + \text{CaO} + \text{C} \Leftrightarrow \text{CaS} + \text{Fe} + \text{CO}$$
- The exothermic combustion of carbon.

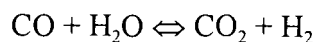
$$\text{C} + \text{O}_2 \Leftrightarrow \text{CO}_2$$
- The endothermic reduction of CO_2 .

$$\text{CO}_2 + \text{C} \Leftrightarrow 2\text{CO} (>1000^\circ\text{C})$$
- The endothermic reduction of moisture in the blast.

$$\text{C} + \text{H}_2\text{O} \Leftrightarrow \text{CO} + \text{H}_2 (>1000^\circ\text{C})$$

2.2. REACTIONS IN THE MIDDLE ZONE (ISOTHERMAL/THERMAL RESERVE)²

The middle zone, where the temperatures of the solids and gas are nearly identical (800°-1000°C), is called the isothermal or thermal reserve zone. Ideally, this zone can occupy up to 60 percent of the furnace volume. A major proportion of indirect reduction of iron oxides according to **Equations 1-3** occurs in this zone. The extent of this zone is important since the wustite should be given as much opportunity as possible for indirect reduction. The start of this zone depends on the level within the furnace where the highly endothermic reactions begin and the extent of indirect reduction depends upon the heat transfer efficiency. Another reaction of importance, which occurs in the middle zone is the so-called water-gas shift reaction (**Equation 6**).



6

This reaction generates hydrogen, which is a more active reductant than CO.



2.3. REACTIONS IN THE UPPER ZONE (PREHEATING/PREPARATION)²

The temperature of the gas ascending from the middle zone falls rapidly from 800-1000°C to 100-250°C in this zone. The temperature of the solids rises from room temperature to 800°C. The main reactions that occur in this zone are:

- The decomposition of carbonates other than that of calcium;
- vapourisation of moisture and hydrated water of the burden;
- carbon deposition
$$2\text{CO} \rightleftharpoons \text{CO}_2 + \text{C}$$
- partial or complete reduction of hematite and magnetite to their lower oxides according to **Equations 1 & 2.**

3. THE DEVELOPMENT OF A FURNACE AND TEST PROCEDURES

Present standard tests (ISO) to determine ore, sinter and pellet qualities only provide information of up to 1100°C⁴. Softening and melting of charges take place in the cohesive zone - >1100°C - of the blast furnace and several tests have been developed world-wide to determine the probable position and size of the cohesive zone for different charges^{1,4,5,6,7,8,9}. Since each blast furnace is unique, an attempt to develop an ISO-standard was unsuccessful due to the difference in operating conditions of the blast furnaces.

The aim was to develop a test that simulated the blast furnace process from loading to melting. The initial furnace and test method purchased by Iscor were designed and developed by SGA in Germany - the so called REAS-furnace (Reduktion, Erweichung und Abschmelzen which means reduction, softening and melting). Since 1985 Iscor Research & Development tested the REAS to determine the repeatability of the REAS test method and certain test parameters. Since 1993 new developments started and a test method for Iscor-blast furnaces was specifically developed. The control systems of the furnace, gas flow and monitoring of data have been computerised and an additional furnace has been built. **Figure 4** is a schematic diagram of the test apparatus.

3.1. TEST APPARATUS

The new apparatus consists of basically two sections, namely:

- Furnace with reactor
- Computerised control system

3.1.1. FURNACE WITH REACTOR

Figure 5 is a schematic diagram of the furnace with the reactor. The outer and inner tubes are made of 99.3% Alumina, while the sample holder, perforated plates and the five drip holders on the scale are made of graphite to eliminate any alumina contamination. The inner and outer diameters of the various tubes are given in **Table 1**. The perforated plate at the bottom has longer slits for better flow. The seals consist of wet (H₂O) Alumina ropes rolled in graphite. S-type thermocouples are used for monitoring both the furnace and sample temperatures. A dead weight system has been developed to place the sample under a constant load. A LVDT (linear variable differential transformer) is used to determine the difference in bed height during the test.

Table 1: Diameters

Diameter (mm)	Outer	Inner
Furnace	890	430
Outer Alumina tube	120	111
Inner Alumina tube	105	93
Sample holder	90	75

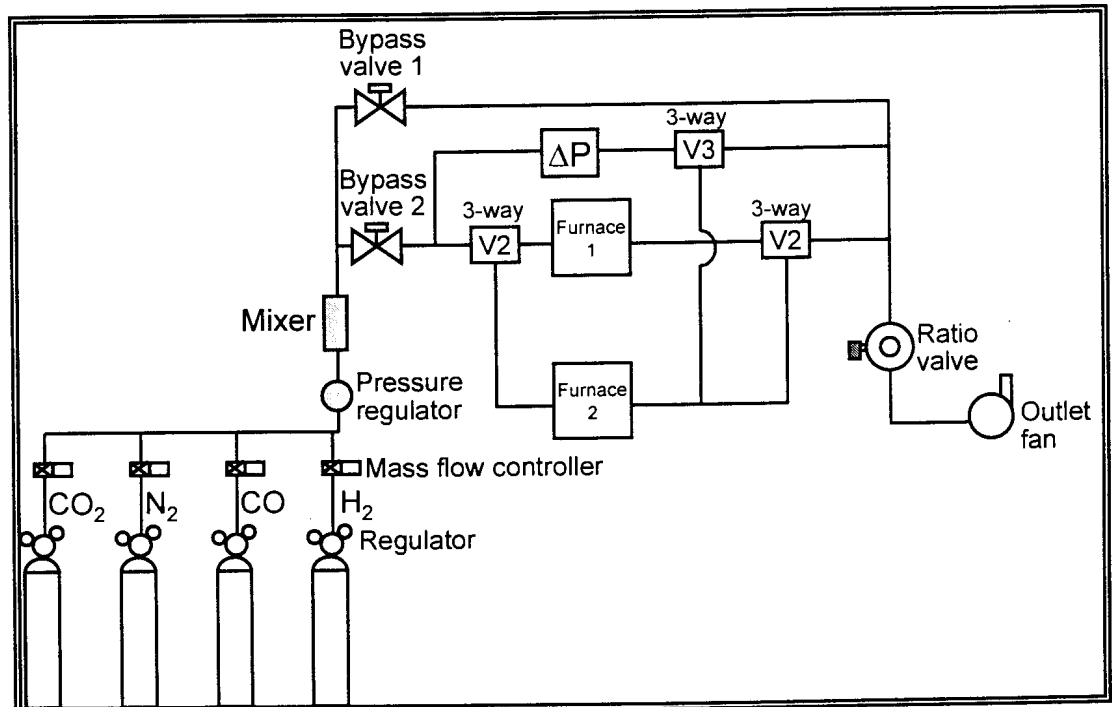


Figure 4: A schematic diagram of the test apparatus.

3.1.2. COMPUTERISED CONTROL SYSTEM.

The gas flow is controlled with mass flow meters. The gas composition is a function of the sample. The total gas flow is kept constant at 1800N/hour.

The pressure drop over the sample bed is determined with a differential pressure unit (DP-unit). This unit was calibrated for a maximum pressure drop of 3000mmH₂O and is connected to the incoming and outgoing gas lines to determine the differential pressure over the sample bed.

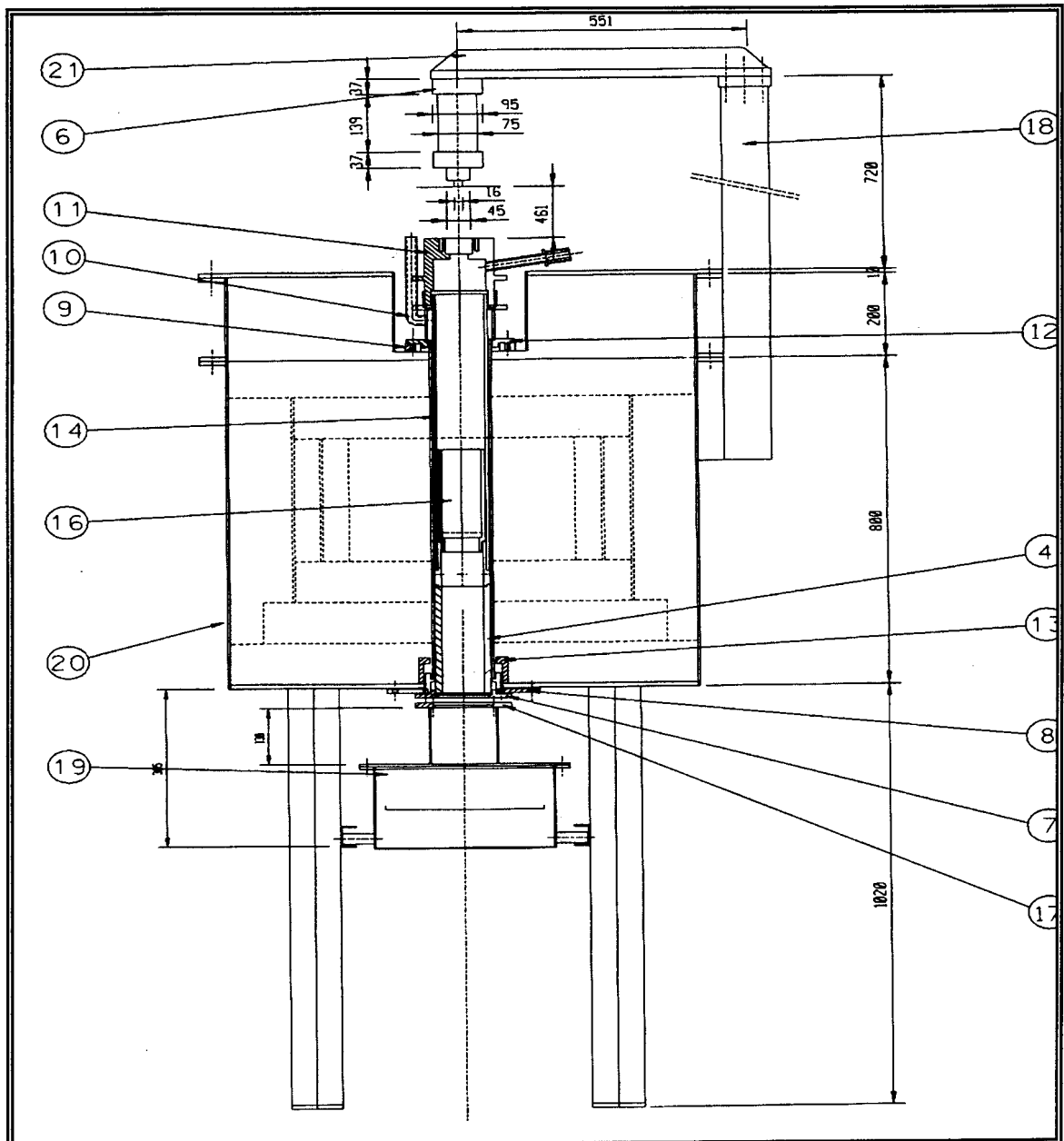


Figure 5: Schematic diagram of the furnace with reactor.

Legend (Figure 5)

4	Supporting ring	13	Guide flange
6	Load system	14	Outer tube
7	Gland	16	Sample holder
8	Tube support	17	Flange
9	Support flange	18	Pillar
10	Exhaust gas gland	19	Scale
11	Gas head gland	20	Furnace shell
12	Flange	21	Supporting beam

3.2. TEST PARAMETERS

The following test parameters are used to simulate the blast furnace conditions:

3.2.1. TIME DURATION

The time scale is more or less eight hours to simulate the retention time of a single particle from charging to melting in the blast furnace.

3.2.2. TEMPERATURE CYCLE

A temperature-time cycle is used to simulate the different phases in the blast furnace. The temperature cycle includes an isothermal phase at 900°C for 70 minutes, representing the thermal reserve zone in the blast furnace. The heating and cooling cycle of the furnace is shown in **Figure 6**.

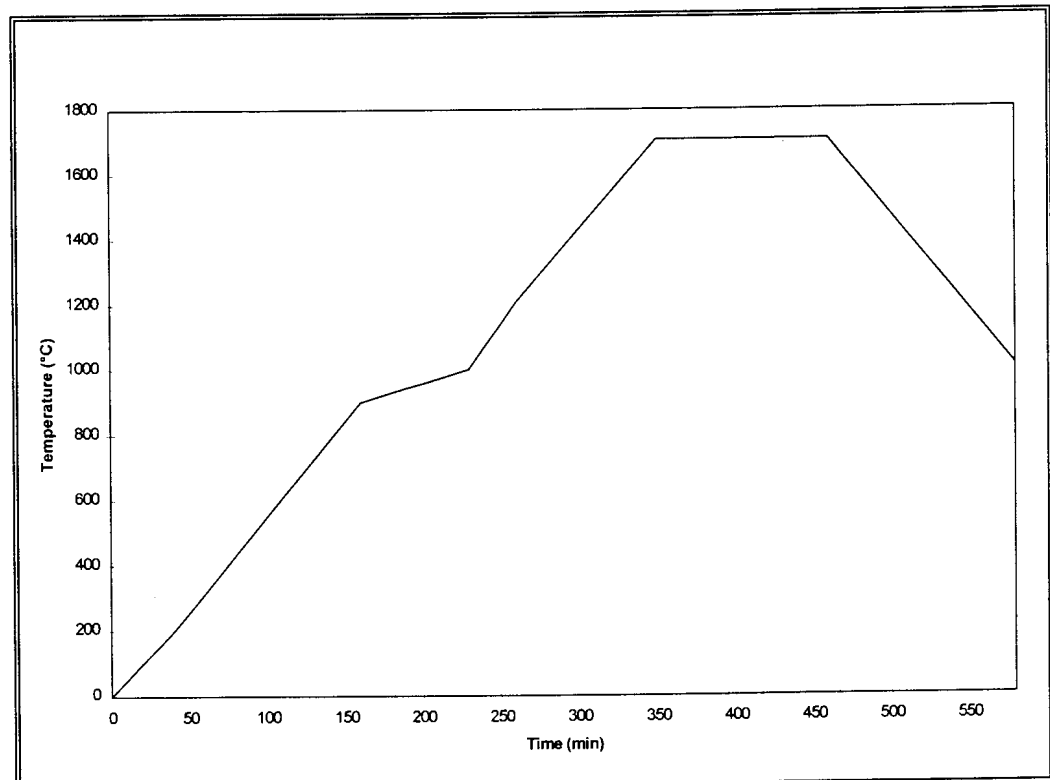


Figure 6: The heating and cooling cycle of the furnace.

3.2.3. GAS COMPOSITION AND FLOW

The gas composition is also a function of the sample temperature. A mixture of four gases, CO, CO₂, N₂, and H₂ is used to simulate blast furnace conditions. The CO/CO₂ ratio is shown in **Figure 7**. The CO plus CO₂ content is always maintained at 40 percent with 60 percent N₂. When H₂ is added, less N₂ is added to maintain the total gas flow of 1800N//min.

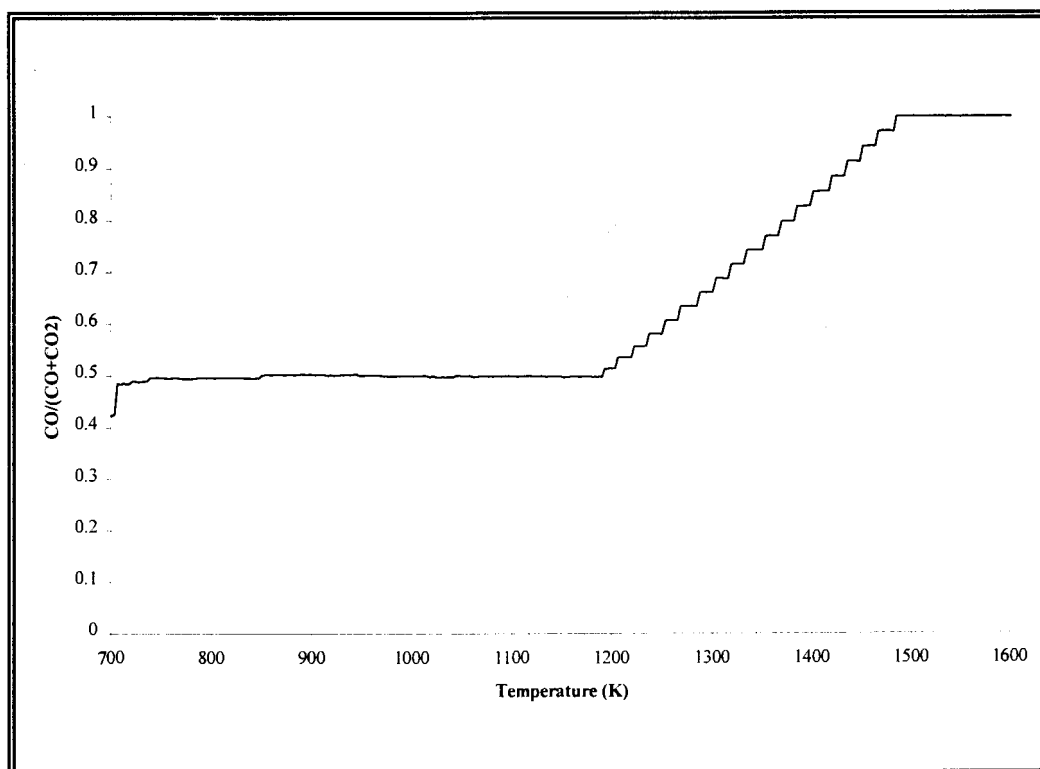


Figure 7: Change in CO/CO₂ ratio with temperature.

3.2.4. LOAD

A constant load of 1kg/cm² is applied to the charge by placing weights on top of the sample as shown in **Figure 5**.

3.2.5. SAMPLE COMPOSITION AND MASS

The sample mass (ore, sinter or pellets) is kept constant at 740g. The coke/graphite layer at the bottom of the sample is 30mm high. The coke/graphite layer at the top varies in height to keep the total packed bed height at 130mm. A schematic diagram of the sample holder is shown in **Figure 8**.

3.2.6. PARTICLE SIZE

The reducibility index is a direct function of the particle size¹. To minimise this effect, a particle size of (-12.5mm+10mm) is used. The particle size of the graphite/coke layers is (-10mm+8mm).

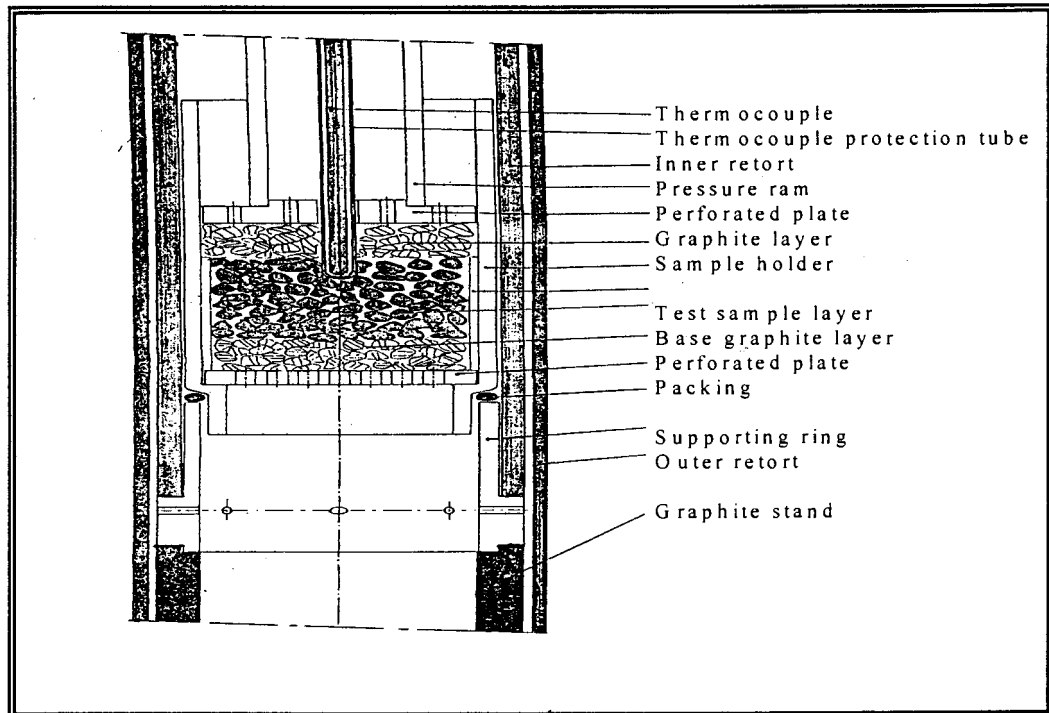


Figure 8: Sample holder with sample

3.3. INDICES

Several indices derived from the parameters obtained during the test are used to characterise the high temperature properties of a blast furnace charge. These indices are:

3.3.1. PERCENTAGE REDUCTION

The oxygen loss during the test is used to calculate the percentage reduction. The percentage CO and CO₂ entering and leaving the furnace (measured by the mass spectrometer) are used to determine the oxygen loss during the test. A complete deduction of the equation is shown in **Appendix 1**. The approximate reduction rate at 40 percent reduction is calculated as the average between 30 percent and 60 percent as follows:

$$\left(\frac{\partial R}{\partial t}\right)_{40} \equiv \frac{33.6}{(t_{60} - t_{30})} (\% / \text{min}), \quad 8$$

where t_{60} = time (min) where 60 percent reduction is reached
and t_{30} = time (min) where 30 percent reduction is reached

3.3.2. MAXIMUM PRESSURE DROP OVER THE SAMPLE BED (ΔP_{MAX}).

The gas pressure drop across the bed increases as the sample softens. The temperature where the maximum pressure drop is recorded as well as the value of the pressure drop are used as indices.

3.3.3. SOFTENING TEMPERATURE (ST)

The temperature where a pressure drop of 100mm H₂O is recorded, is taken as the softening temperature (**Figure 9**).

3.3.4. MELTING TEMPERATURE (MT)

The melting temperature is defined as the temperature where the pressure drop recovers to 100mm H₂O and lower after dripping has occurred (**Figure 9**).

3.3.5. DRIPPING TEMPERATURE (DT)

There are three different temperatures at which this index can be determined;

- First mass recorded on scale.
- Endothermic drop *i.e.* a drop in the sample temperature occurs. This is the commonly used temperature.
- Pressure drop decreases to below 100mm H₂O (**Figure 9**).

3.3.6. RELATIVE DRIPPING MASS

The relative dripping mass is a function of the total mass (**Equation 9**) of the sample and is calculated after the test has been completed.

$$\% \text{Rel Drip Mass} = \frac{\text{Total Drip Mass}}{(\text{Sample mass} - \text{Removable O}_2)} \times 100 (\%) \quad 9$$

3.3.7. COHESIVE AND SOFTENING ZONES

The cohesive zone is defined as the area between the melting and softening temperatures while the softening zone is defined as the area between the dripping and softening temperatures.

3.3.8. VISCOSITY

The area under the pressure drop vs temperature curve between the softening and melting temperatures (**Figure 9**) gives a measure of the viscosity. Because of the way it is defined the two experimental factors which affect the measure the strongest are ΔP_{max} and the cohesive temperature range ($T_M - T_S$). This value

is used to predict possible pressure problems in the blast furnace. The interpretation of this viscosity measure will not be considered further in this thesis.

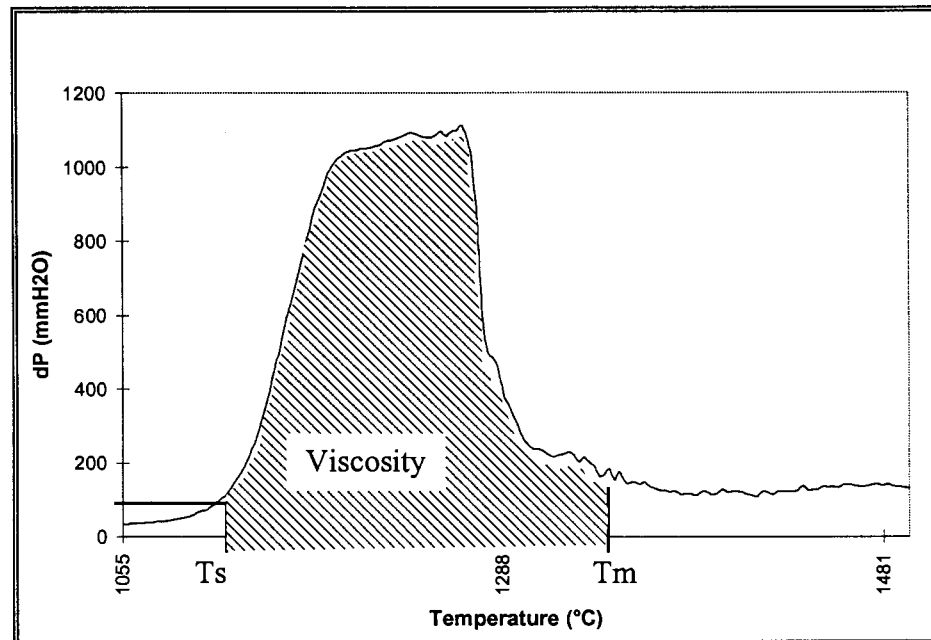


Figure 9: Determination of the viscosity between the softening and melting temperatures.

3.3.9. COMPACTION

The percentage compaction is the compaction at a certain time relative to the total compaction at the end of the test and is calculated using **Equation 10**.

$$\% \text{ Compaction} = \frac{X}{\text{Total Compaction (mm)}} \times 100 \quad 10$$

Where X =
 Compacting at any stage during the test
 Total compaction = Compaction at the end of the test.

3.3.10. CARBON LOSS

The carbon loss is defined as the carbon that has reacted during the Boudouard reaction and is determined by gas analysis. This index can be used in conjunction with the reduction rate and is calculated using **Equation 11**. (see **Appendix 1** for more detail).

$$\text{Carbon loss} = \left[\left((\text{CO}_2)_{\text{out}} + (\text{CO})_{\text{out}} \right) \times \left(\frac{(\%N_2)_{\text{in}}}{(N_2)_{\text{out}}} \right) - \left((\text{CO}_2)_{\text{in}} + (\text{CO})_{\text{in}} \right) \right] \times 14.968 \quad \left(\frac{\text{g}}{\text{min}} \right) \quad 11$$

3.4. CURRENT TESTWORK AND DEVELOPMENTS

All the major iron and steel companies developed test apparatus to ensure better blast furnace control. The following information on high temperature properties of charges is available in the literature:

3.4.1. HIGH TEMPERATURE REDUCIBILITY.

Yamaoka et al¹⁰ states that high temperature properties are affected by the ore reducibility (up to 1000-1200°C) and the composition and volume of the gangue before reduction.

The rate of reduction of a charge depends on the type of charge in terms of sinter, ore or pellets. Hotta et al¹¹ found that reduction proceeds more rapidly for pellets than for sinter until the stage of wustite, whereafter the reduction rate of the pellets tends to decrease significantly due to the formation of a dense metallic shell over the surface portion. He concludes that since FeO is a relatively low melting phase, the difference in softening and melting behaviour of burdens is directly due to the differences in reducibility at about 1000°C (since this determines the amount of FeO remaining) in addition to the composition and volume of gangue before reduction. Clixby⁸ found that one of the major influences on the behaviour of materials at high temperatures is the composition of the slag phase. A slag phase possessing a low melting point is detrimental in that the slag melts and impedes gaseous reduction of the iron oxide phases.

Hsieh et al¹² compared lump ore vs sinter properties and found a much lower reducibility index for the lump ore. This implies a higher FeO content after gaseous reduction that significantly lowers the melting point of the gangue minerals in the lump ore (primarily quartz).

The reducibility of a charge has a direct effect on the fuel efficiency and has a large effect on the configuration of the blast furnace. A high reducibility index leads to higher softening and melting temperatures that means the cohesive zone shifts down the blast furnace⁷. It also increases the degree of indirect reduction that increases the fuel efficiency.

3.4.2. SOFTENING PROPERTIES (SOFTENING (ST) AND MELTING TEMPERATURES (MT)) AND THE EFFECT THESE HAVE ON THE PERMEABILITY OF THE CHARGE.

Clixby⁸ states that the high temperature properties of burden materials depend upon the phases present and their proportions, which are related to the basicity and the degree of reduction. Busby et al¹³ found that cohesive masses are

initiated as a result of the relative stickiness and the softening behaviour of the ferruginous burden. It is attributable in the first place to surface melt formation, usually ferrous in nature. Metallic bonding between particles at temperatures lower than the melting point of pure Fe (1535°C) also takes place. Likely explanations for the latter effect are surface carburisation and the interaction between carburised metallic dust and the newly reduced pure Fe metal.

Melting behaviour ultimately depends on the carburisation of the metal and the gangue melting temperature¹³. The tendency to soften, given the limited formation of any ferrous melt can be related to:

- The gangue:metal ratio; metal with no interspersed gangue, such as that formed from rich ore, is plastic.
- The extent of metal and gangue interspersion
- The nature of the gangue, controlling the minimum temperature of primary slag formation
- The reactions between gangue components.

In the event of reduction being incomplete, the relatively low temperature formation of precursor ferrous melts will influence softening behaviour as also will the fluxing action of alkalis.

Clixby¹⁴ found that the softening and melting process has several distinct stages, namely:

- **Incipient melting** occurs at ~1000°C with acid pellets. Then with the onset of incipient melting, the softening stage commences. Although indirect reduction is still possible, the volume of the liquid slag is increasing with the rise in temperature. The quantity of the liquid slag reaches an amount where the bed becomes blocked (rapid increase in gas pressure drop) and at this point indirect reduction is replaced with direct reduction. Due to the high FeO content, the slag is extremely fluid.
- **Direct reduction**, which result in a considerable amount of FeO-rich slag being converted to slag (with little or no FeO) and metal. The decrease of FeO content causes a rise in the viscosity of the slag. Some dripping may also occur during this stage (dripping occurs when the first liquid drop is recorded on the scale). The effect of the decreased liquid slag volume and the dripping is to lower the quantity of liquid in the voids of the coke and thus the permeability is gradually restored.

Hotta et al¹¹ indicates that acid pellets tend to show an earlier increase in pressure drop over the bed than fluxed pellets due to the generation of molten slag at the core portion of the particle through reactions between wustite and gangue. This leads to lower softening temperatures and an increase in the cohesive zone.

Hsieh et al¹² found a wide cohesive zone for the lump ore ($T_s = 1198^\circ\text{C}$, $T_m = 1524^\circ\text{C}$). They suggest that the low melting $\text{SiO}_2\text{-FeO}$ melt would partially drip down and partially form $\text{SiO}_2 + \text{Fe}$, leaving little FeO before reaching the melting temperature.

The microstructure of the acid pellet before reduction contained hematite and a $\text{SiO}_2\text{-Al}_2\text{O}_3$ gangue system¹¹. Hsieh et al¹² found that at 1100°C the sample mainly consisted of metal and wustite and a slag corresponding to fayalite ($2\text{FeO}\cdot\text{SiO}_2$) with traces of hercynite ($\text{FeO}\cdot\text{Al}_2\text{O}_3$). At 1300°C the core changed to a void and both the peripheral and the core areas exhibit a mixed structure of metal, wustite, fayalite, hercynite and traces of iron-cordierite ($2\text{FeO}\cdot 2\text{Al}_2\text{O}_3\cdot 5\text{SiO}_2$).

Test work conducted by Clixby⁸ indicates that melting of the sample (pellets) started at a temperature of 980°C caused by a reaction between wustite and the slag present in the fully oxidised pellets. The presence of the alkalis in the residual slag served to lower the melting point of the liquid slag to $\sim 980^\circ\text{C}$. Due to the nature of the reaction between wustite and the residual slag he came to the conclusion that there is a maximum area of contact between the wustite and the residual slag.

The permeability of partly reduced iron ore reduces with an increase in the temperature due to softening and compaction of the sample bed. A high softening temperature indicates good permeability of the reduction gas through the furnace. This leads to high gas efficiency and blast furnace production. A low softening temperature on the other hand indicates that problems with permeability of the blast furnace could occur. This would cause uneven gas distribution in the blast furnace that would lead to unstable blast furnace parameters and bad metal quality.

A test was developed by Hoogovens¹⁵ based on vertical probings in the blast furnace at different radial positions. Pellets and sinter were compared regarding reducibility, reduction disintegration, swelling, shrinking and bed permeability. They found that:

- Up to the wustite stage, pellets are reduced faster than sinter due to their higher porosity. Due to a dense iron shell that forms the final reduction (wustite to iron) of the pellet is slow.
- Sinter tends to disintegrate more than pellets.
- A sharp increase in the pressure drop is observed at 1050°C for pellets while sinter starts to soften at higher temperatures.

3.4.3. DRIPPING PROPERTIES.

The percentage residual material (100 – the percentage relative drip material) is an indication of the ease with which meltdown would occur in the blast furnace. A high percentage residual material indicates a low production rate in the blast furnace as well as possible build up of high melting material. Clixby et al⁹ found that the two main chemical factors affecting the quantity of residual material for sinter were the FeO content of the sinter and the CaO/SiO₂ ratio of the sample (**Equation 12**).

$$\% \text{ Residual material} = 17.02 - 3.96 * \% \text{FeO} + 15.84 * \text{CaO/SiO}_2 \quad 12$$

According to this analysis, the basicity of the raw materials should be low and the FeO content high. A blast furnace test in 1984 based on this information gathered by Clixby resulted in some improvement in furnace operation and the number of observed pressure fluctuations decreased. The significance of the sinter lime:silica ratio may be explained by considering the melting mechanism. The slag emanating from the sinter is extremely fluid, due to the fluxing effect of the FeO. During direct reduction, the FeO content of the slag decreases to a very low value. With the decreasing FeO content, the slag properties are dependent upon the properties of CaO, SiO₂, Al₂O₃ and MgO in the slag.

Examination of the relevant phase diagrams shows that the liquidus temperature of the slag rises rapidly as the CaO/SiO₂ ratio increases. The rise in liquidus temperature can easily produce a slag which is not entirely fluid at the temperatures existing in the blast furnace.

Softening and melting tests developed to investigate the melting characteristics of burden materials up to temperatures of 1550°C also indicated a correlation between the residual material and the percentage of indirect reduction that occurred during the test⁸ (**Figure 10**). The higher the percentage indirect reduction, the higher the percentage residual material due to less FeO present to assist as a flowing agent.

Clixby⁸ found that the presence of residual slag will increase the width of the cohesive zone and depending on the quantity of slag and its viscosity may prevent metal from dripping away. The reason for the slag preventing metal dripping is that the FeO-rich slag reacts with the coke or graphite. This reaction removes the FeO, which has the fluidising influence, thus a viscous slag is formed. This viscous slag effectively shields the metal from the coke or graphite, hindering carburisation and meltdown.

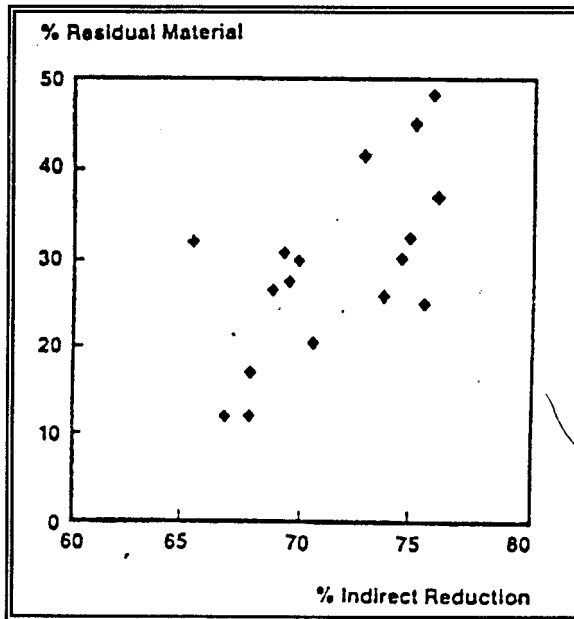


Figure 10: Correlation between the percentage indirect (gas) reduction and the percentage residual material¹⁰

3.4.4. MAXIMUM PRESSURE DROP OVER THE SAMPLE BED.

Studies performed by Clixby⁸ showed that samples with a relatively high percentage of reduction at temperatures higher than 1000°C had a low pressure drop over the bed, whereas samples with a low percentage of reduction had a high pressure drop over the sample bed. The permeability resistance decreased with an increase in the percentage of reduction in the 1000°C-1200°C temperature zone. This leads to a decrease in the high pressure drop zone, with better softening and melting properties.

3.4.5. VISCOSITY

The viscosity of slags depends on the sample composition and temperature. Low viscosity not only helps to increase the reaction rates by its effect on the diffusion of ions to and from the metal/slag reacting interface through the liquid slag but also ensures the smooth running of the furnace. An increase in basic oxides and the temperature above the liquidus temperature of the slag decrease the viscosity.

4. TESTWORK AND RESULTS

4.1. DETERMINATION OF THE VARIOUS PHASES OF IRON (DEGREE OF REDUCTION) DURING THE TESTS

Four tests were performed on a mixture of Sishen and Thabazimbi ore to determine the process of melt down of the test sample. The tests were performed with Vanderbijlpark PCI-coke. The chemical composition of the sample as well as the coke ash is given in **Table 2**. These four tests were stopped at different stages of the full REAS test, characterised by different gas pressure drops across the sample, as follows:

- **Test 1:** $\Delta P = 200\text{mmH}_2\text{O}$
- **Test 2:** $\Delta P = 600\text{mmH}_2\text{O}$
- **Test 3:** $\Delta P = 1200\text{mmH}_2\text{O} = \Delta P_{\text{max}}$
- **Test 4:** Full (normal) tests

Table 2: Chemical composition of the samples used to determine the various Fe-phases during the test.

Chemical component	Ore (mass %)	Coke Ash (mass %)
Fe (tot)	67.2	
Fe ₂ O ₃	95.8	6.77
FeO	0.26	
Fe ^o	0.02	
SiO ₂	2.02	57.1
Al ₂ O ₃	0.98	26.9
CaO	0.036	3.09
MgO	0.031	0.96
TiO ₂	0.05	1.81
Na ₂ O	0.02	0.76
K ₂ O	0.08	1.93
P	0.04	0.122
S	0.036	
C	0.065	
LOI		86.5

The complete REAS test results of tests 1-4 are given in **Appendix 2**. **Figures 11-14** are photos of the residual material of tests 1-3 as well as the drip that formed during test no. 4. The different drip layers were numbered as indicated in **Figure 14**. The conditions at the termination of the various tests are shown in **Table 3**. The residue material of tests 1-3 was prepared for evaluation with a scanning electron microscope (using the backscattered electrons for imaging to yield atomic number contrast). A accelerating voltage of 10kV was used and the average magnification was 1000 times

(see **Figures 15-17** for specific detail). Energy-dispersive X-ray analysis (EDX) was performed on the samples to determine the chemical analysis of the phases. The accelerating voltage used was 20kV. Various phases were identified and the chemical composition of these phases is listed in **Table 4**. Where the composition correlated with the stoichiometric composition of a phase, the phases was named accordingly. The areas in which the liquid phases plotted, were used to name the different phases (see **Appendix 3** for SiO₂, FeO and Al₂O₃ phase diagram)..

Table 3: Development of REAS tests 1-4.

	Test 1	Test 2	Test 3	Test 4
ΔP (mmH ₂ O)	152	555	1204	146
T _{max} (°C)	1218	1299	1315	1549
% Reduction	36.1	40.2	44.2	84.2
Gas composition				
Incoming				
% CO	38.99	38.2	38.14	
% CO ₂	0.03	0.01	0.04	
% N ₂	60.98	61.79	61.82	100
Outgoing				
%CO	36.97	39.37	41.96	
%CO ₂	3.41	1.20	0.47	
% N ₂	59.62	59.43	57.57	100
Drip mass (g)				429.9
Compaction (mm)	33.3	43.2	57	97.8

Table 4: Mass percentage of the three main elements identified in the residues of tests 1-3.

Element	Al ₂ O ₃	SiO ₂	FeO
Metallic iron Phase 1			100% Fe
Wustite Phase 2	<3%	< 3%	>97%
Liquid with fayalite composition Phase 3	0-2.9%	27.66-40.34%	59.43-70.98%
Hercynite Phase 4	60-66%	-	34-40%
Alkali rich liquid * Phase 5	14.94-24.16%	30.39-44.49%	25.04-33.92%

* also contains up to 1.58% Na₂O, 4.8%K₂O

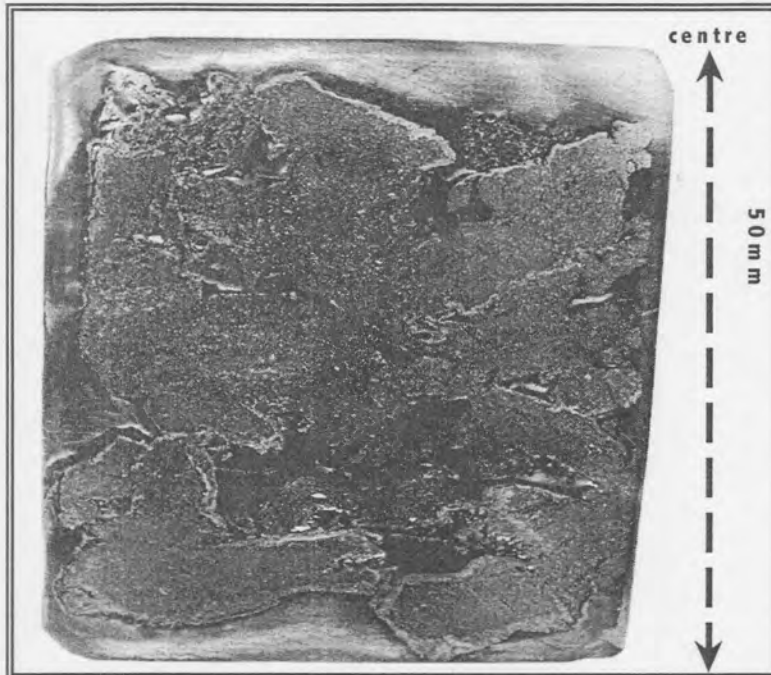


Figure 11: Residual material of test#1.

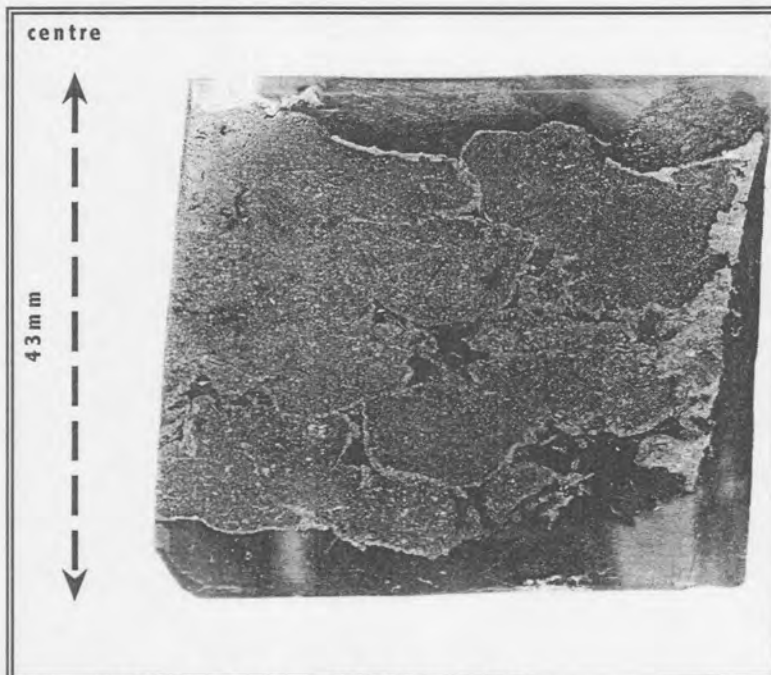


Figure 12: Residual material of test#2.

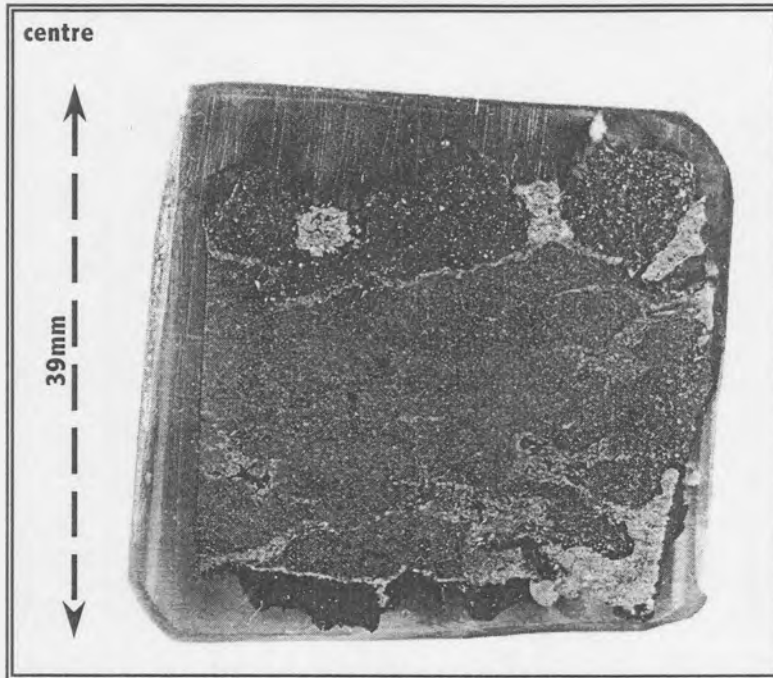


Figure 13: Residual material of test#3.

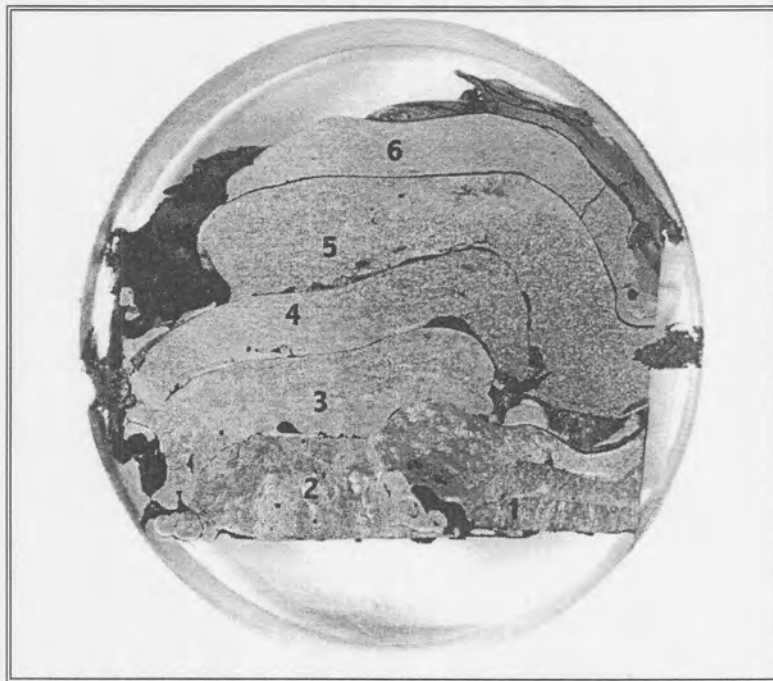


Figure 14: Drip sample of test#4.

Figures 15-17 are photographic images of the different phases observed during the scanning electron microscope (SEM) investigation for tests 1-3 respectively. Each sample was divided into ~8 evenly spaced rows and columns. Additional points were evaluated on the edges of the sample (top, bottom and sides). Making use of backscattered electron imaging (giving compositional contrast), together with energy-dispersive X-ray (EDX) analysis, the phases present in each field of view were assessed. The magnification varied between 130 and 1000 times (see **Figures 15-17** for detail). The numbers occurring on the figures represent the phase numbers as given in **Table 4**. **Table 5** gives an indication of the positions of the phases in the residual material. It indicates that all the phases occurred homogeneously throughout the sample and that particle distribution had no effect on the results gained. **Figures 18-20** indicate the percentage of fields that contained the different phases.

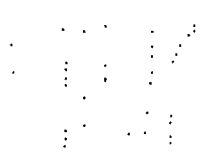


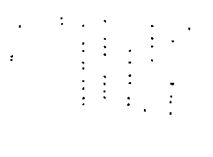
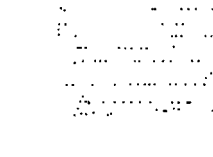

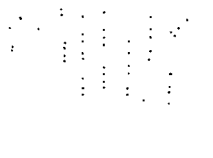
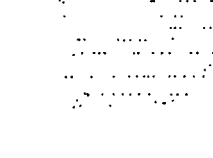
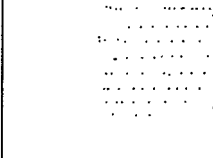


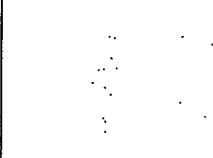

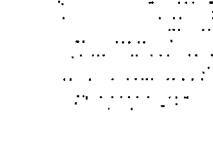

To perform an energy balance on the REAS test, information on the charge in the amount of phases with time (and temperature) is required. The phase distribution was calculated from the observed phases and the chemical analysis; the results are given in **Figures 21 and 22** and **Table 6**. Two issues are of importance in the calculation of the amount of the phases – firstly, using the analysed compositions to estimate the amounts of phases present for Tests 1 to 4, and secondly extrapolation of these to lower temperatures. As far as the first point is concerned, the calculation procedure is given in Appendix 4, and explained briefly below:

It is assumed that all Fe_2O_3 is reduced to FeO before any metallic iron forms. Beyond this time, the assumption that all the iron is present in the form of Fe° and FeO is made (the FeO can be present as pure wustite, as hercynite, in the alkali-rich liquid, as fayalite, or as the fayalite-base liquid). From the average chemical analysis of the alkali-rich liquid phase (as determined by EDX) the amounts of Al_2O_3 , FeO and SiO_2 reporting to the alkali-rich liquid phase was determined, assuming that all Na_2O and K_2O report to this liquid. According to **Table 5**, the rest of the Al_2O_3 was present in phase 4 (Hercynite). The rest of the SiO_2 is present in the liquid with fayalite composition (phase 3). The amount of FeO was then calculated based on the percentage reduction, and the amount of pure FeO found as the balance of that not taken up by the alkali-rich liquid, fayalite-based liquid and hercynite.

The amounts of these phases were then used to calculate the molar percentages given in Figures 21 and 22. These molar percentages were calculated per mole of the relevant compound, i.e. moles of FeO, Fe_2O_3 , Fe° , hercynite (FeAl_2O_4), fayalite-based liquid (Fe_2SiO_4), and the total moles of K_2O , Na_2O , Al_2O_3 , SiO_2 and FeO in the alkali-based liquid. The slag (assumed to take up all oxides) present at the end of Test 4 was assumed to be molten for temperatures above 1400°C (this was based on observation of dripping of slag beyond this temperature); hercynite and the fayalite based liquid are hence assumed to disappear as separate phases as this “dripping” slag develops. The alkali-rich liquid was assumed to melt above 980°C , and to be present as a solid

(with the same composition as in test 1) below this temperature. Any pure FeO was assumed to melt at 1364°C. Below the temperature of Test 1, the amounts of hercynite and fayalite (or fayalite-based liquid) were assumed to develop, as FeO became available by reduction of Fe₂O₃. This means that some unbound SiO₂ and Al₂O₃ were assumed to be present at lower temperatures, but above 400°C sufficient FeO was available to form the alkali-rich phase, hercynite and fayalite. The simplifying assumptions were necessary to allow the amount of the phases to be estimated.

Table 5: A schematic diagram indicating the occurrence of the phases in the residual material.

	Test 1 Right side represents the centre of the sample	Test 2 Left side represents the centre of the sample	Test 3 Left side represents the centre of the sample
Metallic iron (Phase 1)			
Wustite (Phase 2)			
Liquid with fayalite composition (Phase 3)			
Hercynite (Phase 4)			
Alkali rich liquid (Phase 5)			

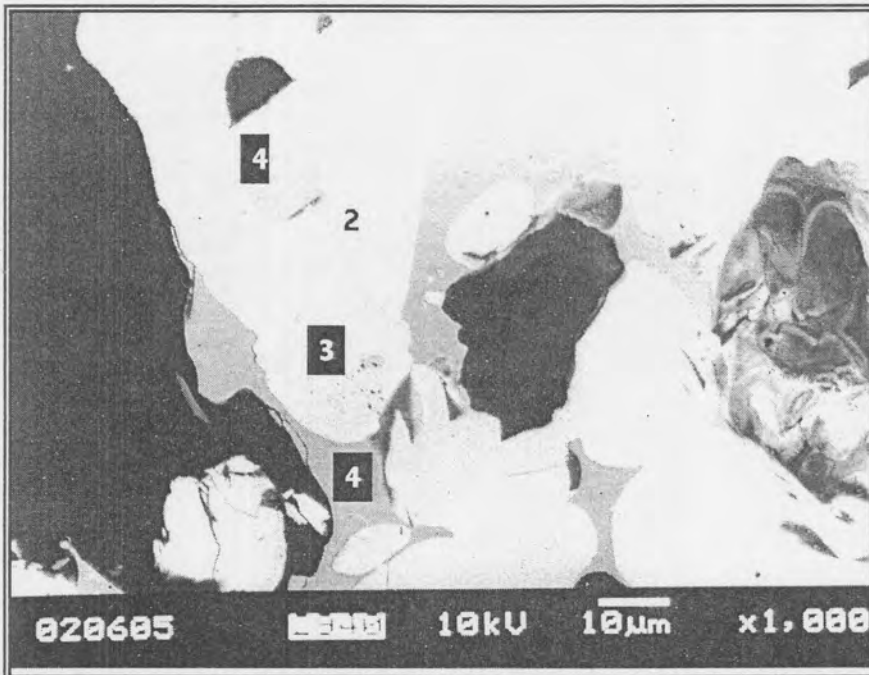


Figure 15 (test1) (The numbers correspond to the phase numbers in Table 5).

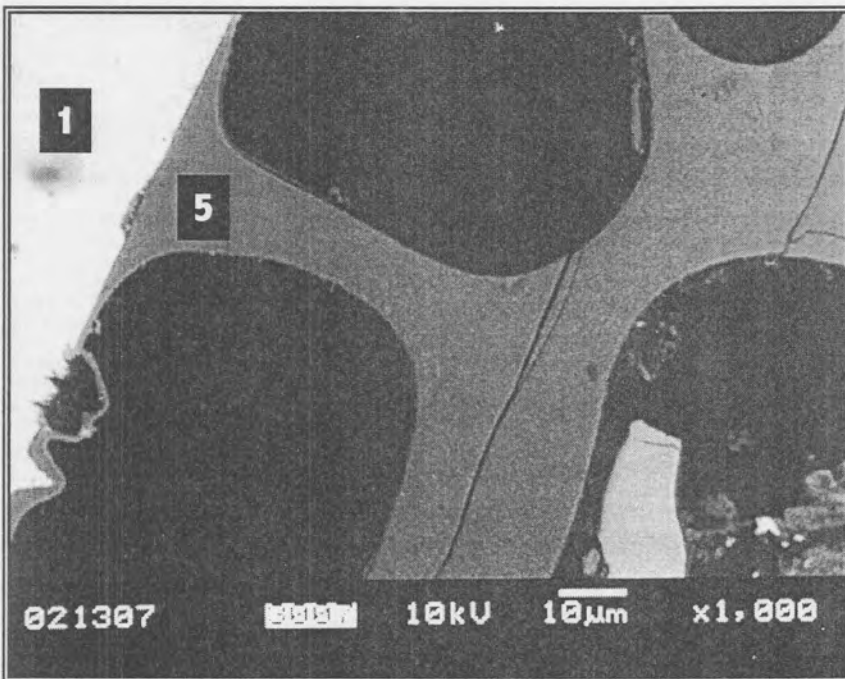


Figure 16 (test2) (The numbers correspond to the phase numbers in Table 5).

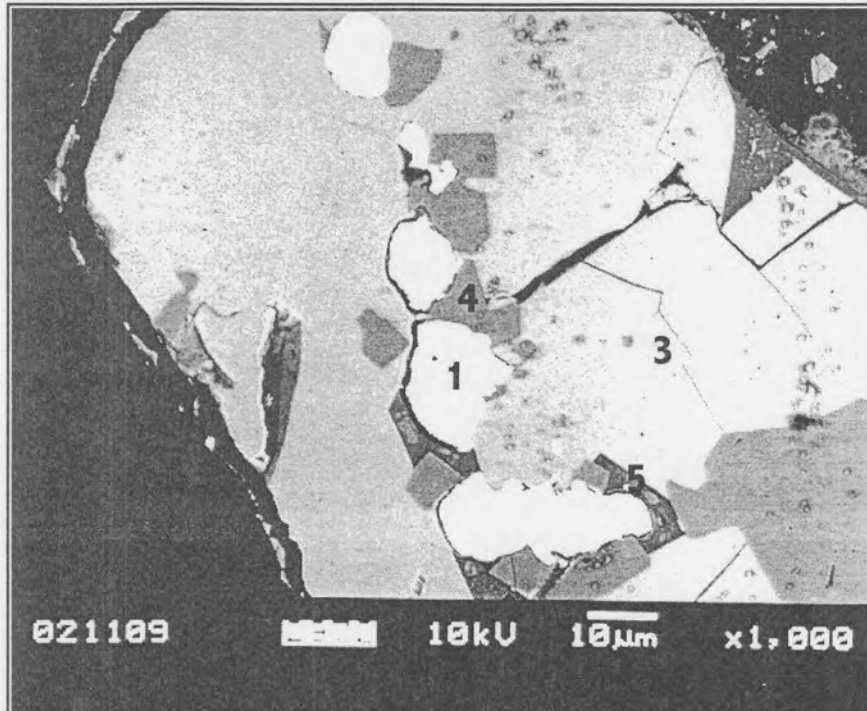


Figure 17 (test3) (The numbers correspond to the phase numbers in Table 5).

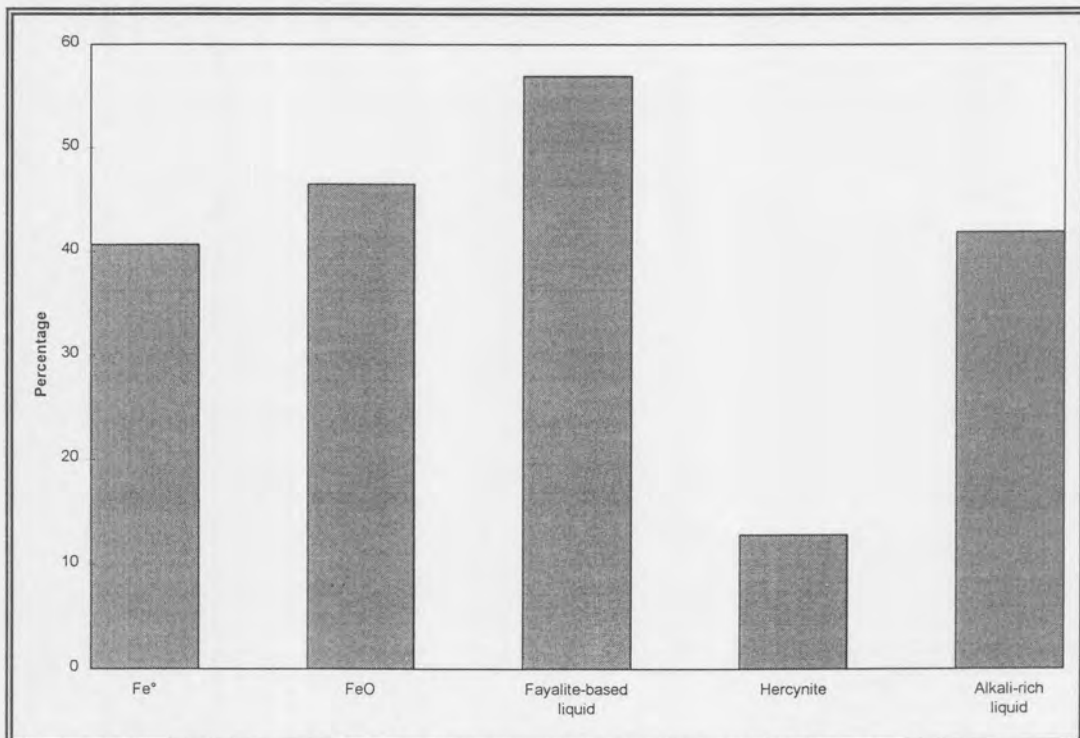


Figure 18: Percentage of fields of view which contained different phases (test #1).

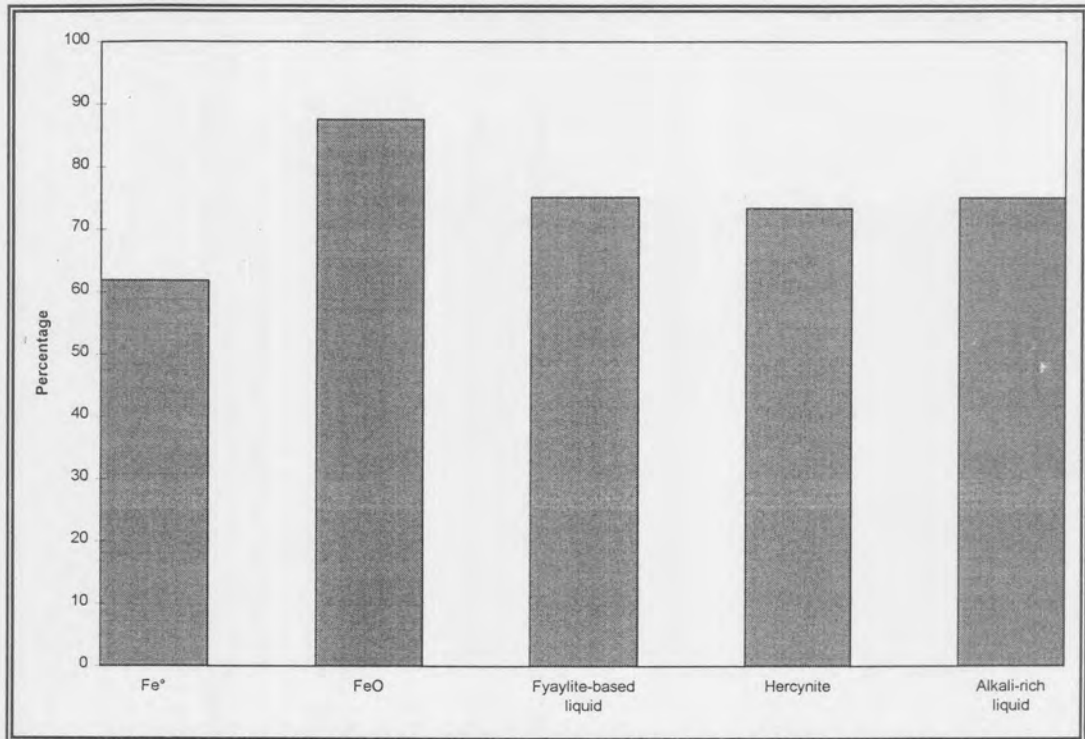


Figure 19: Percentage of fields of view which contained different phases (test #2).

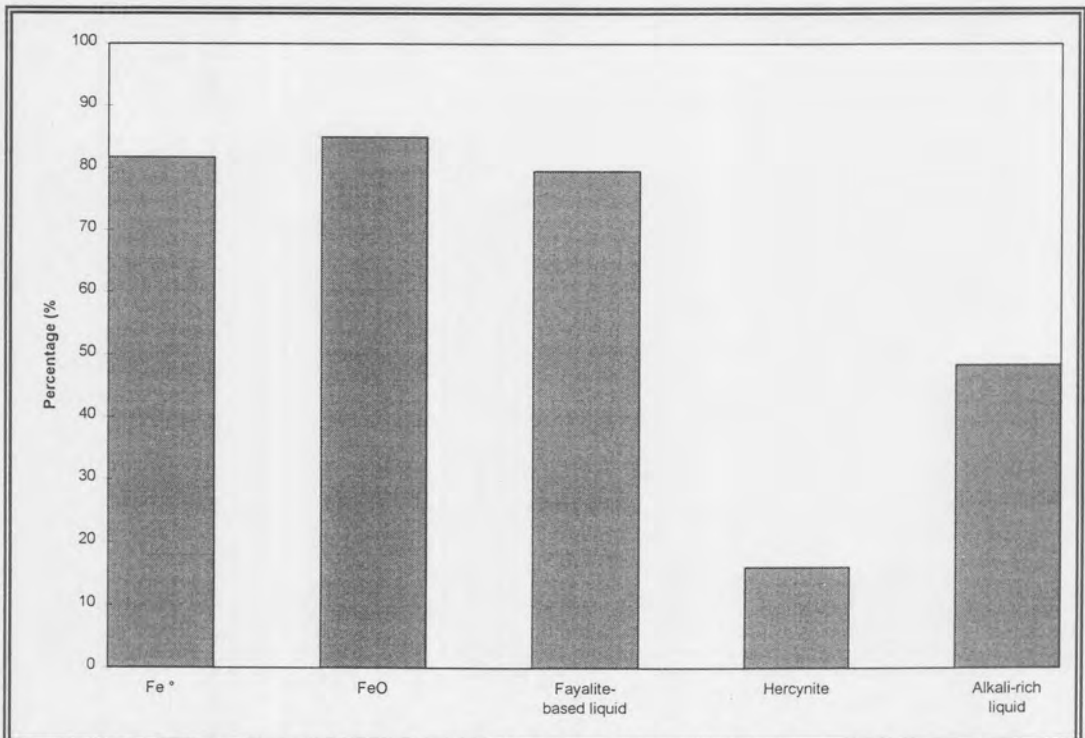


Figure 20: Percentage of fields of view which contained different phases (test #3).

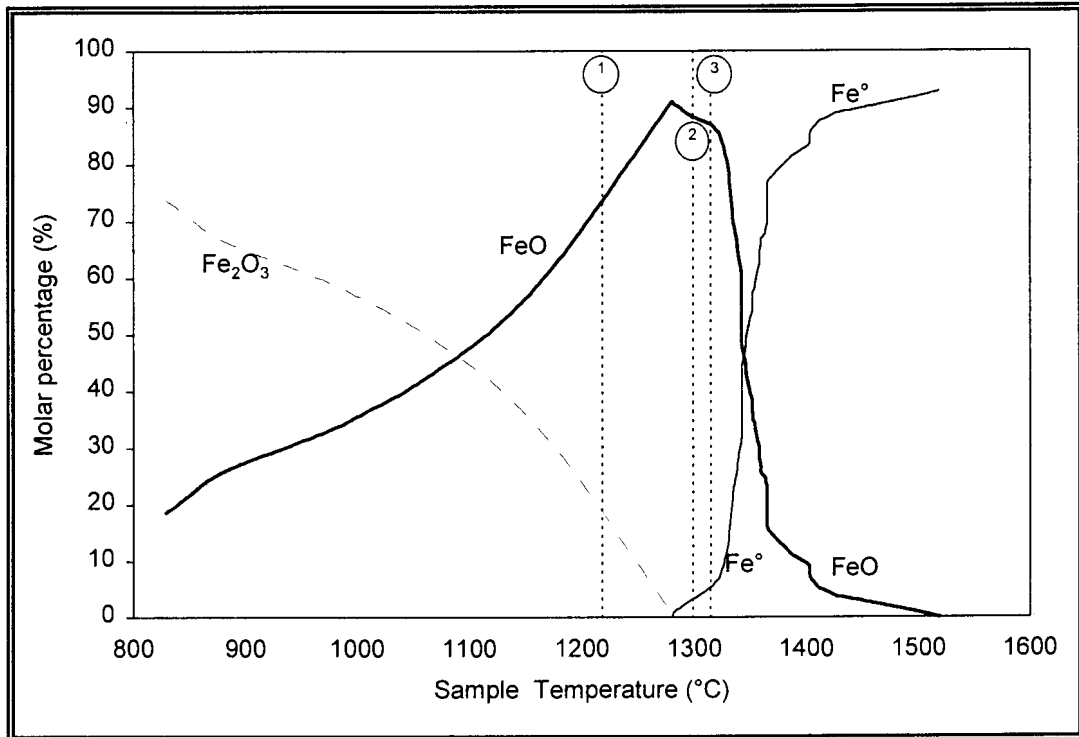


Figure 21: The calculated occurrence of the major iron-containing phases in the sample at different stages of the test. The numbers 1 to 3 in circles indicate the temperatures at which Tests 1 to 3 were terminate for analysis.

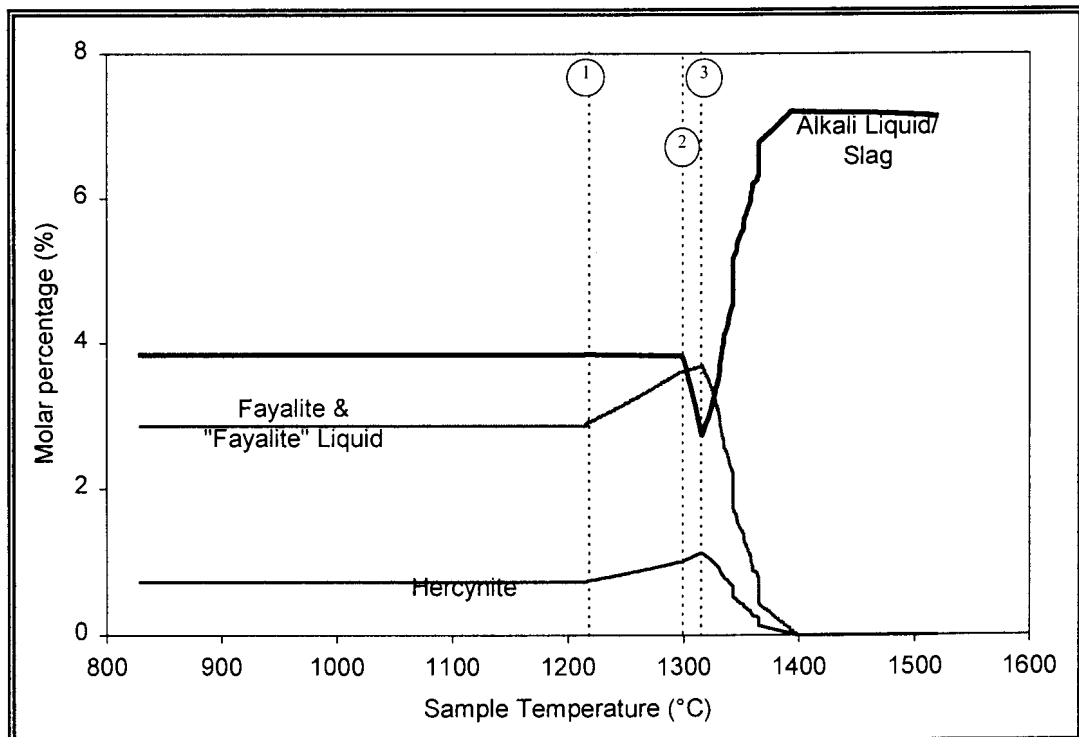


Figure 22: The calculated occurrence of the other phases in the sample at different stages of the test. The numbers 1 to 3 in circles indicate the temperatures at which Tests 1 to 3 were terminate for analysis.

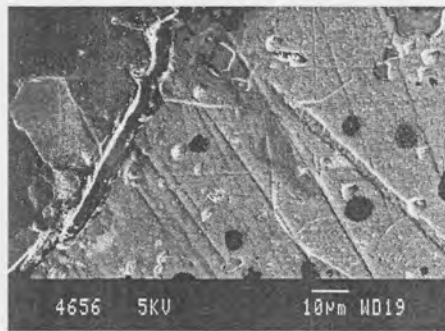
After determining the chemical compositions of the different phases, the samples of tests 1-4 were prepared and etched with nital to determine the microstructure of the metallic residual material with a scanning electron microscope (SEM). **Figures 23-25** are photos indicating the microstructure of the residual materials for **Tests 1-3** respectively. **Figure 26** indicates the microstructure of the drip that formed during test # 4. The amount of carbon in the different layers was estimated by the cementite/pearlite ratio and is shown in **Table 7** (The numbers of the layers correlate to the numbers in **Figures 14 and 26f&g**). The high C-content indicate typical cast iron structures with different melting points (according to **Figure 27¹⁷**).

Table 6: Calculated mole percentages of the different phases at different temperatures (corresponding to tests 1 to 3).

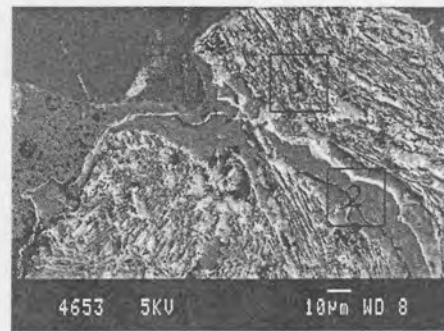
	1218°C	1299°C	1315°C
Fe°	0.02	3.27	5.54
Wustite	80.38	91.88	89.59
Liquid with fayalite composition	0.20	3.43	3.42
Hercynite	0.71	0.93	1.11
Alkali rich liquid	0.49	0.49	0.35
Fe ₂ O ₃	18.21	0	0

Table 7: Estimated amount of carbon in the white cast iron drip layers as indicated in Figure 14.

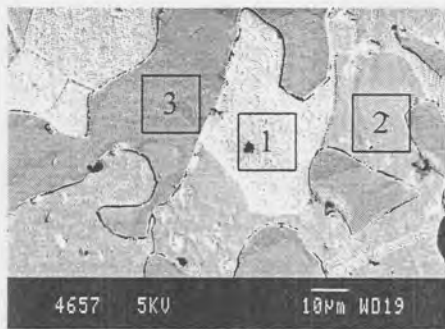
Layers	% Carbon (Estimated)
1 (Figure 14)	4
2 (Fig.26a)	4
3 (Fig.26a)	5
4 (Fig.26a)	5
5 (Fig.26a)	2.5
6 (Fig.26f)	3
7 (Fig.26f)	2.5-3
a (Fig.26a)	5
b (Fig.26a)	2.5
I (Fig.26g)	6
t1 (Fig.26f)	6
t2 (Fig.26f)	6.5
x (Fig.26a)	6
y (Fig.26a)	5
z (Fig.26a)	5



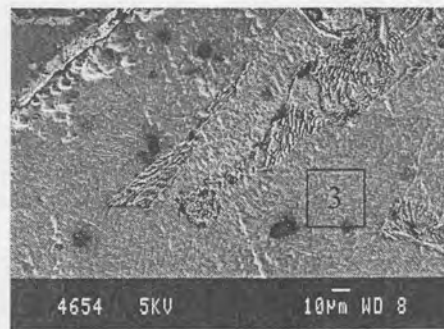
a



a



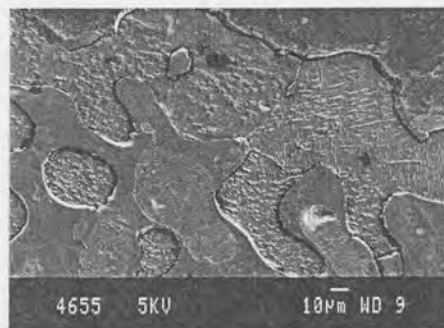
b



b



c



c

Figure 23: Microstructure of residual material of test 1. The various forms in which iron occurs, namely Fe (1), FeO (2) and fayalite-type liquid (3) are clearly indicated.

Figure 24: Microstructure of residual material of test 2. Figure a is the microstructure next to the graphite crucible and consist of pearlite (1) and cementite(2), while in figure b has a ferritic (3) structure with pearlite pockets where the material is in contact with the coke particles at the top. Figure c is the ferritic structure of the material in the middle of the sample.

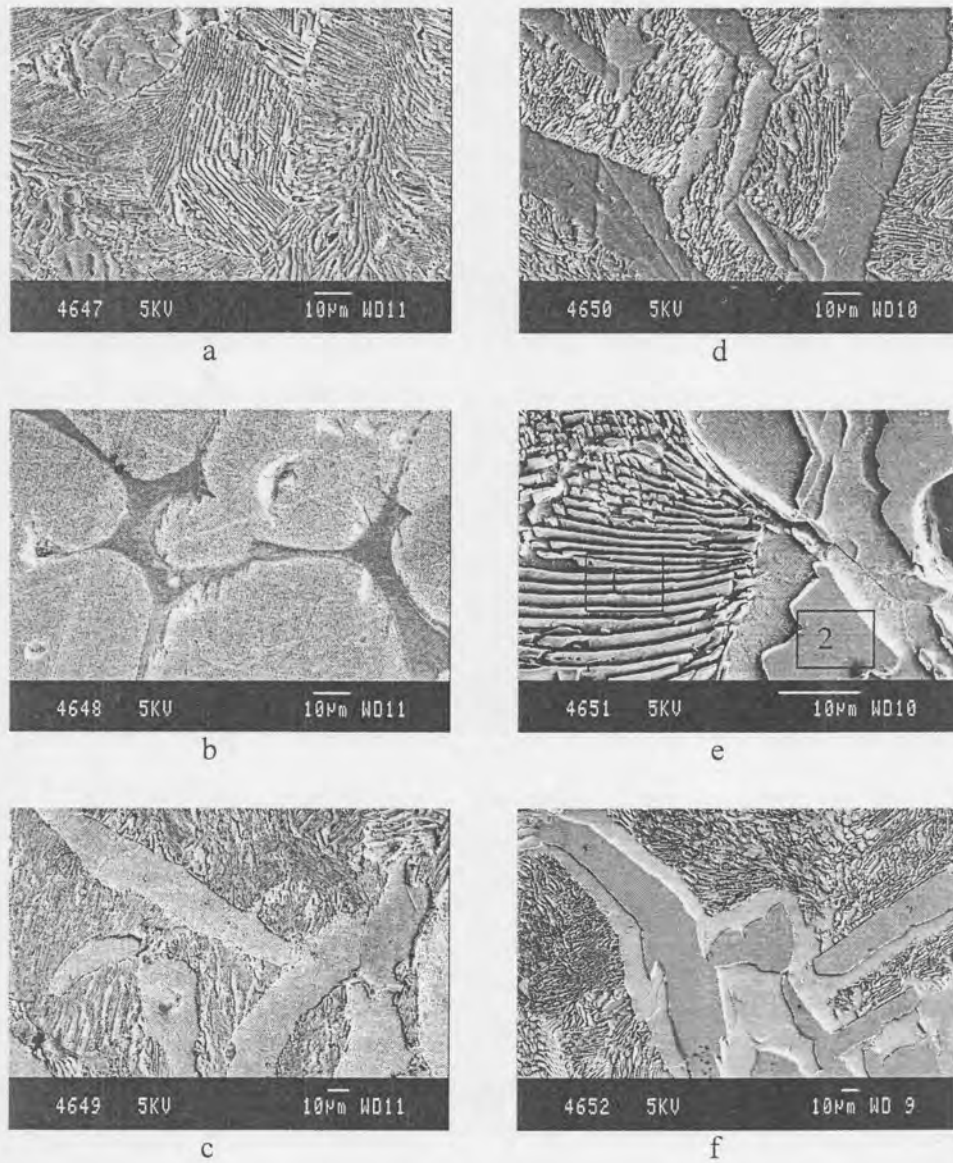


Figure 25: Microstructure of the residual material of test 3. Depending on the position of material, more or less carbon absorption has taken place. This leads to the different amounts of pearlite (1) and cementite (2) found in the microstructures.

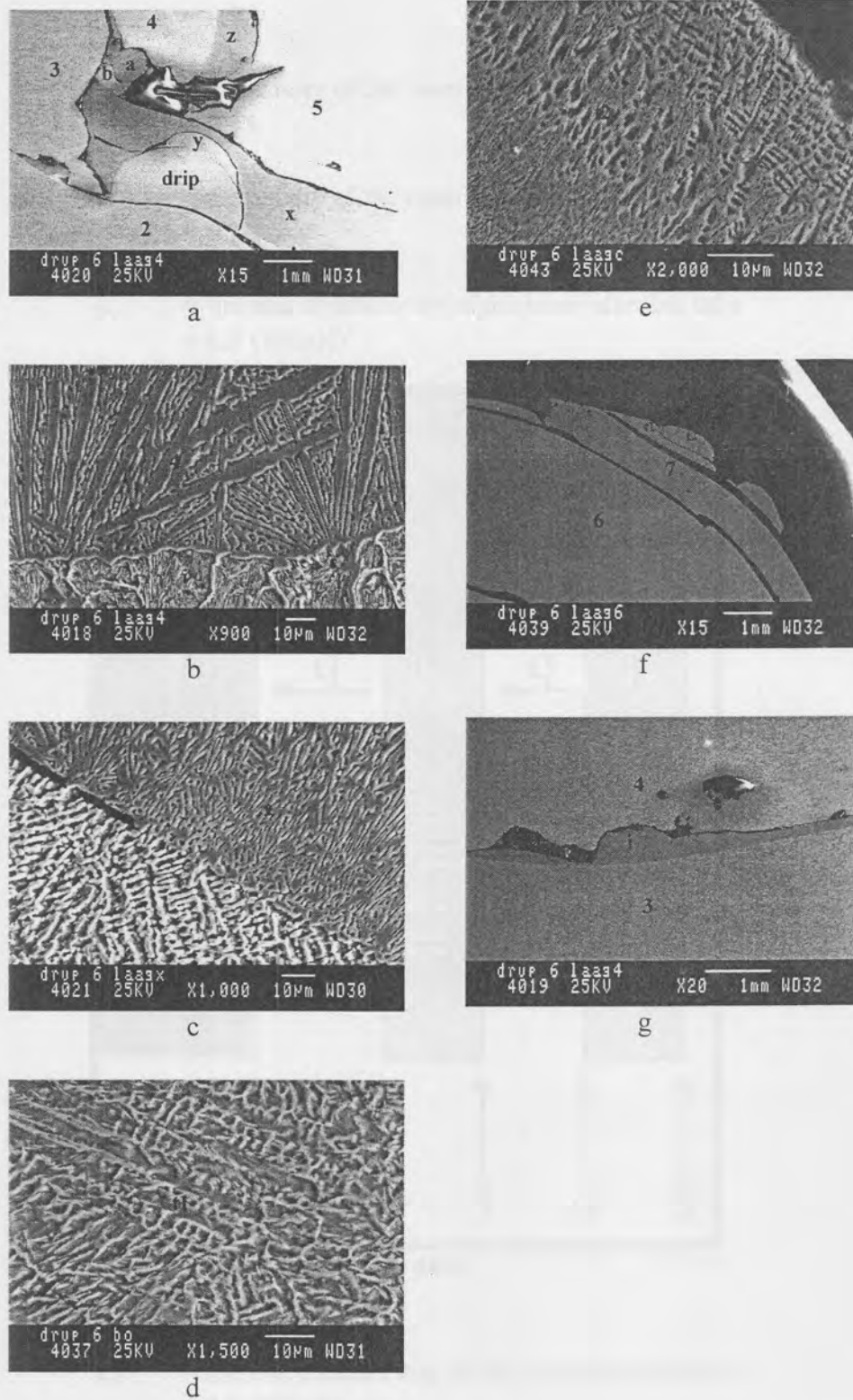


Figure 26: Microstructures of the iron melt produced during test#4. This indicate the different layers of white cast iron which differ regarding the amount of carbon absorbed. The numbers and letters refer to Table 7.

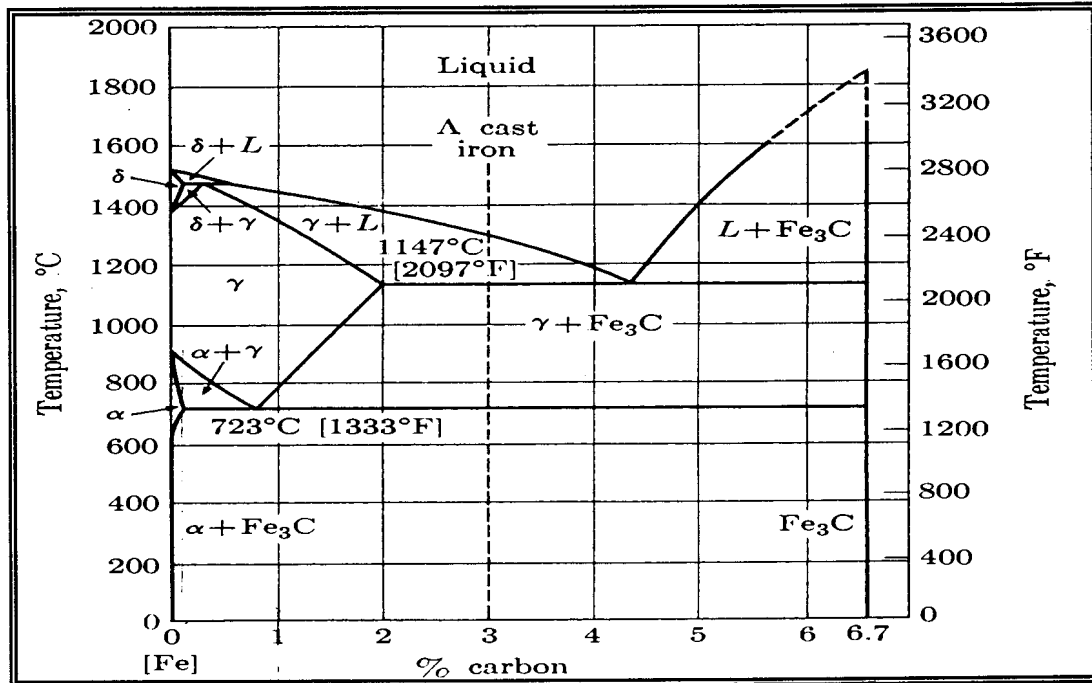


Figure 27: The meta-stable iron-iron carbide phase diagram.¹⁷

4.2. EVALUATION OF THE HEAT TRANSFER RATE DURING THE TEST

During the tests, just before the first drip is observed, the temperature tends to decrease. The extent to which this happens depends on the burden. Values of up to 50°C have been measured. If the blast furnace is operated near the slag liquidus temperature, a sudden drop in temperature could lead to problems with the viscosity and the formation of scabs. To determine the cause of the temperature fall, the heat transfer in the experimental furnace and the enthalpy of the burden have been computed.

4.2.1. ENTHALPY OF THE BURDEN

The calculated heat flow (**Equations 11 & 12**) is based on the values obtained during test 4 as well as the results generated in paragraph 4.1. The chemical analysis of the slag is given in **Table 8**. This analysis was used to determine the heat content of the molten slag using **Equations 13-16**¹¹.

Table 8: Chemical analysis of the slag formed during test#4.

Chemical component	Slag (mole %)
FeO	14.06
SiO ₂	59.86
Al ₂ O ₃	13.58
CaO	7.60
MgO	3.59
TiO ₂	0.89
K ₂ O	0.97
MnO	0.35

Sample:

$$H_T^{\text{sample}} = H_T^\circ(\text{Al}_2\text{O}_3) * n(\text{Al}_2\text{O}_3) + H_T^\circ(\text{Fe}_2\text{SiO}_4) * n(\text{Fe}_2\text{SiO}_4) + \dots \quad 11$$

Enthalpy change during a time interval:

$$\Delta H = H_{\text{current}}^{\text{sample}} - H_{\text{previous}}^{\text{sample}} + \{ [H^\circ(\text{CO})_{\text{out}} * \Delta n(\text{CO})_{\text{out}} + H^\circ(\text{CO})_{\text{out}} * \Delta n(\text{CO}_2)_{\text{out}} + H^\circ(\text{N}_2)_{\text{out}} * \Delta n(\text{N}_2)_{\text{out}}] - [H^\circ(\text{CO})_{\text{in}} * \Delta n(\text{CO})_{\text{in}} + H^\circ(\text{CO})_{\text{in}} * \Delta n(\text{CO}_2)_{\text{in}} + H^\circ(\text{N}_2)_{\text{in}} * \Delta n(\text{N}_2)_{\text{in}}] \} \quad 12$$

Slag:¹¹

$$H_{298}^\circ = -285290 \quad (\text{J/g.atom}) \quad 13$$

$$H_T - H_{298}^{\circ} = 5460 + 49.75T - 6.3 \times 10^{-3}T^2 - 180 \times 10^3 T^{-1} - 1110\sqrt{T} + 1.67 \times 10^{-6} T^3 \quad (\text{J/g.atom}) \quad 14$$

$$\Delta H_m = 0.35 (H_T^{\circ} - H_{298}^{\circ}) - 2.5 \quad (\text{J/g.atom}) \quad 15$$

$$H_{\text{slag}_T} = H_T + \Delta H_m \quad (\text{J/g.atom}) \quad 16$$

4.2.2. HEAT TRANSFER IN THE FURNACE

To calculate the heat transfer within the furnace, the following assumptions have been made:

1. Consider one dimensional (radial) heat transfer
2. Ignore the heat transfer between the reaction gas and the alumina tubes
3. Ignore gas radiation transfer (since the gas contains very small amounts of CO₂ and H₂O)
4. Steady state heat transfer between the furnace and the sample container was considered.

Figure 27 is a diagram of the furnace. **Table 9** lists the various constants and furnace dimensions.

Table 9: Furnace dimensions.

Position	Radii (m)
1 Outer radii of graphite sample holder	0.04
2 Inner radii of inner alumina tube	0.04575
3 Outer radii of inner alumina tube	0.05075
4 Inner radii of outer alumina tube	0.05475
5 Outer radii of outer alumina tube	0.06025

ϵ_1 = emissivity of the graphite sample holder

$$= 0.75$$

ϵ_a = emissivity of the inner alumina tube
= 0.35

ϵ_B = emissivity of the outer alumina tube
= 0.35

k_A = thermal conductivity of the inner alumina tube
= 8.6 (W/mK)

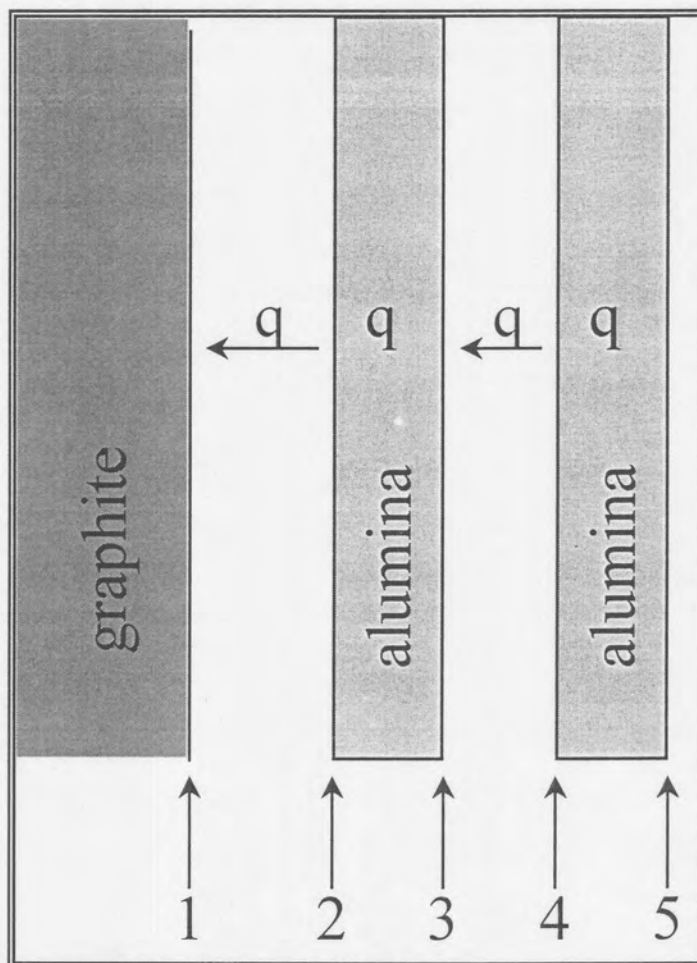


Figure 27: Diagram of furnace

k_B = thermal conductivity of the outer alumina tube
= 8.6 (W/mK)

σ = heat transfer coefficient (Stephan-Boltzmann Constant)
= 5.669×10^{-8} (W/m²K⁴)

The following approach was used:

1. Assume that T_1 (sample temp) and T_5 (furnace temp) are known
2. The same heat flow exists between 1&2, 2&3, 3&4 and 4&5
3. Calculate q per unit length

Equations 17-20 were used to determine q , T_2 , T_3 and T_4 . Solutions at various temperatures are shown in Table 10.

$$q = (T_2^4 - T_1^4)C_{1-2} \quad 17$$

$$\text{where } C_{1-2} = \frac{\sigma}{\frac{1-\varepsilon_1}{\varepsilon_1 A_1} - \frac{1}{A_1} + \frac{1-\varepsilon_A}{\varepsilon_A A_2}}$$

$$q = (T_4^4 - T_3^4)C_{3-4} \quad 18$$

$$\text{where } C_{3-4} = \frac{\sigma}{\frac{1-\varepsilon_3}{\varepsilon_A A_3} - \frac{1}{A_3} + \frac{1-\varepsilon_B}{\varepsilon_B A_4}}$$

$$q = (T_5 - T_4)C_{4-5} \quad 19$$

$$\text{where } C_{4-5} = \frac{2\pi k_B}{\ln(r_5/r_4)}$$

$$q = (T_3 - T_2)C_{2-3} \quad 20$$

$$\text{where } C_{2-3} = \frac{2\pi k_A}{\ln(r_3/r_2)}$$

Table 10: Results of the heat flow calculations.

Furnace temperature (T_5) (K)	Sample temperature (T_1) (K)	q (W/m)	T_2 (K)	T_3 (K)	T_4 (K)
1398	1174	3868.14	1282	1290	1391
1552	1324	5353.10	1430	1440	1543
1744	1598	5117.00	1659	1669	1735
1780	1613	6083.48	1683	1695	1769
1817	1665	5920.34	1728	1739	1807

These results are compared with enthalpy calculations in Chapter 5.

5. DISCUSSION

5.1. DETERMINATION OF THE VARIOUS PHASES OF IRON (DEGREE OF REDUCTION) DURING THE TESTS

The various phases were identified by means of EDX/SEM and the relevant phase diagrams. By determining the different phases, an idea could be formed in which phases the different components, i.e. FeO, SiO₂ and Al₂O₃, reported. This also gave an indication of the course of reduction, the formation of phases, in which state the phases were (solid or liquid) and the expected effect of these on the pressure drop over the sample bed.

5.1.1. TEST NO. 1 (SOFTENING OF SAMPLE STARTED)

In **Table 5** the left side of the sample represents the outer side of the sample in contact with the graphite sample holder while the right side represents the centre of the sample. According to **Table 5**, two liquid phases, the liquid with the fayalite composition and the alkali rich liquid, are present at 1218°C, which probably accounts for the rise in the pressure drop over sample bed at this temperature. The total amount of liquid at this stage is some 7% (molar basis) of the total sample (**Figure 29a**). **Figure 23a** is the microstructure of the residual material occurring in the middle to the left of the sample. Although carbon is readily available, the metallic iron has a ferrite structure with little carbon absorption (less than 0.025%). **Figure 23b** shows the different forms in which iron occurs, namely, Fe, FeO as well as the fayalite type liquid (from light to dark), that were present at this stage of the test. **Figure 23c** is the microstructure of the material adjacent to a coke particle. Very little carbon absorption has taken place at this stage.

5.1.2. TEST NO. 2 ($\Delta P = 600\text{MMH}_2\text{O}$)

In **Table 5** the left side of the sample represents the centre of the sample, whereas the right side represents the outer side of the sample in contact with the graphite sample holder. The percentage material (phases 3 and 5) in a liquid form increased slightly to 7.4 per cent (molar basis) (**Figure 29a/Table 6**). **Figure 24a** indicates the microstructure of the residual material on the right hand side next to the crucible. It consists of cementite, pearlite and ferrite. **Figure 24b** is the microstructure of the material at the top in contact with coke particles. It has a ferritic structure with pearlite pockets.

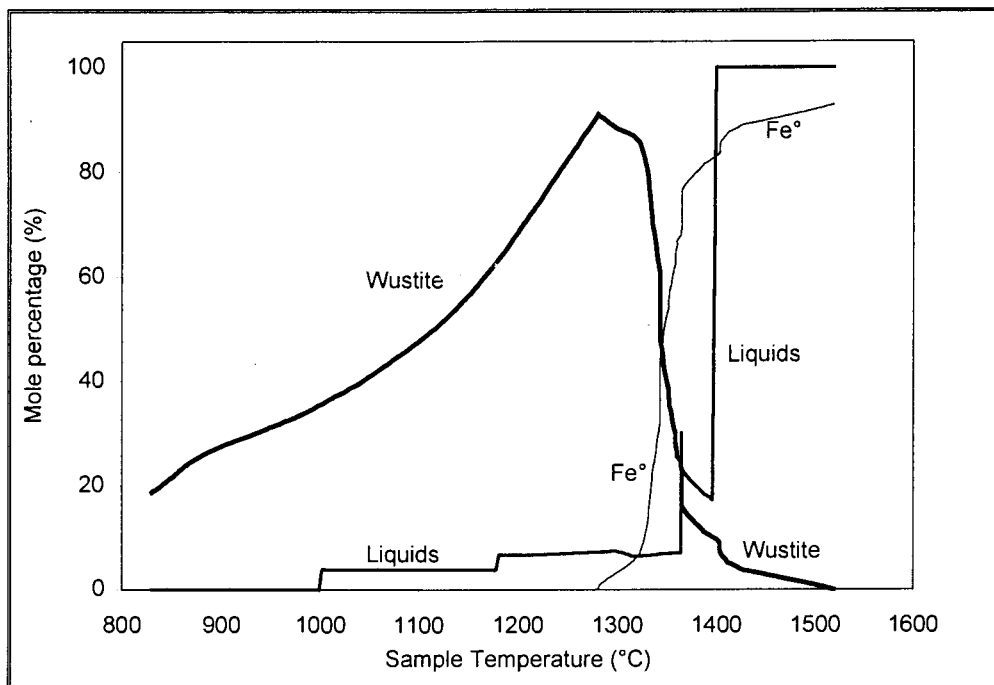


Figure 29a: Calculated percentages of liquid in the sample, together with distribution of iron between oxide and metal during the course of reduction. The amount of liquid shows step increases at 980°C, where the alkali-rich phase is assumed to melt, 1180°C (fayalite melts) , 1360°C (wustite melts), and 1400°C (remaining oxides melt to form slag; metallic iron product – cast iron – melts)

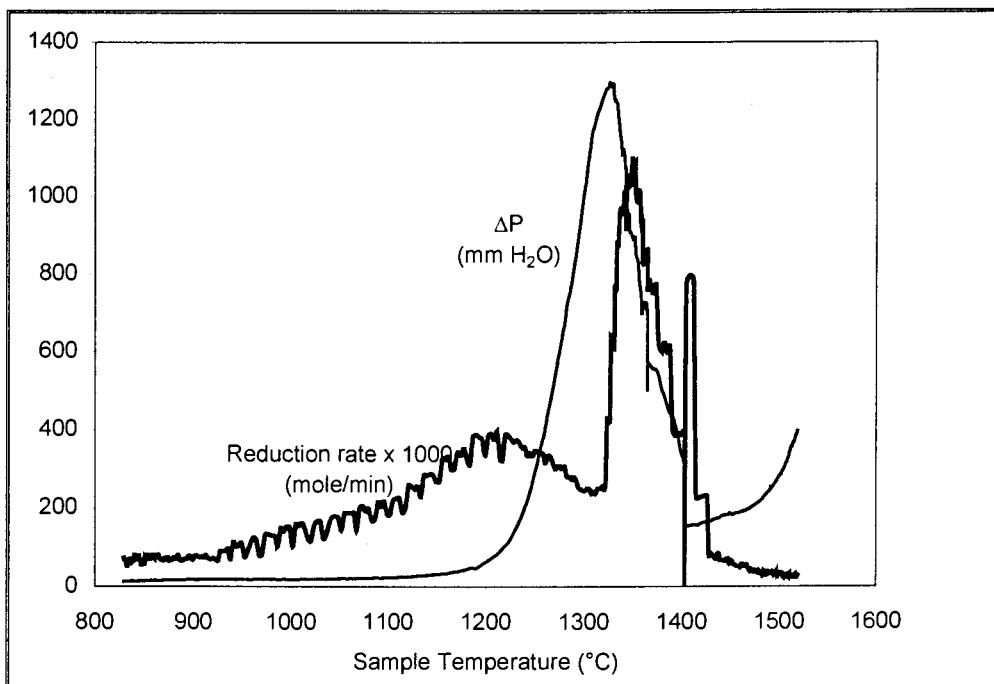


Figure 29b: Differential pressure and rate of reduction vs temperature.

Figure 24c is the microstructure of the residual material in the middle of the sample. It consists of iron with very little carbon absorption. Comparing **Figures 24 a & b**, which are the microstructures of the material next to the graphite crucible and a coke particle respectively, it is clear that carbon is absorbed easier from the graphite than the coke (indicated by the higher pearlite content in the former case).

5.1.3. TEST NO 3: (ΔP MAX REACHED - MATERIAL STARTS FLOWING)

In **Table 5** the left side of the sample represents the centre of the sample, whereas the right side represents the outer side of the sample in contact with the graphite sample holder. According to **Figure 29a** the percentage of liquid present between 1299°C and nearly 1315°C is constant. Despite this, a substantial increase in the pressure drop is observed over this interval – at 1315°C the maximum pressure drop is reached (**Figure 29b**). **Figure 25a** indicates the pearlitic structure that formed at the bottom left hand side of the sample. The different forms in which iron occurs, namely, Fe and FeO, in the middle of the sample are indicated in **Figure 25b**. **Figures 25c & d** show the microstructure of the material just away from the crucible, with the transition in microstructure from the side to the middle, regarding the amounts of ferrite and pearlite. **Figure 25e** indicates cementite lamellae. Due to the high pressure difference over the sample bed in the furnace material is pushed upwards into the top coke layer. **Figure 25f** gives an indication of the microstructure of this material, which consists of cementite and pearlite.

The increase in the occurrence of pearlite from tests 1 to 3 indicates the influence of temperature on the equilibrium and kinetics of carbon uptake in the iron.

5.1.4. TEST NO 4: (COMPLETE TEST)

Figure 29a indicates a small decrease in the percentage of liquid phase between 1315°C and 1369°C, primarily caused by FeO being reduced from the two liquid phases to metallic iron. At 1369°C the remaining wustite melts, which explains the sudden rise in the calculated amount of liquid. The liquid again decreases as the wustite is reduced to metallic iron (which is solid at these temperatures). The final melting point, as determined with the REAS apparatus (based on observed dripping) was 1392°C. **Figure 30** indicates these additional test results for the full test.

The layered appearance of the cast iron which dripped from the sample (**Figures 14 and 26**) suggest that separate incidents of dripping occur, rather than a continuous process. The transition from one layer of cast iron to the next is sudden with definite carbon contents on either side (e.g. **Figure 26b,c**). The sharp increase in the carbon content indicates longer retention of the molten iron in the coke layer. It should be noted that although layer 1 drips onto the graphite drip holder, it contains less carbon than layers 3,4, a, I, t1, t2, x, y & z – indicating that the observed carbon contents do correspond to that during dripping rather than reflecting contamination by the graphite drip pad. The isolated dripping incidents are also visible on the plot of drip mass (**Figure 30**) which displays a series of steps in the drip mass.

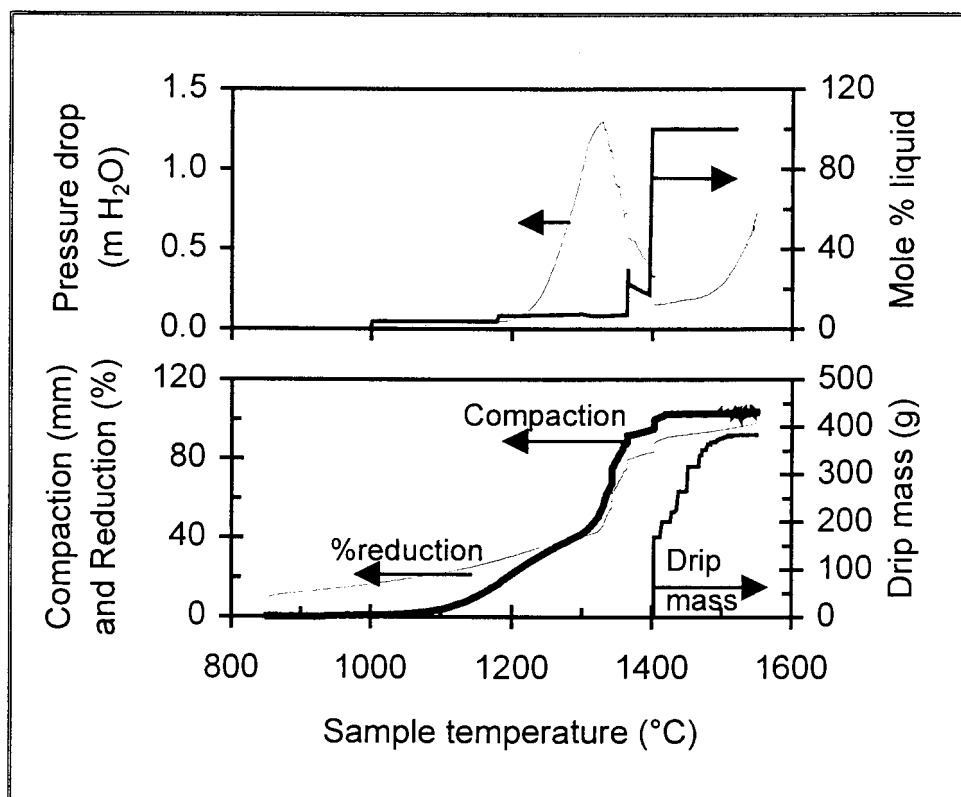


Figure 30: Results of REAS test #4.

Of the 5 phases that are present at 1200°C, the liquid with fayalite composition (phase3) as well as the alkali rich liquid phase (phase 5) are in a liquid state. It appears that liquid formation around 1200°C is associated with the first increase in the pressure drop. However, in contrast with the literature results, it does not appear (**Figure 30**) that the subsequent changes in the pressure drop are caused by changes in the amount of liquid present – well past the peak pressure the amount of liquid is calculated to remain unchanged. The pressure increase rather seems to be associated with substantial compaction of the sample, probably because of elimination of voids.

The subsequent decrease in the pressure drop is probably caused by the lowered viscosity of the slag phase at increased temperatures: the viscosity of ‘pure’ fayalite-

based liquid ($\text{FeO}/\text{SiO}_2 = 65/35$) varies from 3-5 poise between 1150-1200°C (**Figure 31 & 32**). Above 1200°C the viscosity lowers gradually to less than 2 poise by the time 1300°C is reached. The increase in the amount of carbon in the metallic phase (as evidenced by the drip sample of test 4) simultaneously lowers the melting point of the cast iron. Both of these factors probably favour the decrease in pressure.

In addition, above ca. 1370°C the amount of liquid decreases due to the reduction of FeO, which may also contribute to the lowered pressure drop. However, this effect can be of only secondary importance, since it is found well past the peak in the pressure drop (**Figure 30**). Similarly, removal of liquid from the sample by "dripping" should also contribute to the pressure decrease. However, **Figure 30** shows that this can only be responsible for the last decrease in the pressure when the sample reaches 1400°C (and dripping occurs) – again well past the peak in the pressure curve.

According to **Figure 33**, the melting point of the alkali-rich liquid could be as low as 900°C (in line with the literature observations). Hence the alkalis favour early liquid formation. However, the observation that the pressure drop only increases once the sample temperature reaches 1200°C (**Figure 30**) indicates that in this case the alkalis have a limited effect on the gas permeability of the furnace charge.

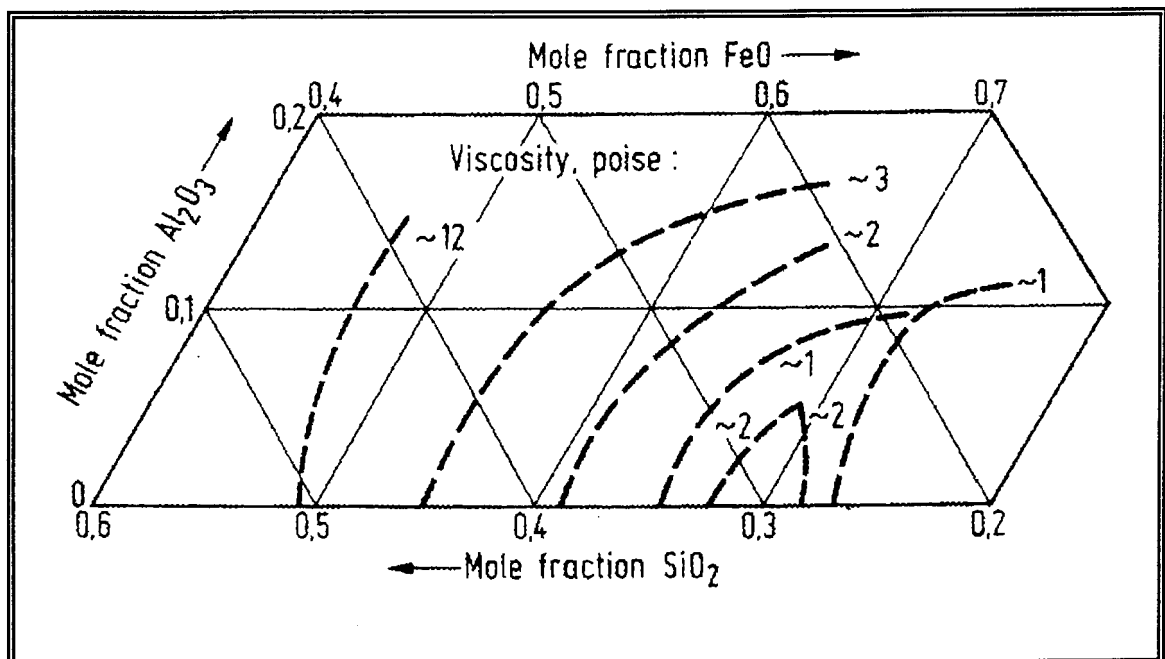


Figure 31: Viscosity of $\text{FeO}/\text{SiO}_2/\text{Al}_2\text{O}_3$ slag at 1250°C.¹⁸

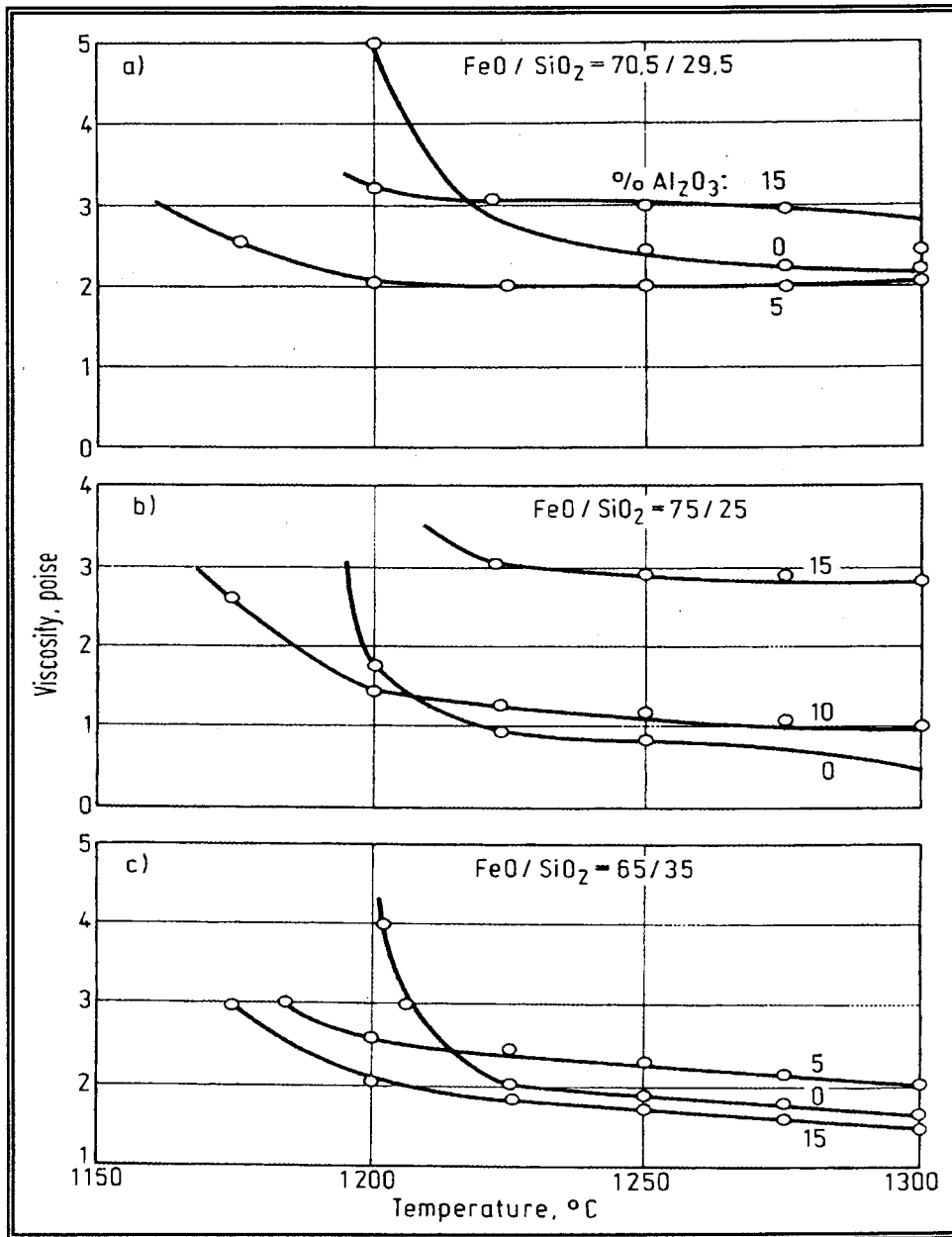


Figure 32: Viscosity of FeO/SiO₂ slags at various temperatures.¹⁸

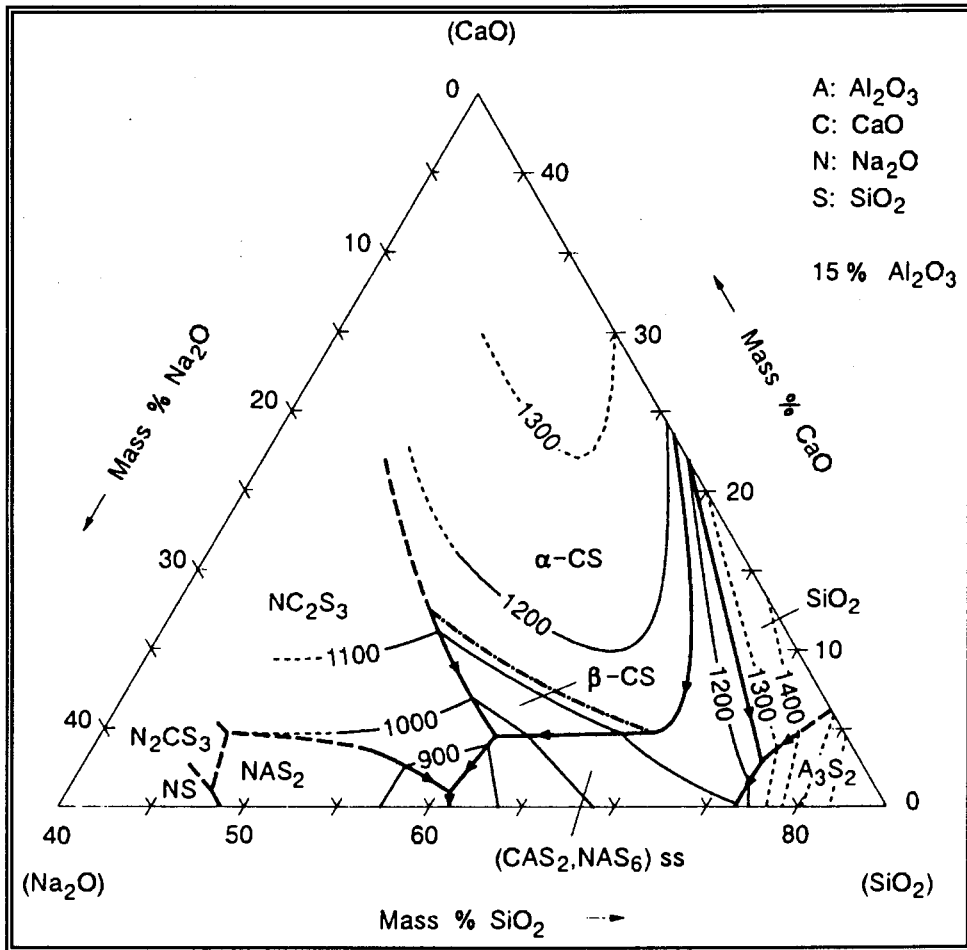


Figure 33: CaO-SiO₂-Na₂O phase diagram with 15% Al₂O₃¹⁹

5.2. EVALUATION OF HEAT TRANSFER DURING THE TEST

Figure 34 shows the calculated rate of radiative heat transfer to the sample together with the rate of enthalpy change of the sample. It should be noted that the change in sample height was considered in the radiation calculations (i.e. as the sample is compacted, the rate of heat transfer reduces). While the two calculations agree fairly well at lower temperatures (the lack of agreement may well be due to differences between the actual and assumed emissivities), the two calculations diverge substantially above 1200°C. Beyond this point the calculated rate of one-dimensional heat transfer by radiation decreases strongly because the sample height is substantially smaller (see **Figure 30**); however, from this point the assumption of simple one-dimensional (i.e. all radial and no axial) heat transfer is much less valid, specifically because of the smaller sample height. For this reason, the sample energy balance (indicated by "enthalpy change" in **Figure 34**) was used in subsequent comparisons between heat flow and temperature arrests.

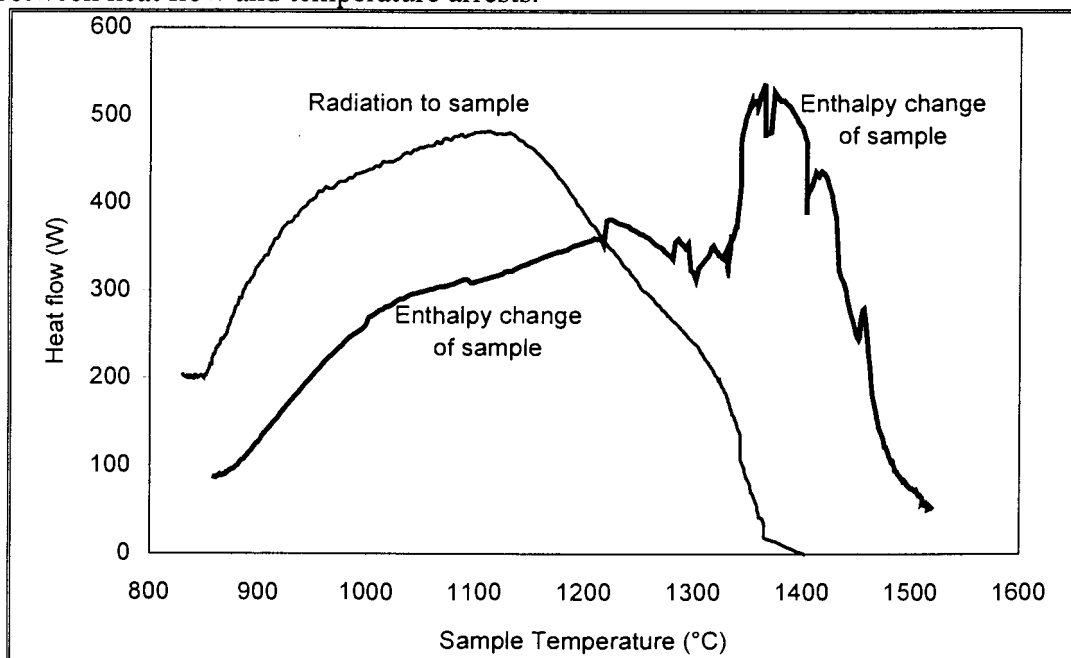


Figure 34: Calculated rate of radiative heat transfer to the sample, compared with the calculated rate of change of the sample enthalpy.

The purpose of the energy balance is to determine the origin of the temperature arrests during the test, to determine whether these arrests can give some information on the nature of the reactions in the sample. As **Figure 34** indicates, one broad endothermic peak is centred on 1200°C, a second around 1360°C, and a third around 1400°C. The peak around 1200°C appears to be largely associated with latent heat requirements in the sample (e.g. melting of fayalite). If this is indeed the case, the arrest at this temperature should coincide with the increase in pressure drop across the sample bed (since liquid formation is thought to be responsible for the sharp increase in pressure drop). This suggestion is tested in **Figure 35**, which compares the rate of heating (differential of the sample temperature - time curve) with the pressure drop, for quite

different types of samples. It is apparent that the heating rate decreases significantly (i.e. a temperature arrest occurs) as soon as the differential pressure rises, both for the ore currently used at Iscor Vanderbijlpark (**Figure 35a**) and for sinter manufactured from a possible alternative ("calcitic") hematite ore (**Figure 35b & c**).

The only endothermic reaction occurring during the reduction process is the Boudouard (carbon gasification) reaction. Hence sharp increases in the rate of carbon gasification may also give rise to temperature arrests. The rate of carbon gasification does vary significantly during the test: the calculated rates of the reduction and carbon gasification reactions are given in **Figure 36**. These are based on the gas analyses as given in **Appendix 2**. According to this figure, the rate of reduction outstrips carbon gasification in the early stages of the process – where the sample temperature is low. In line with the high activation energy of the Boudouard reaction, the difference between the two reaction rates diminishes at the higher temperatures. The importance of the Boudouard reaction for the observed temperature changes is illustrated by **Figure 37**, which shows a larger energy requirement around ca. 1360° to coincide with a higher rate of carbon gasification. This net endothermic effect does coincide with a strong temperature arrest, which means that this temperature arrest gives some indication of the rate of reduction (which corresponds to the rate of the Boudouard reaction – **Figure 36**) of molten wustite, and of FeO from the fayalite-based liquid.

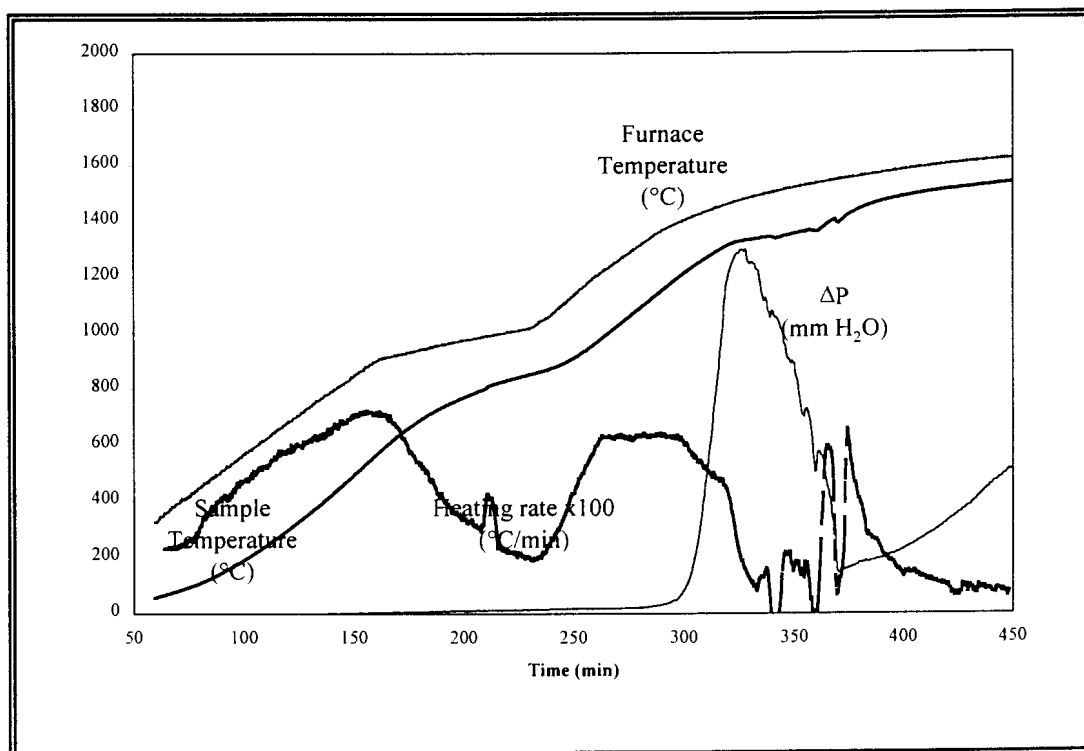


Figure 35a: Heating rate of the Vanderbijlpark ore. Note the significant decrease in heating rate associated with the increase in differential pressure.

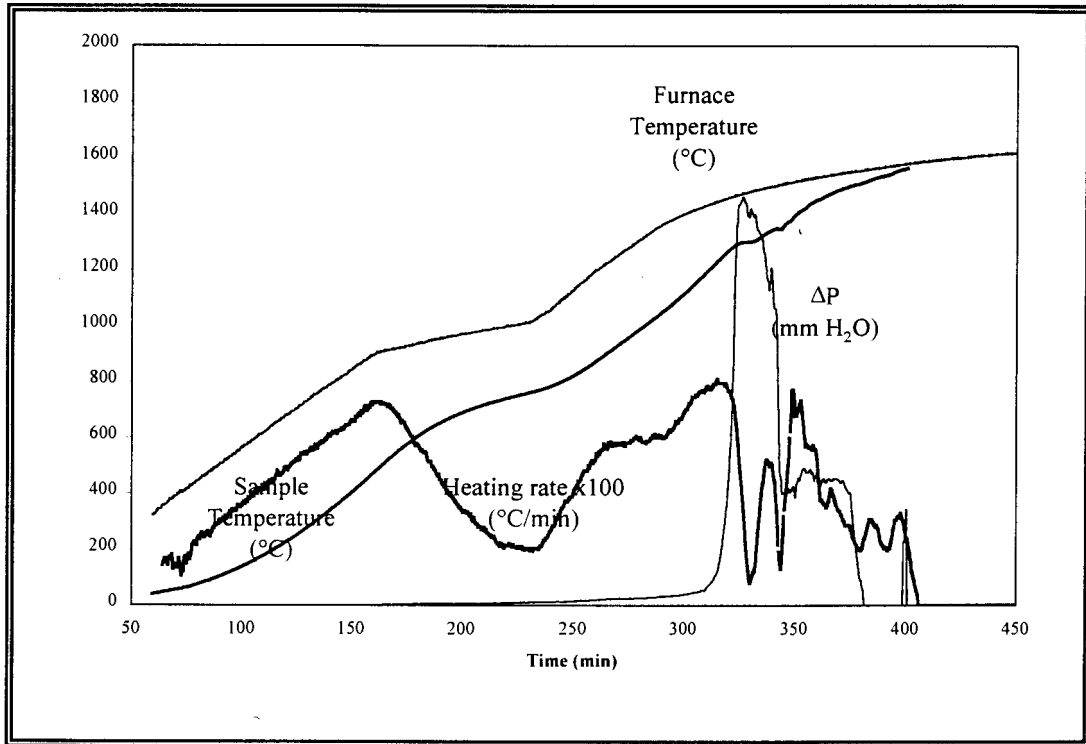


Figure 35b: Heating rate of calcitic ore sinter1. The same decrease in heating rate is noticeable as in Figure35a.

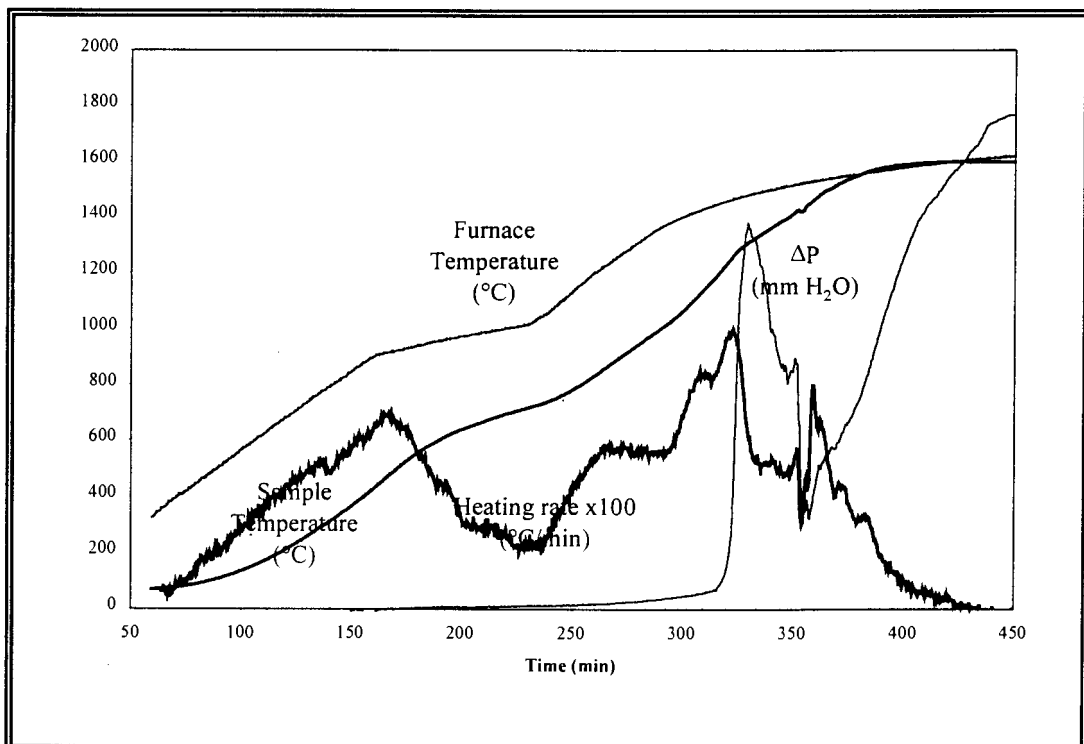


Figure 35c: Heating rate of calcitic ore sinter2. The same decrease in heating rate is noticeable as in Figure35a.

The subsequent increase in heat requirement (around 1400°C) appears to be related to latent heat requirements (melting of the cast iron product and the slag) rather than any specific chemical reactions.

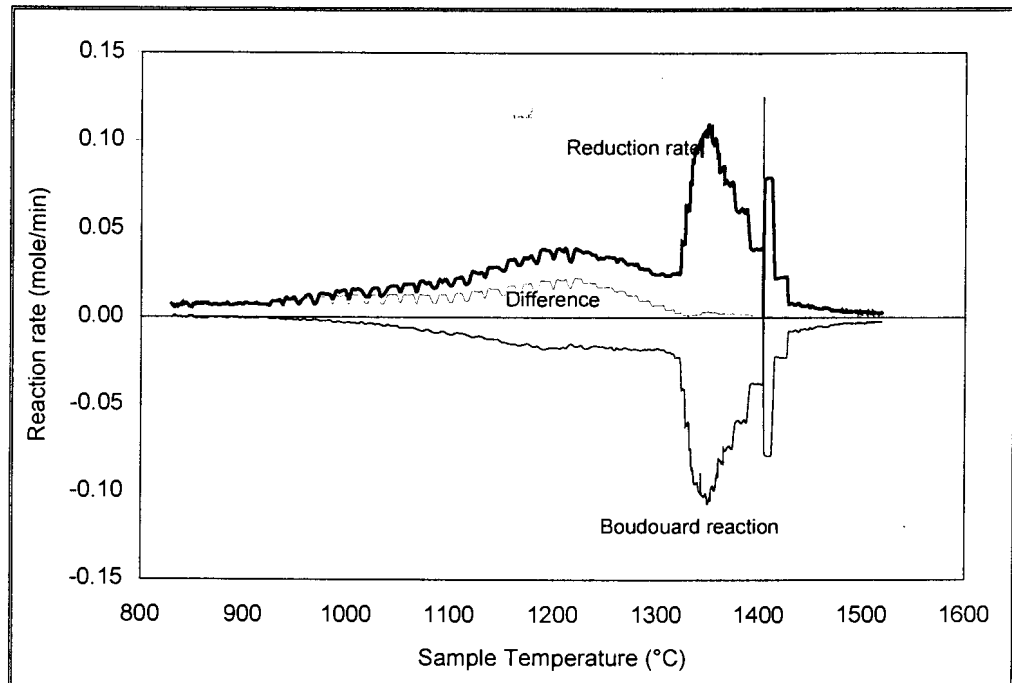


Figure 36: Relationship between the reduction rate and rate of carbon gasification (Boudouard reaction).

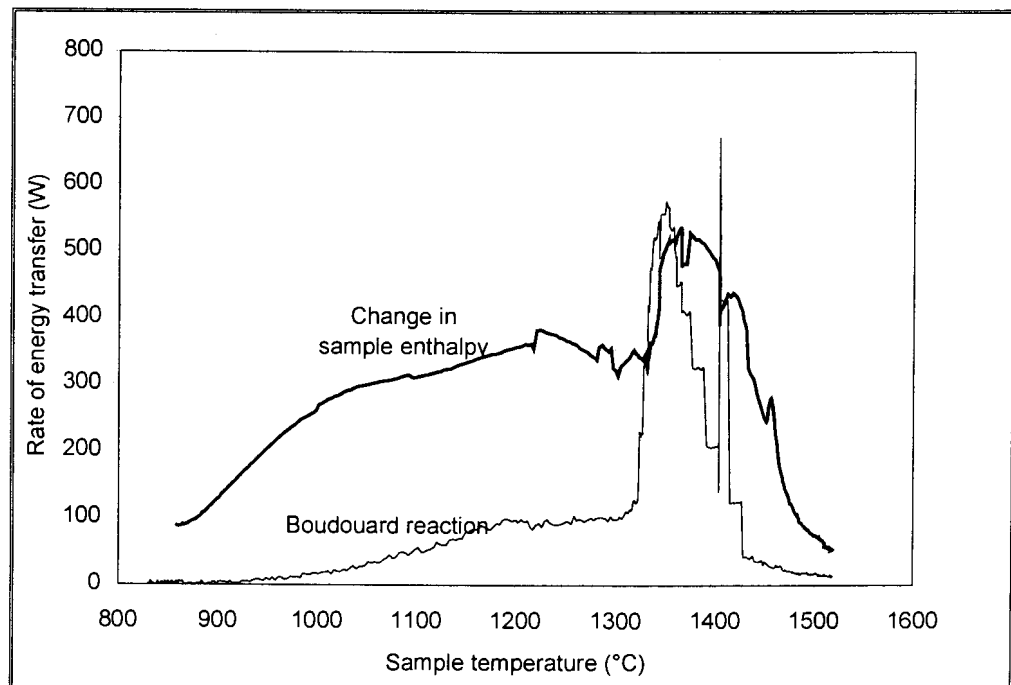


Figure 37: Net energy requirement of sample (from energy balance), compared with the energy requirement of the carbon gasification (Boudouard) reaction.

6. CONCLUSION

By using the REAS apparatus – a high temperature reduction vessel that simulates the blast furnace process from stockline to melting - the high temperature properties of burden materials have been investigated. The REAS process not only provides an insight into the reactions occurring during the softening and melting process but also a range of indices with which to judge the blast furnace performance.

The REAS is loaded with blast furnace burden material, i.e. sinter, pellets and iron ore, between two layers of coke/graphite. The sample is heated for approximately eight hours from room temperature to 1600°C.

During the reduction of the iron ore, mainly five phases are present. Above 1200°C two liquid phases, an alkali rich phase and a liquid phase with a fayalite composition are present. The rest of the iron reports at different stages in various forms of metallic iron and wustite. Small amounts of a high melting slag phase, hercynite, also occurs.

Softening of the sample is said to occur when the ΔP over the sample bed increases by more than 200 mm H₂O. For the specific tests evaluated, this occurred at 1200°C. At this temperature, the liquid with a fayalite composition as well as the alkali rich liquid are present. The formation of the low melting fayalite phase with a high viscosity appears to cause the sudden rise in ΔP . A temperature arrest occurs at the same time supporting the suggestion that liquid formation is responsible for the pressure increase.

The results indicate that the mechanisms responsible for the observed pressure drop (decreased gas permeability) and dripping may well be different from those given in the literature (as discussed in §3.4). The literature mechanisms emphasise the importance of the amount of FeO available to act as flux for the silica which is present as gangue; hence a greater degree of (indirect) reduction below the melting point of fayalite gives poorer fluxing of silica since less FeO is available. However, the charge materials considered in this study appear to be of substantially higher grade than those used in the previous work. For this reason, there does not appear to be any shortage of FeO to act as flux (see, for example, **Figures 21&22**, which show that most of the FeO remains unbound at the melting point of fayalite; there is more than enough FeO to flux the silica). This abundance of FeO, and the observation that the peak in pressure drop is not associated with any great change in the amount of liquid (**Figure 30**), together imply that the literature mechanism regarding changes in the amount and composition of the liquid (i.e. becoming more SiO₂-rich and viscous as the FeO is reduced) cannot explain the pressure fluctuations observed here. Rather, the increase in pressure appears to be a joint effect of liquid being present (giving the first increase in pressure) and compaction of the sample; **Figure 30** shows the pressure increase curve to parallel the compaction curve. Loss of voidage in the sample by this substantial amount of compaction (which is quite apparent in the macrographs shown in **Figures 11-13**) appears the

likely cause of the pressure increase. The subsequent decrease in the pressure drop is probably associated with lower viscosity as the sample temperature increases.

The importance of compaction means that the amount of indirect reduction does play a role in the development of the pressure drop, but not for the reasons cited in the literature. Pure iron is more malleable than the oxides, and reduction gives a porous iron structure which is more easily compacted. For both these reasons, the metallic product of indirect reduction favours compaction (and hence the pressure increase). This is again apparent from **Figure 30**, revealing the shape of the compaction curve to be very similar to the curve which shows the degree of reduction of the sample. The sharp increase in reduction rate close to the peak pressure (**Figure 29b**) presumably results from better contact between the remaining iron oxide (in the fayalite-based liquid, and wustite) with the coke reductant, so favouring direct reduction; this increased reduction (endothermic because of the Boudouard reaction) results in one of the noticeable temperature arrests on the sample temperature curve.

The correspondence between the temperature arrests and the changes within the sample does imply that these arrests can be used to gain some information on the reduction mechanisms. However, the reliability of the temperature arrests as indicators of the state of the sample and the reaction conditions within the sample must be tested by further work.

8. REFERENCES

1. YAMAOKA, Y; HOTTA, H; KAJIKAWA, S.; **Testing method of high temperature properties of blast furnace burdens**, *Transactions ISIJ*, Vol. 22, 1982, pp. 164-171
2. BISWAS, AK.; **Principles of blast furnace ironmaking**, *Cootha Publishing House*, Australia, pp1-13, 54.
3. COUDURIER, L; HOPKINS, DW., WILKOMIRSKY, I; **Fundamentals of metallurgical processes**, *Pergamon Press*, pp. 246-250
4. OJA, KG.; **Melting studies of blast furnace burdens**, *Skilling's Mining Review*, Sept. 25, 1993, pp.4-14
5. OMORI, Y.; **Testing methods for the softening under load and meltdown properties and continuous test method for the behaviour of iron ore**, *Research Institute of Mineral Dressing and Metallurgy*, Tokyo University, Katahire, Sendai, Japan. (Not published in open literature.)
6. RELF, R.; **Temperature programmed softening test for blast furnace iron bearing burden materials**, *Welsh Laboratories*, British Steel Corp, 1980
7. BERGSTRAND, R.C.; FRAY, T.A.T.; **The high temperature reduction, softening and melting properties of ferrous burden materials in the laboratory, with particular reference to hydrocarbon injection at the tuyeres**, *Second European Ironmaking Congress*, Glasgow, 1991
8. CLIXBY, G.; **Simulated blast furnace reduction of acid pellets in temperature range 950°C-1350°C**, *Ironmaking and Steelmaking*, Vol. 2, 1980, pp. 68-75
9. CLIXBY, G; PARRAT, J.E.; **An alternative view in sinter properties for stable and efficient blast furnace operation**, *Ironmaking Conference Proceedings*, 1989, pp. 459-469
10. Yamaoka, Y., Hotta, H., Takasaki, Y., Ohzeki, S.; **On the high temperature properties of blast furnace burdens**; *Australia Japan Extractive Metallurgy Symposium*, Sydney, Australia, 1980; pp1-12



11. Hotta, H., Yamaoka, Y.; **Softening and melting behaviour of sinter and pellets**, *Transactions ISIJ*, Vol 25, 1985, pp294-301
12. Hsieh, L., Liu, K.; **The high temperature softening and melting properties of blast furnace ferrous burdens**, *China Steel Technical Report*, No. 6, 1992, pp. 88-95
13. Busby, N.J., Fray, T.A.T., Goldring, D.C.; **Nature of cohesive zone in blast furnace**, *Ironmaking and Steelmaking*, Vol 21, no.3, 1994, pp229-236
14. Clixby, G.; **Influence of softening and melting properties of burden materials on blast furnace operation**, *Ironmaking and Steelmaking*, Vol 13, no. 4, 1986, pp. 169-175
15. CHAIGNEAU, R., SPORTEL, H., TROUW, J., VOS, R., DROOG, J.; **Blast furnace burden quality: laboratory simulation**, *Ironmaking and Steelmaking*, Vol 24, 1997, pp. 461-467
16. TURKDOGAN, E.T.; **Physicochemical properties of molten slags and glasses**; *The metal society of London*; 1983, pp. 128-140.
17. GUY, A.G., HREN, J.J.; **Elements of physical metallurgy**; 3rd edition, *Addison-Wesley Publishing Company*; p.333.
18. Verein Deutscher Eisenhüttenleute (eds.) *Slag Atlas*, 2nd edition (1995). Verlag Stahleisen, pp 164 & 204.



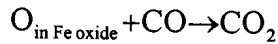
APPENDIX 1

DERIVATION OF THE WORKING EQUATION FOR REDUCTION RATE



The calculations are based on a continuous oxygen balance by analysing and comparing the composition of inlet and outlet reducing gases.

The reaction taking place in the high temperature zone can be described by



The reduction rate can be calculated from the following relationship

$$\left(\frac{dR}{dt}\right)_{\%/\text{min}} = \frac{\Delta O}{[O]_0} \times 100$$

Where: ΔO Oxygen removed, (g/min)

$[O]_0$ Original amount of oxygen bound to Fe in sample (g)

This can be expressed by:

$$\left(\frac{dR}{dt}\right)_{\%/\text{min}} = \left(\frac{\sum O_{\text{out}} - \sum O_{\text{in}}}{[O]_0}\right) \times 100$$

where $\sum O_{\text{out}}$ oxygen in the outgoing gas, (g/min)

$\sum O_{\text{in}}$ oxygen in the incoming gas, (g/min)

This can be expressed in terms of the gas analysis

$$\left(\frac{dR}{dt}\right)_{\%/\text{min}} = \left(\frac{(\% \text{CO} + 2\% \text{CO}_2)_{\text{out}} * (\% \text{N}_2)_{\text{in}} / (\% \text{N}_2)_{\text{out}} - (\% \text{CO} + 2\% \text{CO}_2)_{\text{in}}}{[O]_0}\right) \times k$$

where k is a factor converting the gas flow, (l/hr), to oxygen mass flow, (g/min). For a gas flow of 1800 l/hr measured at 20°C and 1 atm pressure

$$k = \left(\frac{1800 \times 16}{60 \times 22.41}\right) \times \left(\frac{273.16}{293.16}\right) = 19.96$$

where 16 is the atomic mass of oxygen

22.4 is the molar volume at NTP

Substituting for k and rearranging

$$\left(\frac{dR}{dt}\right)_{\%/\text{min}} = \left(\frac{(\% \text{CO} + 2\% \text{CO}_2)_{\text{out}} * (\% \text{N}_2)_{\text{in}} / (\% \text{N}_2)_{\text{out}} - (\% \text{CO} + 2\% \text{CO}_2)_{\text{in}}}{[O]_0}\right) \times 19.96$$



DETERMINATION OF THE COKE CONSUMPTION DURING THE TEST



The determination of the carbon loss is based on the same principles as the working equation for the reduction rate. The k factor is changed accordingly to determine C instead of oxygen.

$$k = \left(\frac{1800 \times 12}{60 \times 22.41} \right) \times \left(\frac{273.16}{293.16} \right) = 14.97$$

The carbon loss is then determined with the following equation:

$$\left(\frac{dM_{\text{carbon}}}{dt} \right)_{\text{g/min}} = \left(\frac{(\%CO + \%CO_2)_{\text{out}} * (\%N_2)_{\text{in}} / (\%N_2)_{\text{out}} - (\%CO + \%CO_2)_{\text{int}}}{100} \right) \times 14.97$$



APPENDIX 2

REAS TEST RESULTS – TEST 4



Time	FT	ST	dP	dH	CO in	CO2 in	CO out	CO2 out	k	Total Reduction	Drip mas
0.0002	498.2	24.1925	0	0	0.1465	0.1538	0.9524	0.8278	19.95776	0.100620329	0
1.0012	491.362	24.084	-34.048	0	0.1319	0.1538	0	0.044	19.95776	0.100620329	0
1.5077	487.731	24.2853	-33.059	0	0.1319	0.1099	0.0147	0.0366	19.95776	0.100620329	0
2.001	483.149	24.3045	-33.938	0	0.0733	0.0879	0.044	0.0733	19.95776	0.100620329	0
2.5076	480.815	24.3038	-34.268	0	0	0	0	0.0366	19.95776	0.104039897	0
3.0006	478.283	24.2309	-33.865	0	0.0147	0	0	0.0586	19.95776	0.108828227	0
3.5069	475.39	23.7711	-34.982	0	0	0	0.0586	0.0879	19.95776	0.11977832	0
4.0069	471.521	23.9371	-35.696	0	0	0	0	0.0293	19.95776	0.122515843	0
4.5002	468.798	23.9922	-33.627	0.0839	0	0	0.0293	0.022	19.95776	0.125940083	0
5	466.453	23.7345	-33.663	0.1053	0	0	0	0.0659	19.95776	0.132097174	0
5.5067	463.435	24.1179	-35.019	-0.0176	0	0.0147	0.0147	0.022	19.95776	0.133465936	0
6.0065	460.775	23.7532	-35.806	0.013	0	0	0	0.022	19.95776	0.135521414	0
6.5064	457.786	24.2107	-35.183	0.0984	0.0586	0.0147	0	0.0293	19.95776	0.135521414	0
7.0063	455.307	23.6245	-34.103	0.1198	0.044	0.044	0.0733	0.0073	19.95776	0.135521414	0
7.5064	453.617	23.9738	-35.605	0.0443	0	0	0	0.044	19.95776	0.139632371	0
8.0128	450.611	23.7006	-34.579	0.0099	0	0	0	0.044	19.95776	0.143743327	0
8.5062	448.863	24.1761	-34.78	0.0977	0	0	0	0.0293	19.95776	0.14648085	0
9.0059	447.182	23.7156	-36.465	0.0076	0	0	0	0.0147	19.95776	0.147854283	0
9.5059	445.011	23.4599	-35.165	0.0572	0	0	0	0.0073	19.95776	0.148536328	0
10.0065	442.243	23.6262	-36.392	0.042	0	0	0	0.0293	19.95776	0.151273852	0
10.5123	440.384	23.4414	-35.293	-0.0221	0	0	0	0	19.95776	0.151273852	0
11.0122	437.882	23.6083	-34.671	0.0382	0.0293	0	0	0.0513	19.95776	0.154698091	0
11.5055	436.663	22.8004	-35.312	0.0351	0	0	0	0.0073	19.95776	0.155380136	0
12.0121	435.412	23.1111	-33.627	0.074	0.0147	0.0073	0.0147	0.0293	19.95776	0.157435615	0
12.5055	431.731	23.3873	-33.48	0.0282	0	0.022	0	0	19.95776	0.157435615	0
13.006	430.337	23.4057	-35.641	0.0542	0	0	0	0	19.95776	0.157435615	0
13.5053	427.825	23.8072	-35.367	-0.0534	0	0	0	0	19.95776	0.157435615	0
14.0051	426.722	23.131	-35.44	0.0443	0	0	0	0.0366	19.95776	0.160855183	0
14.5049	424.384	23.403	-35.861	0.0244	0	0	0	0	19.95776	0.160855183	0
15.0117	423.798	23.3488	-34.121	0.0527	0.0293	0.0147	0.0147	0.022	19.95776	0.160855183	0
15.5114	421.283	22.8908	-35.715	0.0717	0	0	0	0.0147	19.95776	0.162228616	0
16.0047	418.753	23.1474	-34.707	-0.0107	0	0	0	0	19.95776	0.162228616	0
16.5046	417.658	23.387	-34.945	0.0069	0	0	0	0.022	19.95776	0.164284094	0
17.0045	415.244	23.2398	-35.586	0.0153	0	0	0.0879	0.0513	19.95776	0.17318338	0
17.5052	413.83	23.791	-35.257	-0.074	0	0	0	0	19.95776	0.17318338	0
18.0045	412.037	22.9845	-35.421	0.0336	0	0	0.0293	0.0147	19.95776	0.175925575	0
18.5044	411.024	22.6901	-36.117	0.0137	0	0	0	0	19.95776	0.175925575	0
19.0041	409.939	23.5877	-34.854	0.0023	0.0293	0.0147	0.0147	0.0147	19.95776	0.175925575	0
19.5107	407.672	22.7793	-35.11	-0.0618	0	0	0	0	19.95776	0.175925575	0
20.0107	406.94	23.479	-34.982	0.0786	0	0.0147	0	0.0073	19.95776	0.175925575	0
20.5106	404.447	24.1178	-35.586	-0.0351	0	0	0	0	19.95776	0.175925575	0
21.0039	402.6	22.8374	-35.476	-0.058	0	0	0.0293	0.022	19.95776	0.179349815	0
21.504	402.649	22.984	-35.403	-0.0092	0.0147	0.0147	0.044	0.022	19.95776	0.181400622	0
22.0037	401.464	23.2229	-32.931	-0.0466	0	0	0.0147	0	19.95776	0.182087338	0
22.5102	400.046	23.389	-35.11	0.0137	0.0586	0.022	0	0	19.95776	0.182087338	0
23.0042	398.731	23.7359	-35.074	-0.0267	0	0	0	0	19.95776	0.182087338	0
23.5101	397.548	23.1272	-35.678	-0.0412	0	0.0147	0	0	19.95776	0.182087338	0
24.004	394.868	23.9557	-33.517	-0.0427	0	0	0.0147	0.0073	19.95776	0.1834561	0
24.5098	393.302	23.754	-35.183	0.0069	0	0	0	0.0073	19.95776	0.184138145	0
25.0033	391.795	23.075	-35.733	-0.0458	0	0	0	0.0073	19.95776	0.18482019	0
25.503	391.427	24.1387	-34.158	-0.0397	0.0293	0.0073	0.0147	0.022	19.95776	0.185511578	0
26.003	390.381	24.2302	-33.682	0.0229	0.0293	0.0073	0.0147	0.022	19.95776	0.186202966	0
26.5095	389.276	24.6337	-34.854	0.0443	0	0	0	0.022	19.95776	0.188258444	0
27.0027	387.792	23.643	-36.374	-0.1473	0	0	0	0	19.95776	0.188258444	0
27.5027	386.782	24.3769	-33.865	-0.0756	0.0293	0	0.0147	0.022	19.95776	0.189631878	0
28.0025	384.867	24.615	-35.165	-0.1206	0	0	0.0293	0.0366	19.95776	0.194420207	0
28.5091	383.868	24.4492	-35.165	-0.0717	0.0147	0.0147	0.0147	0.022	19.95776	0.195102252	0
29.0092	382.116	24.7618	-35.898	-0.045	0	0	0.0293	0	19.95776	0.196471014	0
29.5091	381.02	24.9254	-34.268	-0.1648	0	0	0	0.0073	19.95776	0.197153059	0
30.0024	379.673	24.9988	-35.715	-0.0878	0.044	0.0293	0	0.0073	19.95776	0.197153059	0
30.5087	379.566	25.3433	-35.037	-0.0443	0	0	0	0.0073	19.95776	0.197835104	0
31.0086	377.479	25.4895	-35.806	-0.0336	0.0733	0.0366	0	0	19.95776	0.197835104	0
31.5027	375.94	26.2379	-35.238	-0.058	0	0	0	0	19.95776	0.197835104	0
32.0026	374.662	26.0192	-36.484	-0.0061	0.0879	0.022	0	0.0147	19.95776	0.197835104	0
32.5084	374.913	25.7095	-36.246	-0.0504	0.0293	0.022	0	0	19.95776	0.197835104	0
33.0016	372.094	25.8565	-36.099	-0.0771	0	0	0	0	19.95776	0.197835104	0
33.5017	372.965	26.8922	-35.074	-0.0778	0	0.022	0.0293	0.0073	19.95776	0.197835104	0
34.0022	372.869	26.5299	-33.993	-0.0885	0.0293	0.0147	0.0293	0.022	19.95776	0.198517149	0
34.5081	369.188	26.9842	-35.11	0.0557	0	0.0147	0	0	19.95776	0.198517149	0
35.0015	368.097	27.6577	-35.403	-0.0824	0	0	0.0293	0.0293	19.95776	0.202623434	0
35.502	367.405	27.5843	-34.487	-0.0748	0.0147	0	0	0.0147	19.95776	0.203310151	0



Time	FT	ST	dP	dH	CO in	CO2 in	CO out	CO2 out	k	Total Reduction	Drip mas
36.0011	366.288	27.8739	-36.594	-0.103	0	0	0.0147	0.0073	19.95776	0.204678912	0
36.501	365.776	28.7457	-35.66	-0.0114	0	0	0.044	0.0366	19.95776	0.210153959	0
37.0017	363.161	28.5808	-36.374	0.0053	0.0586	0.0073	0	0	19.95776	0.210153959	0
37.5009	363.306	28.2386	-35.312	-0.0282	0	0	0.0586	0.0293	19.95776	0.215629005	0
38.0015	361.53	29.5598	-35.953	-0.1152	0	0	0	0	19.95776	0.215629005	0
38.5073	361.385	28.9971	-36.099	-0.1839	0	0	0	0	19.95776	0.215629005	0
39.0072	360.173	30.1912	-35.165	-0.0519	0	0	0	0.0073	19.95776	0.21631105	0
39.5012	358.984	29.5959	-36.612	-0.0839	0	0	0	0	19.95776	0.21631105	0
40.0012	358.047	31.0048	-36.282	-0.1412	0.0293	0	0	0	19.95776	0.21631105	0
40.507	357.865	30.8241	-35.202	-0.0855	0	0	0.0293	0	19.95776	0.217679812	0
41.0002	355.968	31.5816	-35.476	-0.0382	0	0	0	0	19.95776	0.217679812	0
41.5001	355.016	31.9239	-34.432	-0.013	0.0147	0	0	0	19.95776	0.217679812	0
42.0008	353.814	32.5871	-36.209	-0.0969	0.044	0.0586	0	0	19.95776	0.217679812	0
42.5007	351.632	33.2178	-36.923	0.016	0	0.0147	0.0147	0	19.95776	0.217679812	0
43.0067	352.502	32.3029	-36.502	-0.0412	0.0293	0.0073	0.0147	0.022	19.95776	0.2183712	0
43.5066	350.477	33.5416	-36.41	-0.1091	0	0	0	0	19.95776	0.2183712	0
44.0064	350.694	33.7906	-35.44	-0.0412	0.0586	0.0293	0	0.0073	19.95776	0.2183712	0
44.5063	349.186	33.9729	-35.715	-0.1374	0.0293	0.022	0	0.022	19.95776	0.2183712	0
45.0069	348.799	35.5262	-36.52	-0.0916	0	0	0	0	19.95776	0.2183712	0
45.5002	347.558	35.69	-35.605	-0.0069	0	0	0	0	19.95776	0.2183712	0
46.0061	345.771	36.3488	-36.612	-0.1168	0.0147	0.044	0	0	19.95776	0.2183712	0
46.5067	344.817	36.2225	-36.813	-0.0946	0	0	0	0	19.95776	0.2183712	0
47.006	344.235	37.1253	-37.418	-0.0382	0	0	0.044	0.0366	19.95776	0.223846246	0
47.5058	343.048	37.4184	-36.96	-0.1335	0	0	0	0	19.95776	0.223846246	0
48.0058	341.888	38.6616	-37.638	-0.0923	0	0.0513	0	0	19.95776	0.223846246	0
48.5122	341.671	39.5288	-35.934	0.0046	0	0	0	0	19.95776	0.223846246	0
49.0121	340.594	39.5111	-36.319	-0.1007	0	0	0	0	19.95776	0.223846246	0
49.512	339.143	39.6707	-36.484	-0.0557	0	0	0	0	19.95776	0.223846246	0
50.0053	338.522	41.1919	-34.396	0.0031	0.0147	0.0073	0	0	19.95776	0.223846246	0
50.5053	337.906	42.0714	-36.978	-0.1641	0.0147	0	0.044	0.0293	19.95776	0.227952531	0
51.0052	336.45	42.0917	-37.546	-0.1519	0	0	0	0	19.95776	0.227952531	0
51.5051	336.316	42.6194	-36.594	-0.1404	0.044	0.0147	0	0	19.95776	0.227952531	0
52.0116	333.828	43.6219	-37.363	-0.0977	0	0	0	0	19.95776	0.227952531	0
52.5056	335.031	44.7614	-36.85	-0.1114	0	0	0	0	19.95776	0.227952531	0
53.0114	333.525	44.7787	-36.484	-0.1305	0	0.0073	0	0	19.95776	0.227952531	0
53.5114	334.216	45.4961	-36.154	-0.013	0.0586	0	0.0147	0.022	19.95776	0.227957203	0
54.0113	332.54	46.474	-35.33	-0.1198	0.0147	0	0.0147	0.0147	19.95776	0.229330636	0
54.5121	331.91	47.6423	-34.982	-0.0168	0	0.0147	0	0	19.95776	0.229330636	0
55.011	330.266	48.6668	-36.191	-0.1488	0	0.022	0	0	19.95776	0.229330636	0
55.511	330.426	49.2414	-35.458	-0.0977	0.0147	0	0.0147	0.0073	19.95776	0.230012681	0
56.0042	328.807	50.7123	-35.898	-0.0435	0	0	0	0	19.95776	0.230012681	0
56.5042	329.246	50.7309	-35.806	-0.1381	0	0	0	0	19.95776	0.230012681	0
57.0107	328.624	51.648	-35.824	-0.119	0	0	0	0	19.95776	0.230012681	0
57.5107	327.005	53.0081	-36.704	-0.1458	0	0	0.0147	0.0073	19.95776	0.231381442	0
58.004	326.69	53.4234	-35.641	-0.103	0	0.0073	0.0293	0.0147	19.95776	0.233441592	0
58.5039	325.151	54.8656	-37.326	-0.1954	0.0293	0.0147	0	0	19.95776	0.233441592	0
59.0038	325.518	55.7218	-37.125	-0.0702	0	0	0.0733	0.044	19.95776	0.240976788	0
59.5036	324.482	56.8682	-36.429	-0.1641	0.0147	0.0147	0.0147	0.0147	19.95776	0.240976788	0
60.0101	323.944	58.1827	-35.202	-0.1366	0	0	0.0147	0	19.95776	0.241663505	0
60.5034	325.92	58.9826	-36.356	-0.2091	0	0	0.0147	0	19.95776	0.242350222	0
61.0036	329.853	60.0198	-35.715	-0.1603	0.0147	0.0073	0.0147	0	19.95776	0.242350222	0
61.5033	335.891	61.1221	-35.568	-0.1404	0	0	0	0	19.95776	0.242350222	0
62.0098	342.227	62.3562	-35.605	-0.0611	0.0293	0	0	0	19.95776	0.242350222	0
62.5098	344.357	63.8066	-35.806	-0.1412	0.0147	0.0073	0.0147	0	19.95776	0.242350222	0
63.003	346.204	65.0016	-36.868	-0.1542	0	0	0	0	19.95776	0.242350222	0
63.5098	348.222	66.0744	-35.623	-0.1496	0	0	0	0	19.95776	0.242350222	0
64.0028	355.439	66.8789	-35.421	-0.0145	0	0.0073	0	0	19.95776	0.242350222	0
64.5035	358.045	68.0498	-36.52	-0.0687	0	0	0	0	19.95776	0.242350222	0
65.0027	359.176	69.6833	-35.898	-0.0694	0.0147	0.0147	0	0	19.95776	0.242350222	0
65.5092	362.874	70.6144	-36.667	-0.1534	0.0879	0.0293	0	0	19.95776	0.242350222	0
66.0092	364.72	71.6589	-35.733	-0.0809	0	0	0	0	19.95776	0.242350222	0
66.5032	370.935	72.6523	-36.649	-0.0756	0.0879	0	0.0293	0	19.95776	0.242350222	0
67.0024	372.787	74.124	-36.209	-0.0954	0	0	0.0147	0	19.95776	0.243036938	0
67.5023	380.4	75.3267	-36.081	-0.1068	0.0147	0.0073	0.0147	0.0073	19.95776	0.243036938	0
68.0028	378.792	76.4617	-37.528	-0.0992	0	0	0	0	19.95776	0.243036938	0
68.5086	380.794	77.5275	-35.769	-0.1801	0.0147	0	0.0147	0.0073	19.95776	0.243718983	0
69.0085	385.603	78.7707	-36.282	-0.1206	0	0	0	0	19.95776	0.243718983	0
69.5019	389.822	80.0765	-36.484	-0.1748	0	0	0.0147	0.0073	19.95776	0.245087745	0
70.0084	392.745	81.2827	-36.997	-0.0771	0	0.0147	0	0	19.95776	0.245087745	0
70.5016	393.396	82.3863	-37.326	-0.1694	0	0	0	0	19.95776	0.245087745	0
71.0083	397.534	83.3437	-36.209	-0.1267	0	0.044	0	0	19.95776	0.245087745	0



Time	FT	ST	dP	dH	CO in	CO2 in	CO out	CO2 out	k	Total Reduction	Drip mas
71.5014	400.305	84.6062	-36.539	0.0053	0	0.0073	0	0	19.95776	0.245087745	0
72.0015	408.226	86.2679	-35.824	-0.0466	0.0147	0	0.0147	0	19.95776	0.245087745	0
72.5079	405.735	87.186	-37.088	-0.0679	0.0586	0	0	0	19.95776	0.245087745	0
73.002	405.166	88.8071	-35.66	-0.1267	0.0147	0.0073	0	0.0073	19.95776	0.245087745	0
73.5012	408.109	89.7037	-36.429	-0.0176	0.0293	0.0147	0.0293	0.0073	19.95776	0.245087745	0
74.0077	408.664	91.1914	-36.868	-0.1168	0.0586	0	0.0586	0.0147	19.95776	0.246461178	0
74.5017	413.972	92.0518	-37.802	-0.0351	0	0	0	0	19.95776	0.246461178	0
75.0016	415.916	93.8316	-36.539	-0.174	0	0	0	0	19.95776	0.246461178	0
75.5009	419.213	95.4503	-37.07	-0.1259	0	0	0	0	19.95776	0.246461178	0
76.0073	419.987	96.4327	-37.216	-0.2854	0.0293	0	0	0	19.95776	0.246461178	0
76.5073	428.425	97.7571	-36.099	-0.1381	0	0.0293	0	0	19.95776	0.246461178	0
77.0006	427.192	99.1431	-36.649	-0.0977	0	0	0	0	19.95776	0.246461178	0
77.5011	430.512	100.148	-36.374	-0.1206	0	0	0	0	19.95776	0.246461178	0
78.0004	435.516	101.605	-37.674	-0.0893	0	0.0147	0	0	19.95776	0.246461178	0
78.501	435.423	103.258	-38.242	-0.0992	0.0586	0.0147	0	0	19.95776	0.246461178	0
79.0068	440.77	104.929	-37.821	-0.0664	0	0	0	0	19.95776	0.246461178	0
79.5067	446.913	106.436	-36.649	-0.0534	0.0147	0	0	0	19.95776	0.246461178	0
80.0066	446.739	107.985	-35.696	-0.0122	0.0147	0.0073	0.0147	0.0073	19.95776	0.246461178	0
80.5	446.985	109.915	-36.282	-0.0328	0.0147	0.0073	0	0.0073	19.95776	0.246461178	0
81.0065	451.369	111.9	-36.758	-0.1664	0	0	0	0	19.95776	0.246461178	0
81.5072	455.108	113.296	-36.172	-0.1488	0	0	0.0147	0	19.95776	0.247147894	0
82.0003	461.217	114.873	-36.905	-0.161	0	0	0	0	19.95776	0.247147894	0
82.5061	462.344	117.023	-36.978	-0.1045	0	0	0	0	19.95776	0.247147894	0
83.0061	462.215	118.801	-36.502	-0.1328	0	0	0	0	19.95776	0.247147894	0
83.5067	467.138	120.059	-36.594	-0.0694	0	0.0073	0	0.0073	19.95776	0.247147894	0
84.0059	467.787	122.191	-36.722	-0.0809	0.0293	0.0073	0	0	19.95776	0.247147894	0
84.5058	472.182	123.983	-36.172	-0.0443	0.0293	0	0	0	19.95776	0.247147894	0
85.0058	477.796	126.055	-35.879	-0.0351	0.044	0.022	0	0	19.95776	0.247147894	0
85.5124	481.751	128.075	-35.348	-0.0038	0.0293	0.0147	0.0147	0.0073	19.95776	0.247147894	0
86.0057	480.248	130.325	-35.861	-0.1618	0	0	0.0293	0	19.95776	0.248516656	0
86.5054	485.261	131.56	-36.667	-0.1007	0	0	0	0	19.95776	0.248516656	0
87.0055	485.977	133.799	-35.367	-0.0137	0	0	0	0	19.95776	0.248516656	0
87.5055	492.492	135.29	-35.495	-0.0374	0	0.0147	0	0.0073	19.95776	0.248516656	0
88.0059	492.733	137.545	-36.319	-0.1107	0	0.0073	0	0	19.95776	0.248516656	0
88.5118	494.91	139.921	-35.898	-0.0458	0	0	0	0	19.95776	0.248516656	0
89.0117	496.601	142.014	-34.927	-0.1045	0.0293	0.0073	0.0147	0.0073	19.95776	0.248516656	0
89.5057	502.213	144.01	-36.502	0.0351	0	0.0366	0	0	19.95776	0.248516656	0
90.0116	505.118	146.189	-35.788	-0.1793	0	0	0	0	19.95776	0.248516656	0
90.5047	506.746	148.405	-35.421	-0.0328	0.044	0.0147	0	0	19.95776	0.248516656	0
91.0048	509.408	150.281	-35.568	-0.0549	0	0	0	0	19.95776	0.248516656	0
91.5054	511.333	152.309	-36.301	-0.1549	0	0	0	0	19.95776	0.248516656	0
92.0044	517.572	154.434	-34.689	-0.0901	0	0	0	0	19.95776	0.248516656	0
92.5111	523.685	156.407	-35.055	-0.0656	0.0733	0	0.0147	0.0147	19.95776	0.248516656	0
93.005	520.841	157.961	-34.561	-0.0885	0	0	0.0586	0.0293	19.95776	0.253991703	0
93.5043	523.389	160.123	-34.964	-0.0389	0.0147	0.0073	0	0	19.95776	0.253991703	0
94.0108	525.477	162.915	-35.861	-0.2244	0	0	0	0	19.95776	0.253991703	0
94.5107	531.428	164.37	-34.744	-0.1473	0	0	0.0293	0.0147	19.95776	0.256733897	0
95.0039	533.718	167.483	-33.846	-0.0923	0.0293	0	0.044	0.0147	19.95776	0.258794047	0
95.5038	535.162	169.223	-33.462	-0.0389	0.0147	0.0147	0.0147	0	19.95776	0.258794047	0
96.0039	540.608	171.979	-35.806	-0.0534	0.0586	0.0147	0	0	19.95776	0.258794047	0
96.5037	540.766	174.322	-35.202	-0.0412	0.0147	0.0366	0.0586	0	19.95776	0.258794047	0
97.0036	543.414	176.128	-33.975	-0.0313	0.0293	0.0073	0	0	19.95776	0.258794047	0
97.5037	547.303	178.776	-33.59	-0.0496	0	0	0	0	19.95776	0.258794047	0
98.0036	551.235	181.069	-33.81	-0.0542	0.0147	0.0073	0.0147	0.0147	19.95776	0.259485435	0
98.5101	553.455	183.41	-33.59	0.0557	0.0293	0	0.0586	0.0293	19.95776	0.26359172	0
99.0099	556.451	185.484	-35.385	-0.0847	0	0	0	0	19.95776	0.26359172	0
99.5031	561.105	187.866	-34.048	-0.0916	0	0	0	0	19.95776	0.26359172	0
100.003	565.044	190.583	-34.744	-0.0397	0	0	0	0	19.95776	0.26359172	0
100.503	566.577	192.597	-35.568	-0.1335	0	0	0	0	19.95776	0.26359172	0
101.009	570.048	195.568	-33.132	-0.0183	0	0.0073	0.0147	0.0073	19.95776	0.264278437	0
101.503	572.704	197.975	-33.132	-0.0603	0	0.0073	0	0	19.95776	0.264278437	0
102.002	573.548	199.998	-34.542	-0.158	0	0	0	0	19.95776	0.264278437	0
102.503	578.538	202.661	-34.726	-0.0656	0	0	0	0	19.95776	0.264278437	0
103.009	579.727	204.593	-35.788	-0.0908	0	0	0	0	19.95776	0.264278437	0
103.503	581.803	207.336	-36.282	-0.0466	0	0	0	0.022	19.95776	0.266333915	0
104.009	585.94	209.817	-33.352	-0.042	0	0	0	0	19.95776	0.266333915	0
104.508	589.759	212.677	-33.81	-0.1007	0.0293	0.0147	0	0	19.95776	0.266333915	0
105.002	591.952	214.64	-33.828	-0.0603	0	0	0	0	19.95776	0.266333915	0
105.502	595.192	217.854	-33.755	-0.0466	0.0879	0	0.0147	0.0073	19.95776	0.266333915	0
106.002	597.483	220.189	-34.084	-0.0885	0	0	0	0	19.95776	0.266333915	0
106.501	600.383	222.833	-33.59	-0.0565	0	0.0073	0.0147	0.0073	19.95776	0.267020631	0



Time	FT	ST	dP	dH	CO in	CO2 in	CO out	CO2 out	k	Total Reduction	Drip mas
107.002	602.881	225.169	-33.846	0.0084	0	0	0	0	19.95776	0.267020631	0
107.501	608.448	228.126	-32.747	-0.0939	0.0147	0	0.0147	0.0073	19.95776	0.267702676	0
108.002	609.06	230.384	-34.378	0.0008	0	0	0	0	19.95776	0.267702676	0
108.501	613.217	232.937	-34.671	-0.0824	0	0	0.0147	0	19.95776	0.268389393	0
109.002	613.739	235.833	-34.506	-0.0328	0.044	0	0.0147	0	19.95776	0.268389393	0
109.508	615.66	238.269	-34.011	-0.0404	0	0	0	0	19.95776	0.268389393	0
110.001	619.454	240.713	-34.799	-0.0542	0	0.022	0	0	19.95776	0.268389393	0
110.501	623.508	243.936	-33.425	0.1305	0	0	0	0	19.95776	0.268389393	0
111.007	625.633	246.405	-32.986	0.013	0	0	0	0	19.95776	0.268389393	0
111.501	627.513	248.703	-33.608	-0.0832	0	0	0	0.022	19.95776	0.270444871	0
112.007	632.915	251.52	-33.7	-0.042	0	0.0147	0	0	19.95776	0.270444871	0
112.507	635.011	254.523	-34.176	-0.0427	0.0147	0.0073	0	0	19.95776	0.270444871	0
113	638.276	257.276	-34.121	-0.0343	0	0	0	0	19.95776	0.270444871	0
113.507	641.337	260.163	-33.205	-0.0694	0	0	0	0	19.95776	0.270444871	0
114.007	642.778	263.005	-32.967	-0.0412	0	0	0	0	19.95776	0.270444871	0
114.5	647.12	265.524	-33.041	-0.0992	0	0	0.0147	0.0073	19.95776	0.271813633	0
115	650.743	268.544	-33.553	-0.0061	0	0	0	0	19.95776	0.271813633	0
115.507	653.244	271.343	-33.443	0.0183	0	0	0.0147	0.0073	19.95776	0.273182394	0
116.007	656.245	274.049	-33.077	-0.0656	0	0	0	0	19.95776	0.273182394	0
116.5	658.37	277.087	-33.279	0.0366	0.0293	0	0	0.0147	19.95776	0.273187066	0
117	660.766	280.407	-32.143	-0.0107	0	0	0	0	19.95776	0.273187066	0
117.506	663.64	282.583	-33.498	0.0435	0	0	0	0.0073	19.95776	0.273869111	0
118.006	669.108	285.854	-33.37	-0.0015	0.0147	0	0	0	19.95776	0.273869111	0
118.506	669.349	288.931	-33.004	-0.0679	0	0	0	0	19.95776	0.273869111	0
119.007	671.943	291.356	-33.077	-0.1007	0	0.0147	0	0	19.95776	0.273869111	0
119.513	676.308	294.236	-31.85	0.0412	0	0	0	0	19.95776	0.273869111	0
120.006	681.222	296.987	-32.857	-0.0023	0	0	0	0	19.95776	0.273869111	0
120.506	680.961	300.018	-32.619	-0.0481	0	0.0293	0	0	19.95776	0.273869111	0
121.006	683.469	303.167	-31.997	0.0298	0	0	0.0147	0	19.95776	0.274555827	0
121.506	684.023	306.138	-31.978	-0.029	0	0	0	0	19.95776	0.274555827	0
122.012	687.992	309.055	-32.857	-0.0153	0.0147	0	0	0	19.95776	0.274555827	0
122.506	691.641	312.605	-32.143	-0.058	0	0	0	0	19.95776	0.274555827	0
123.012	694.096	314.592	-32.418	-0.0862	0	0	0	0	19.95776	0.274555827	0
123.505	697.652	317.875	-32.711	-0.0031	0	0	0	0	19.95776	0.274555827	0
124.012	698.192	320.712	-32.546	0.0359	0	0	0	0	19.95776	0.274555827	0
124.506	702.423	323.851	-33.004	-0.029	0.0293	0	0	0	19.95776	0.274555827	0
125.012	704.622	326.997	-32.198	0.0443	0	0.0073	0	0	19.95776	0.274555827	0
125.505	706.711	330.04	-32.125	-0.013	0	0.0073	0	0.0073	19.95776	0.274555827	0
126.005	711.585	332.909	-31.264	0.0038	0	0	0.0147	0.0147	19.95776	0.276615977	0
126.511	713.261	335.944	-33.737	-0.0221	0	0	0	0	19.95776	0.276615977	0
127.011	716.375	338.829	-31.923	-0.0198	0	0	0	0	19.95776	0.276615977	0
127.511	718.156	342.026	-33.242	-0.0504	0	0	0	0.0147	19.95776	0.27798941	0
128.005	722.659	345.097	-32.143	-0.0435	0	0	0	0.0147	19.95776	0.279362844	0
128.511	726.629	347.922	-52.143	-0.0374	0	0	0	0.0147	19.95776	0.280736277	0
129.004	729.314	351.19	-30.165	-0.0168	0	0	0	0.0073	19.95776	0.281418322	0
129.505	731.054	354.334	-33.846	-0.0466	0.0293	0	0.0147	0.022	19.95776	0.282791755	0
130.004	733.242	357.305	-33.627	0.0351	0	0	0	0	19.95776	0.282791755	0
130.504	737.977	360.644	-31.813	-0.0023	0	0	0	0.022	19.95776	0.284847233	0
131.005	738.638	363.692	-29.231	-0.0176	0.0293	0	0.0147	0.0073	19.95776	0.284847233	0
131.504	745.14	366.832	-27.106	-0.0107	0	0	0	0.0073	19.95776	0.285529278	0
132.004	746.16	369.417	-24.744	-0.0649	1.5971	2.0952	0.0293	0	19.95776	0.285529278	0
132.51	750.089	373.327	-21.575	-0.0588	1.5385	2.0659	0.8938	1.3187	19.95776	0.285529278	0
133.01	754.743	376.205	-20.605	-0.042	1.5385	2.0733	0.8938	1.326	19.95776	0.285529278	0
133.51	755.22	379.592	-19.231	-0.0046	1.5238	2.0806	0.9524	1.3407	19.95776	0.285529278	0
134.003	756.67	382.261	-14.158	-0.0504	1.5385	2.0733	0.9231	1.326	19.95776	0.285529278	0
134.51	759.814	385.225	-11.887	-0.0412	7.4872	7.9267	0.9084	1.3407	19.95776	0.285529278	0
135.01	761.907	388.852	-10.403	-0.0267	7.4432	7.9487	5.7436	6.4176	19.95776	0.285529278	0
135.51	766.27	391.631	-8.004	0.0191	7.5018	7.9121	5.7582	6.4542	19.95776	0.285529278	0
136.01	767.799	395.439	-8.535	-0.0404	7.4579	7.9414	5.7143	6.3956	19.95776	0.285529278	0
136.503	771.584	398.271	-4.194	-0.0183	7.4872	7.9414	5.6996	6.3956	19.95776	0.285529278	0
137.003	774.806	401.468	-2.619	0.0107	13.5092	14.1026	5.7436	6.4176	19.95776	0.285529278	0
137.509	776.51	404.377	0	0.0069	13.5092	14.1026	5.7436	6.4176	19.95776	0.285529278	0
138.003	777.647	407.969	0.384	-0.0702	13.4652	14.1319	11.5018	12.7106	19.95776	0.285529278	0
138.509	781.271	411.002	-0.605	-0.0565	13.4945	14.1099	11.5018	12.7473	19.95776	0.285529278	0
139.003	782.668	414.752	0.952	-0.0435	13.4799	14.0806	11.4579	12.7326	19.95776	0.285529278	0
139.502	787.911	417.908	0.165	-0.0763	13.4945	14.0879	11.4579	12.7326	19.95776	0.285529278	0
140.009	789.745	420.696	-0.037	-0.0603	19.2234	19.4799	11.4579	12.7326	19.95776	0.285529278	0
140.509	790.174	424.423	-0.898	-0.0237	19.1941	19.4945	16.8645	19.6117	19.95776	0.285529278	0
141.002	794.966	427.452	1.08	-0.0114	19.2381	19.4872	16.8791	19.619	19.95776	0.285529278	0
141.509	795.53	431.335	1.703	-0.0114	19.2381	19.5018	16.8938	19.6337	19.95776	0.285529278	0
142.002	800.001	434.406	-0.037	-0.1107	19.2234	19.4945	16.8791	19.6117	19.95776	0.285529278	0



Time	FT	ST	dP	dH	CO in	CO2 in	CO out	CO2 out	k	Total Reduction	Drip mas
142.502	800.409	438.035	-0.202	0.0038	19.1355	19.5018	16.8938	19.6117	19.95776	0.285529278	0
143.008	806.829	441.123	0.311	-0.0099	19.1355	19.5458	17.6264	20.7106	19.95776	0.323859275	0
143.502	806.84	444.581	-0.257	-0.058	19.1648	19.5092	17.7289	20.7473	19.95776	0.372457319	0
144.008	809.411	447.593	1.923	-0.0176	19.1502	19.5238	17.7436	20.7546	19.95776	0.42174208	0
144.508	811.263	451.324	0.091	0.0244	19.1795	19.5238	17.7582	20.7619	19.95776	0.47102217	0
145.001	816.542	454.947	1.245	-0.0053	19.1648	19.5751	17.6996	20.7473	19.95776	0.512094361	0
145.508	816.105	458.311	1.611	-0.0817	19.0916	19.5531	17.7875	20.7619	19.95776	0.564111974	0
146.008	820.099	461.671	1.593	-0.1084	19.1209	19.5458	17.9341	20.5421	19.95776	0.601755254	0
146.501	821.998	465.005	2.161	-0.0214	19.1209	19.5751	17.9194	20.5495	19.95776	0.636665683	0
147.008	825.033	468.208	0.329	-0.0725	19.1355	19.5531	17.9634	20.5641	19.95776	0.676369113	0
147.502	826.605	471.94	0.183	-0.0046	19.1941	19.5311	17.9634	20.5421	19.95776	0.713335019	0
148.008	829.49	475.102	1.007	-0.0259	19.1941	19.4945	17.9341	20.5568	19.95776	0.753725166	0
148.501	833.964	479.025	0.494	-0.0404	19.2234	19.5385	18.1685	20.4176	19.95776	0.786580116	0
149.001	838.936	482.145	-0.641	-0.0572	19.2088	19.5385	18.1099	20.381	19.95776	0.81396002	0
149.507	840.204	485.841	0.806	-0.016	19.1795	19.5165	18.1245	20.4029	19.95776	0.847492343	0
150.001	843.386	489.843	1.172	0.0122	19.2088	19.5311	18.1685	20.4176	19.95776	0.881720727	0
150.501	845.722	493.415	1.758	-0.0252	19.1795	19.5018	18.1392	20.4103	19.95776	0.918004588	0
151	849.197	496.477	1.923	-0.0496	19.2088	19.4945	18.2125	20.3223	19.95776	0.94880406	0
151.507	852.081	500.364	1.209	0.0031	19.2381	19.5165	18.2418	20.337	19.95776	0.978921487	0
152.007	855.007	503.638	1.025	-0.0351	19.2088	19.5092	18.2125	20.3223	19.95776	1.008347526	0
152.507	858.389	507.001	2.326	0.0366	19.2234	19.5165	18.2271	20.337	19.95776	1.038464953	0
153.001	861.104	510.395	2.161	0.0885	19.2381	19.5238	18.2418	20.337	19.95776	1.067900335	0
153.5	863.764	514.221	2.253	-0.0313	19.2381	19.5238	18.1832	20.3223	19.95776	1.093224761	0
154.006	863.784	517.917	1.703	-0.0664	19.2234	19.5165	18.1978	20.337	19.95776	1.121973426	0
154.5	867.556	521.231	3.461	-0.0122	19.2527	19.5385	18.2125	20.3443	19.95776	1.148666613	0
155.006	868.681	525.342	1.593	-0.0359	19.2088	19.5238	18.3004	20.381	19.95776	1.186319236	0
155.5	874.741	528.809	2.014	-0.0275	19.1941	19.5385	18.1832	20.3223	19.95776	1.212325707	0
156	876.188	532.387	1.978	-0.0122	19.1795	19.5458	18.2418	20.2857	19.95776	1.237650133	0
156.513	878.449	536.029	1.666	0.0038	19.1355	19.5311	18.2418	20.2857	19.95776	1.26640347	0
157.007	881.055	539.337	2.546	-0.0466	19.1795	19.5531	18.1978	20.2857	19.95776	1.288990372	0
157.5	884.493	542.824	2.894	0.0153	19.1941	19.5311	18.1832	20.3004	19.95776	1.313642096	0
158	885.498	546.16	2.271	-0.0137	19.4579	19.3187	18.2564	20.3077	19.95776	1.349916614	0
158.506	888.84	550.116	3.425	-0.0183	19.4872	19.3333	18.2271	20.2784	19.95776	1.379351996	0
159.006	892.4	553.66	2.619	0.0679	19.4725	19.326	18.4908	20.0586	19.95776	1.401938898	0
159.506	893.851	556.917	2.234	-0.0023	19.4286	19.3114	18.4615	20.044	19.95776	1.425207846	0
160.005	895.138	560.634	3.022	0.0229	19.4579	19.3114	18.4322	20.0586	19.95776	1.44710336	0
160.505	897.61	564.077	3.498	0.0145	19.5311	19.3407	18.4615	20.0513	19.95776	1.463528499	0
161.012	901.11	567.774	4.304	0.074	19.4725	19.2967	18.4908	20.0513	19.95776	1.48817088	0
161.505	902.9	571.513	3.681	0.0839	19.4286	19.2894	18.4469	20.0513	19.95776	1.513495306	0
162.005	905.911	575.056	3.736	-0.029	19.4579	19.2894	18.4615	20.0733	19.95776	1.540188493	0
162.506	906.204	578.011	4.194	0.0862	19.4725	19.3114	18.5055	20.0806	19.95776	1.56688168	0
163.012	905.225	582.03	4.267	-0.1061	19.4286	19.304	18.4908	20.0733	19.95776	1.5949483	0
163.505	908.587	585.64	4.249	-0.0931	19.4432	19.2674	18.4615	20.0586	19.95776	1.623010249	0
164.005	909.071	588.81	3.461	0.0176	19.4872	19.2821	18.4469	20.0586	19.95776	1.646961242	0
164.511	908.84	592.289	4.084	0.0786	19.4725	19.2601	18.4908	20.0806	19.95776	1.677760714	0
165.011	911.553	595.999	4.926	0.0321	19.4286	19.2674	18.4469	20.0659	19.95776	1.706504708	0
165.505	912.36	599.505	4.725	0.0305	19.4872	19.2821	18.4762	20.0733	19.95776	1.733197895	0
166.004	912.138	602.749	4.377	-0.0229	19.4725	19.3187	18.4615	20.0733	19.95776	1.756471514	0
166.511	912.551	606.124	3.315	-0.0328	19.4139	19.3187	18.4469	20.1245	19.95776	1.786584269	0
167.004	914.899	609.24	4.469	0.0725	19.4286	19.326	18.3443	20.0879	19.95776	1.807115693	0
167.504	915.342	613.186	4.029	0.0664	19.4286	19.3187	18.4322	20.1172	19.95776	1.835172971	0
168.011	915.453	616.594	4.945	0.0313	19.4139	19.3187	18.4469	20.1245	19.95776	1.865285726	0
168.504	916.55	619.633	4.34	0.074	19.3846	19.3187	18.4322	20.1172	19.95776	1.895398481	0
169.004	918.081	622.547	5.183	0.0237	19.4139	19.326	18.4469	20.1172	19.95776	1.924147147	0
169.504	917.336	626.067	5.714	0.0023	19.3553	19.2894	18.4908	20.2198	19.95776	1.970689713	0
170.01	919.238	629.538	5.274	0.016	19.3846	19.326	18.4469	20.2125	19.95776	2.009711098	0
170.504	919.831	632.674	5.897	-0.0229	19.4139	19.326	18.4322	20.2051	19.95776	2.045985617	0
171.003	920.758	635.851	4.798	0.0412	19.3993	19.2967	18.4908	20.2125	19.95776	2.089108615	0
171.504	920.938	638.904	5.641	-0.0168	19.4725	19.304	18.3883	20.1832	19.95776	2.120604146	0
172.003	921.561	641.778	4.707	0.0343	19.4725	19.2967	18.3883	20.293	19.95776	2.163040428	0
172.51	924.185	644.825	5.586	-0.013	19.4579	19.3187	18.3297	20.2637	19.95776	2.19862823	0
173.01	923.2	647.792	5.458	0.0504	19.5311	19.2967	18.4029	20.2857	19.95776	2.238326988	0
173.503	924.376	650.679	5.348	0.0359	19.4872	19.2821	18.3297	20.2711	19.95776	2.276656985	0
174.003	924.286	653.651	6.135	-0.016	19.3993	19.348	18.3736	20.2784	19.95776	2.315669026	0
174.51	927.741	656.675	5.824	-0.0488	19.3407	19.348	18.3004	20.3663	19.95776	2.362211593	0
175.009	928.924	659.794	6.74	0.0107	19.3846	19.348	18.2857	20.3883	19.95776	2.408072114	0
175.509	928.603	662.506	6.611	0.0015	19.3993	19.3553	18.2418	20.3663	19.95776	2.448457589	0
176.003	928.713	664.833	6.63	0.0168	19.4139	19.3626	18.2564	20.3736	19.95776	2.488843064	0
176.503	931.662	667.376	6.245	0.0275	19.4432	19.3773	18.2418	20.3736	19.95776	2.525804299	0
177.009	931.572	670.495	6.941	0.071	19.4139	19.3773	18.1245	20.5055	19.95776	2.570978104	0
177.502	931.4	673.23	6.465	-0.0061	19.4286	19.3773	18.1245	20.5055	19.95776	2.615465192	0



Time	FT	ST	dP	dH	CO in	CO2 in	CO out	CO2 out	k	Total Reduction	Drip mas
178.002	933.536	675.864	7.088	-0.0176	19.4139	19.37	18.1392	20.5055	19.95776	2.662007758	0
178.509	932.946	678.735	6.74	0.0321	19.3993	19.3993	18.0806	20.4982	19.95776	2.703075278	0
179.009	934.608	681.159	7.491	0.0046	19.37	19.4139	18.1245	20.5128	19.95776	2.747562366	0
179.503	937.682	683.58	7.106	-0.0145	19.3553	19.4139	18.1245	20.5128	19.95776	2.792736171	0
180.002	938.343	686.595	7.124	0.0412	19.3407	19.4359	17.9634	20.6447	19.95776	2.841334215	0
180.502	938.183	689.369	7.491	-0.0466	19.3553	19.3919	18.0366	20.6667	19.95776	2.898836218	0
181.002	939.613	691.199	7.802	0.0244	19.3114	19.4066	18.0366	20.6667	19.95776	2.957015594	0
181.508	940.334	694.055	6.868	0.0313	19.3407	19.3993	18.0073	20.6593	19.95776	3.012448103	0
182.002	940.933	696.25	7.564	-0.0809	19.37	19.3919	18.022	20.6667	19.95776	3.068581344	0
182.508	939.884	699.252	7.472	-0.0137	19.326	19.3846	17.9194	20.7179	19.95776	3.127442765	0
183.001	941.474	701.572	7.069	-0.0473	19.37	19.3919	17.9194	20.7033	19.95776	3.182202572	0
183.502	943.143	703.675	8.15	0.0427	19.37	19.3846	17.978	20.7399	19.95776	3.243801516	0
184.008	945.312	706.498	8.37	-0.0038	19.326	19.3773	17.9927	20.7473	19.95776	3.309516088	0
184.501	947.267	708.715	7.71	-0.0183	19.37	19.3993	17.9341	20.7253	19.95776	3.366326702	0
185.002	947.009	711.351	7.454	-0.074	19.37	19.3993	17.9048	20.7912	19.95776	3.427925647	0
185.501	948.166	713.006	8.077	-0.0183	19.37	19.4066	17.9048	20.7985	19.95776	3.489524591	0
186.007	948.475	714.649	7.619	0.029	19.3846	19.3993	17.9048	20.8059	19.95776	3.551814923	0
186.507	950.241	717.773	8.168	-0.0366	19.3553	19.3919	17.9048	20.7985	19.95776	3.615474017	0
187.001	950.76	719.939	8.351	0.0435	19.3993	19.4212	17.9194	20.7985	19.95776	3.675022154	0
187.5	951.917	722.093	8.553	0.0229	19.4432	19.4286	17.8315	20.8205	19.95776	3.72977729	0
188	952.276	723.945	8.003	0.0038	19.4139	19.3919	17.8901	20.8498	19.95776	3.794805145	0
188.507	955.275	725.925	8.754	0.0458	19.4725	19.4139	17.8608	20.8425	19.95776	3.852989193	0
189.007	954.887	727.797	9.066	-0.0527	19.4139	19.4066	17.8755	20.8498	19.95776	3.91596157	0
189.5	954.697	730.031	8.718	0.0259	19.326	19.4139	17.8755	20.8511	19.95776	3.983040232	0
190	955.762	731.9	8.223	-0.0488	19.2674	19.4359	17.8022	20.8791	19.95776	4.049432178	0
190.501	957.924	734.397	8.956	-0.0114	19.3846	19.3993	17.7875	20.9377	19.95776	4.118556975	0
191.007	956.818	735.986	8.809	0.0252	19.3846	19.4359	17.7729	20.8938	19.95776	4.179478545	0
191.5	958.123	738.299	8.883	0.0092	19.2821	19.4286	17.7875	20.8938	19.95776	4.246552536	0
192	958.422	739.928	8.791	0.0298	19.2821	19.4432	17.8462	20.9304	19.95776	4.318424199	0
192.506	960.152	741.812	8.278	-0.0389	19.2821	19.4505	17.7875	20.9011	19.95776	4.3841341	0
193.006	961.356	743.621	9.377	0.0061	19.2088	19.4505	17.7875	20.9744	19.95776	4.46011672	0
193.5	961.326	745.247	9.395	-0.0633	19.3407	19.4799	17.7436	20.9524	19.95776	4.523084425	0
194.006	962.449	747.213	9.066	-0.0061	19.2821	19.4579	17.7729	20.967	19.95776	4.593577984	0
194.5	962.499	749.05	8.937	-0.058	19.2234	19.4505	17.8022	20.9817	19.95776	4.670247321	0
195.006	963.265	750.874	10.146	-0.0549	19.3114	19.4212	17.8168	20.989	19.95776	4.746907314	0
195.512	965.291	752.349	10.073	-0.0214	19.2674	19.4286	17.7582	21.011	19.95776	4.824249352	0
196.006	965.302	754.459	9.377	-0.0176	19.3114	19.4359	17.7582	21.0037	19.95776	4.898171822	0
196.512	966.126	756.175	10.549	0.0122	19.2821	19.4505	17.7582	21.0037	19.95776	4.972098964	0
197.005	966.046	757.678	9.231	0.0534	19.3407	19.4505	17.7582	21.0037	19.95776	5.043288583	0
197.505	967.506	759.741	9.926	-0.0122	19.3846	19.3553	17.8168	21.033	19.95776	5.126797055	0
198.005	968.171	761.518	9.011	-0.0374	19.3846	19.3773	17.8022	20.9524	19.95776	5.200037481	0
198.506	969.351	762.871	9.817	-0.042	19.37	19.3773	17.8022	20.9597	19.95776	5.274641996	0
199.012	969.957	764.614	10.055	-0.0771	19.37	19.3846	17.7729	20.967	19.95776	5.347877749	0
199.512	971.881	766.229	9.487	-0.0748	19.37	19.3919	17.7729	20.9524	19.95776	5.419067368	0
200.005	972.883	767.474	10.238	-0.0549	19.3993	19.4286	17.8022	20.9744	19.95776	5.488883553	0
200.505	972.694	769.72	9.652	-0.0237	19.37	19.4139	17.8022	20.9451	19.95776	5.55870441	0
201.005	972.714	771.543	11.172	-0.0511	19.3553	19.4212	17.8022	20.9524	19.95776	5.629211983	0
201.505	972.287	772.839	10.183	-0.0092	19.37	19.4212	17.8022	20.967	19.95776	5.70039693	0
202.011	974.865	774.471	10.494	-0.0504	19.4579	19.4139	17.8022	20.9597	19.95776	5.767475592	0
202.505	973.735	775.934	9.89	-0.0282	19.3553	19.4066	17.8315	20.9524	19.95776	5.840716017	0
203.005	975.172	777.564	10.641	-0.0359	19.3407	19.4432	17.8022	20.9524	19.95776	5.909850158	0
203.505	975.934	779.256	10.916	-0.0572	19.2821	19.4286	17.7875	20.967	19.95776	5.983763285	0
204.004	976.668	780.748	10.824	-0.045	19.3553	19.4579	17.7143	20.9451	19.95776	6.046053617	0
204.504	977.678	782.334	10.787	-0.1015	19.3407	19.4359	17.7729	20.967	19.95776	6.115865131	0
205.004	979.112	784.212	11.117	-0.0565	19.3407	19.4359	17.7582	20.9597	19.95776	6.184307883	0
205.505	979.023	785.46	11.355	-0.029	19.3553	19.4212	17.7729	20.9597	19.95776	6.254128739	0
206.004	979.528	786.981	11.593	-0.0488	19.37	19.4432	17.6996	20.9524	19.95776	6.317101117	0
206.504	980.399	788.563	11.52	0.0176	19.3553	19.4212	17.7582	20.9597	19.95776	6.386235257	0
207.004	981.656	789.799	11.557	-0.0282	19.3846	19.4212	17.7875	20.9524	19.95776	6.454687352	0
207.51	982.209	791.118	11.721	-0.0458	19.3553	19.4359	17.7582	20.9524	19.95776	6.521766014	0
208.01	981.922	792.95	10.97	0.0046	19.3553	19.4139	17.7582	20.967	19.95776	6.592264245	0
208.51	984.365	794.152	11.337	-0.0099	19.37	19.4139	17.7729	20.9597	19.95776	6.66208043	0
209.01	984.177	795.302	12.124	0.0275	19.3114	19.4139	17.7729	20.967	19.95776	6.735316183	0
209.503	985.313	798	11.52	0.0061	19.3553	19.3993	17.7582	20.967	19.95776	6.807178504	0
210.004	985.649	800	11.154	-0.0809	19.3553	19.4139	17.7875	20.967	19.95776	6.879045496	0
210.51	986.528	803	11.905	-0.0786	19.3407	19.4725	17.7582	20.9744	19.95776	6.945442113	0
211.003	986.074	806	11.611	-0.0534	19.3553	19.4725	17.7729	20.967	19.95776	7.011152013	0
211.51	987.298	809.569	11.959	-0.0778	19.3407	19.4505	17.7582	20.9597	19.95776	7.078230675	0
212.009	987.733	810.963	11.923	-0.0168	19.3407	19.4432	17.7729	20.9597	19.95776	7.146678099	0
212.503	988.424	812.097	11.85	-0.1	19.3846	19.4286	17.8168	20.9524	19.95776	7.215807568	0
213.009	990.083	813.261	12.546	-0.0679	19.3993	19.4286	17.7875	20.9377	19.95776	7.281508125	0



Time	FT	ST	dP	dH	CO in	CO2 in	CO out	CO2 out	k	Total Reduction	Drip mas
213.509	991.237	814.539	11.648	-0.0046	19.3114	19.4212	17.7729	20.9524	19.95776	7.352697743	0
214.002	991.72	815.775	11.776	-0.0702	19.3114	19.4359	17.8315	20.9451	19.95776	7.424569407	0
214.509	992.282	816.854	12.729	-0.0641	19.3993	19.4286	17.8022	20.9744	19.95776	7.494385592	0
215.002	992.292	818.286	13.003	-0.0359	19.3553	19.4212	17.8315	20.967	19.95776	7.567626017	0
215.502	993.159	819.199	12.93	-0.0313	19.37	19.4212	17.8168	20.9597	19.95776	7.638810964	0
216.009	993.603	820.465	11.941	0.0313	19.4139	19.4066	17.9048	21.011	19.95776	7.718213152	0
216.509	994.57	821.18	12.271	-0.1015	19.3993	19.4286	17.7875	20.9597	19.95776	7.785969188	0
217.002	995.191	822.631	12.948	0.0305	19.3553	19.4212	17.8022	20.9597	19.95776	7.857158806	0
217.509	996.895	823.76	12.344	-0.0427	19.3993	19.4212	17.7875	20.967	19.95776	7.926282275	0
218.003	996.403	824.961	12.875	-0.0618	19.3553	19.4359	17.8315	20.9597	19.95776	7.997473222	0
218.509	996.964	825.8	13.187	-0.0832	19.3407	19.4066	17.8315	20.967	19.95776	8.072759782	0
219.002	998.5	827.228	13.223	0.0282	19.4286	19.4286	17.8462	20.9744	19.95776	8.143262684	0
219.501	999.751	827.973	13.132	-0.0679	19.3846	19.4286	17.8168	20.967	19.95776	8.213756243	0
220.002	1000.11	829.441	13.168	-0.0466	19.4432	19.4286	17.8022	20.9744	19.95776	8.281521621	0
220.508	1001.76	830.588	13.443	-0.0588	19.3993	19.4286	17.8315	20.9744	19.95776	8.352706568	0
221.002	1001.11	831.208	13.754	-0.0397	19.37	19.4359	17.8168	20.9744	19.95776	8.423891515	0
221.502	1001.92	832.262	13.571	-0.0672	19.3114	19.4359	17.7875	20.9231	19.95776	8.491652222	0
222.002	1001.59	833.367	12.967	-0.1023	19.3407	19.4652	17.8168	20.9158	19.95776	8.555993361	0
222.508	1003.56	834.513	13.187	-0.1053	19.37	19.4359	17.8462	20.9524	19.95776	8.626496263	0
223.001	1003.06	835.824	13.077	-0.0794	19.4432	19.4286	17.8168	20.9524	19.95776	8.692888209	0
223.502	1005.04	836.629	14.249	-0.0664	19.3407	19.4066	17.8315	20.9451	19.95776	8.766128634	0
224.008	1006.54	837.918	14.139	0.0595	19.3846	19.4139	17.8608	20.9524	19.95776	8.838687014	0
224.507	1005.52	838.876	12.93	-0.0351	19.3553	19.4139	17.8755	20.9597	19.95776	8.913982917	0
225.001	1006.21	839.845	13.937	-0.0206	19.3846	19.3993	17.9048	20.9744	19.95776	8.992016343	0
225.507	1006.07	840.659	13.37	-0.0328	19.3407	19.3993	17.8462	20.9451	19.95776	9.06662553	0
226	1009.14	841.638	13.351	-0.1091	19.3553	19.4066	17.8462	20.9451	19.95776	9.139870627	0
226.501	1009.9	842.997	14.084	-0.0595	19.4432	19.4066	17.8901	20.9597	19.95776	9.212424335	0
227	1009.4	844.119	13.406	-0.0176	19.4432	19.4066	17.9048	20.9451	19.95776	9.28430067	0
227.507	1010.07	844.87	14.359	-0.0046	19.4286	19.4139	17.8462	20.9304	19.95776	9.352066049	0
228.001	1011.84	846.012	14.231	-0.0466	19.3993	19.4432	17.9341	20.9084	19.95776	9.420513473	0
228.507	1012.46	846.917	14.231	-0.0198	19.4432	19.4359	17.8022	20.9084	19.95776	9.481430372	0
229	1013.51	847.585	14.414	-0.0778	19.326	19.4066	17.8462	20.9304	19.95776	9.554670797	0
229.5	1012.98	848.972	14.011	-0.1358	19.326	19.4066	17.9194	20.8718	19.95776	9.625855744	0
230	1013.28	849.805	13.718	-0.1152	19.326	19.4139	17.8315	20.9158	19.95776	9.696363317	0
230.5	1015.68	850.791	14.762	-0.087	19.2821	19.4066	17.8901	20.9231	19.95776	9.77302331	0
231.006	1016.45	851.653	14.377	-0.1107	19.3407	19.3993	17.8315	20.9158	19.95776	9.844208257	0
231.507	1018.89	852.772	14.926	-0.0252	19.3553	19.3993	17.8462	20.9158	19.95776	9.915397876	0
232	1021.12	853.634	14.707	-0.0549	19.3553	19.4066	17.9194	20.9231	19.95776	9.990007063	0
232.506	1022.73	854.526	14.89	-0.0466	19.3407	19.4139	17.9048	20.9304	19.95776	10.06461625	0
233.006	1026.7	855.562	14.817	-0.0694	19.3407	19.3993	17.8901	20.9158	19.95776	10.13853872	0
233.512	1027.57	856.875	15.531	0.013	19.4286	19.4212	17.8901	20.9158	19.95776	10.20630877	0
234.012	1031.62	857.397	14.981	-0.1343	19.3114	19.4432	17.9048	20.9304	19.95776	10.27954919	0
234.506	1035.25	858.617	14.377	-0.074	19.326	19.4359	17.9487	20.9451	19.95776	10.35621386	0
235.006	1037.19	859.866	15.274	0.0305	19.3407	19.4579	17.9194	20.967	19.95776	10.4308137	0
235.505	1040.8	860.829	15.513	0.0321	19.326	19.4505	17.9341	20.9597	19.95776	10.50679632	0
236.005	1041.98	861.801	15.11	-0.0748	19.2967	19.4505	17.9341	20.9524	19.95776	10.58346566	0
236.505	1043.97	862.763	15.091	-0.1015	19.326	19.4432	17.9194	20.967	19.95776	10.66012565	0
237.005	1046.43	864.471	15.439	0.0076	19.3553	19.4286	17.9487	20.9597	19.95776	10.73746769	0
237.512	1049.14	865.177	14.981	-0.2015	19.3553	19.4505	17.8608	20.9451	19.95776	10.80729322	0
238.005	1051.34	866.454	15.366	-0.1152	19.3407	19.4286	17.8462	20.9451	19.95776	10.87916488	0
238.506	1052.17	867.691	14.908	-0.0389	19.3407	19.4286	17.8608	20.9451	19.95776	10.95171859	0
239.012	1054.69	868.968	15.476	-0.0557	19.3407	19.4212	17.8462	20.9451	19.95776	11.02428164	0
239.511	1057.43	870.703	16.373	-0.0481	19.3553	19.4652	17.8755	20.9451	19.95776	11.09342045	0
240.005	1061.78	871.826	16.099	-0.0778	19.3553	19.4579	17.8755	20.9524	19.95776	11.16392336	0
240.505	1064.93	873.284	16.227	-0.0923	19.3846	19.4579	17.8755	20.9524	19.95776	11.2330575	0
241.011	1069.83	874.702	16.227	-0.0618	19.326	19.4432	17.8755	20.9451	19.95776	11.30562055	0
241.504	1072.08	876.2	16.758	-0.0252	19.3553	19.4579	17.8755	20.9597	19.95776	11.3768055	0
242.004	1076.15	877.596	15.622	-0.0511	19.3114	19.4799	17.9048	20.9524	19.95776	11.44867249	0
242.511	1080.4	879.174	17.033	0.0221	19.2527	19.4725	17.8755	20.9524	19.95776	11.5226043	0
243.011	1082.49	880.762	15.861	0.0763	19.2967	19.4799	17.8755	20.9817	19.95776	11.59652677	0
243.511	1087.21	882.267	15.861	-0.0397	19.3114	19.4872	17.8755	20.9744	19.95776	11.66839843	0
244.011	1088.12	883.986	17.051	-0.0183	19.2967	19.4725	17.8901	20.9817	19.95776	11.74369434	0
244.51	1093.38	885.592	16.758	-0.0565	19.326	19.4359	17.8315	20.967	19.95776	11.81693009	0
245.004	1096.16	887.288	16.337	-0.058	19.326	19.4359	17.8462	20.9597	19.95776	11.89017052	0
245.504	1100.26	889.156	16.209	-0.1244	19.3114	19.4212	17.8608	20.9304	19.95776	11.96341094	0
246.003	1102.36	891.074	17.088	0.0092	19.326	19.4359	17.8755	20.9377	19.95776	12.03596465	0
246.51	1105.92	893.102	17.271	-0.1091	19.37	19.4505	17.8315	20.9524	19.95776	12.10441674	0
247.01	1108.51	894.977	18.168	-0.0473	19.2821	19.4359	17.8901	20.9524	19.95776	12.18107674	0
247.503	1114.1	897.135	17.491	-0.0641	19.326	19.4286	17.9048	20.9524	19.95776	12.25705469	0
248.003	1116.62	898.977	17.582	-0.0504	19.3407	19.4505	17.8755	20.9524	19.95776	12.32893102	0
248.51	1119.61	900.93	17.6	-0.0923	19.3407	19.4359	17.8901	20.9451	19.95776	12.40217145	0



Time	FT	ST	dP	dH	CO in	CO2 in	CO out	CO2 out	k	Total Reduction	Drip mas
249.01	1122.9	903.347	17.216	-0.0595	19.3407	19.4286	17.9048	20.9597	19.95776	12.47814472	0
249.503	1126.82	905.671	18.425	-0.0923	19.326	19.4432	17.9194	20.9597	19.95776	12.55412267	0
250.003	1128.93	908.094	17.509	0.0008	19.326	19.4725	17.9048	20.9597	19.95776	12.62668105	0
250.503	1134.13	910.385	18.15	0.0023	19.3846	19.4799	17.8755	20.9524	19.95776	12.69375971	0
251.003	1136.92	912.381	17.839	-0.0992	19.326	19.4799	17.9341	20.9744	19.95776	12.7683689	0
251.509	1141.7	914.538	18.022	-0.1183	19.326	19.4579	17.8901	20.967	19.95776	12.8422867	0
252.003	1143.79	917.257	18.351	-0.0359	19.326	19.4725	17.9341	20.9744	19.95776	12.91758727	0
252.503	1148.5	919.622	17.967	-0.0832	19.956	18.8352	17.8901	20.9744	19.95776	13.02094513	0
253.009	1152.66	922.086	18.022	-0.0214	19.8828	18.8791	17.8755	20.9377	19.95776	13.11950998	0
253.509	1156.03	924.819	17.948	-0.0389	20	18.8425	18.2564	20.674	19.95776	13.20917554	0
254.002	1158.68	927.249	17.93	-0.0763	19.956	18.8425	18.2418	20.6593	19.95776	13.29884111	0
254.502	1160.93	930.079	17.436	0.0626	19.956	18.8425	18.2271	20.6593	19.95776	13.38781995	0
255.002	1165.71	932.906	18.37	0.1236	20.7619	18.022	18.2418	20.696	19.95776	13.51992647	0
255.502	1167.74	935.221	18.498	0.1755	20.7619	18.0293	18.2857	20.674	19.95776	13.65134627	0
256.002	1172.25	937.794	18.553	0.2953	20.7912	18.0513	18.9158	20.0586	19.95776	13.75127988	0
256.508	1175.66	940.695	18.15	0.3632	20.7619	18.0073	18.9304	20.0733	19.95776	13.85874869	0
257.002	1178.38	943.454	18.04	0.3984	20.8059	18.0586	18.9158	20.0366	19.95776	13.95525807	0
257.508	1182.54	946.351	17.985	0.4144	20.7619	18.0293	18.9304	20.0586	19.95776	14.05929796	0
258.001	1185.29	949.096	18.223	0.4945	21.6117	17.1941	18.9451	20.0659	19.95776	14.20304129	0
258.508	1188.86	952.297	17.582	0.5746	21.6117	17.1941	19.619	19.4066	19.95776	14.31666719	0
259.008	1193.53	954.977	17.857	0.6899	21.5971	17.1941	19.6484	19.4212	19.95776	14.43371266	0
259.502	1195.56	958.213	17.362	0.6769	21.685	17.2381	19.5751	19.3773	19.95776	14.53501503	0
260.008	1199.69	961.287	17.802	0.6548	21.6117	17.1941	19.6484	19.4286	19.95776	14.65206984	0
260.501	1200.98	964.239	18.48	0.6983	22.5495	16.2418	19.6484	19.4212	19.95776	14.81359773	0
261.001	1203.12	967.428	18.754	0.7357	22.5348	16.2344	20.4542	18.652	19.95776	14.94228001	0
261.508	1206.29	970.474	18.022	0.654	22.5495	16.2637	20.381	18.63	19.95776	15.062063	0
262.001	1210.06	973.548	18.205	0.7135	22.5495	16.2564	20.4396	18.652	19.95776	15.18732103	0
262.507	1212.57	976.797	18.901	0.7036	22.5201	16.2711	20.3956	18.652	19.95776	15.31052359	0
263.001	1214.77	980.044	17.857	0.7204	23.5604	15.2527	20.4542	18.652	19.95776	15.48301559	0
263.507	1218.54	983.268	18.315	0.7502	23.5751	15.2747	20.4103	18.6374	19.95776	15.64935049	0
264	1220.36	986.401	17.692	0.7112	23.5458	15.2527	21.4066	17.8022	19.95776	15.78761877	0
264.507	1224.52	989.521	17.839	0.8051	23.5604	15.2454	21.3919	17.8022	19.95776	15.92520033	0
265.001	1226.68	992.599	18.535	0.7761	23.5604	15.2601	21.4066	17.8022	19.95776	16.06209518	0
265.507	1229.22	995.547	18.132	0.7418	24.6154	14.1685	21.4212	17.8095	19.95776	16.25305845	0
266	1231.92	998.738	18.077	0.8738	24.6154	14.1685	21.4212	17.8168	19.95776	16.44470376	0
266.5	1234.61	1001.71	17.784	0.8181	24.5861	14.1685	22.4029	16.8059	19.95776	16.58912913	0
267.007	1237.25	1005	17.985	0.9196	24.6007	14.1758	22.4176	16.8205	19.95776	16.73424122	0
267.5	1240.62	1008.05	17.894	0.8982	24.6007	14.1685	22.4029	16.8278	19.95776	16.88003068	0
268.006	1242.65	1011.34	18.48	1.0073	24.6154	14.1905	22.4469	16.8059	19.95776	17.02308729	0
268.5	1246.88	1014.29	18.535	0.9753	25.7143	13.1868	22.359	16.7985	19.95776	17.20378718	0
269.006	1248.6	1017.56	18.425	0.9776	25.641	13.1429	23.4725	15.8388	19.95776	17.35436497	0
269.513	1250.96	1020.5	18.608	0.973	25.6703	13.1575	23.4725	15.8242	19.95776	17.50084582	0
270.007	1253.27	1023.99	18.736	1.0348	25.6703	13.1282	23.5311	15.8388	19.95776	17.65416581	0
270.5	1256.32	1027.02	19.011	1.0295	25.5971	13.1355	23.5165	15.8388	19.95776	17.80954127	0
271.006	1259.38	1030.31	19.304	1.1218	26.696	12.0659	23.5018	15.8388	19.95776	18.01282807	0
271.506	1262.68	1033.01	18.974	1.1233	26.7253	12.0733	24.6447	14.7473	19.95776	18.16546601	0
272.006	1265.99	1036.35	18.699	1.2538	26.696	12.0659	24.674	14.7619	19.95776	18.32289695	0
272.5	1267.79	1039.76	19.359	1.2462	26.652	12.0952	24.6154	14.7253	19.95776	18.47348876	0
273.006	1271.54	1042.69	19.414	1.3362	26.696	12.0586	24.6886	14.7692	19.95776	18.63296584	0
273.512	1273.95	1045.82	20.183	1.4499	27.7216	11.0403	24.674	14.7619	19.95776	18.83830811	0
274.005	1277.03	1048.64	19.926	1.5011	27.707	11.011	24.6886	14.7619	19.95776	19.04775199	0
274.506	1279.22	1051.8	20.476	1.6323	27.7216	11.0256	25.9048	13.6923	19.95776	19.21203142	0
275.012	1282.31	1055	21.007	1.7079	27.707	11.0256	25.8755	13.685	19.95776	19.37494208	0
275.506	1284.4	1058.12	19.633	1.701	27.7216	11.0256	25.8755	13.685	19.95776	19.53717069	0
276.012	1287.12	1061.25	20.842	1.9086	28.7326	9.978	25.8608	13.685	19.95776	19.74936144	0
276.512	1291.13	1064.45	20.384	2.0017	28.6886	9.956	25.8755	13.685	19.95776	19.96634987	0
277.005	1292.2	1067.45	20.549	2.0383	28.7912	9.9707	27.1209	12.5568	19.95776	20.12994257	0
277.511	1296.64	1070.44	20.531	2.2146	28.7033	9.9634	27.1355	12.5568	19.95776	20.29900565	0
278.011	1299.13	1073.5	20.916	2.3222	28.7033	9.956	27.1648	12.5714	19.95776	20.47149297	0
278.505	1301.08	1076.89	21.611	2.4977	28.7179	9.956	27.1502	12.5568	19.95776	20.64125212	0
279.005	1304.86	1079.95	20.842	2.5626	29.7582	8.9304	27.1355	12.5348	19.95776	20.85549367	0
279.504	1307.73	1083.37	21.941	2.848	29.8315	8.9084	28.2637	11.5678	19.95776	21.03072319	0
280.004	1310.89	1086.58	22.234	2.9418	29.7729	8.8864	28.293	11.5824	19.95776	21.21347856	0
280.511	1312.46	1089.77	22.271	3.1487	29.7729	8.9011	28.2637	11.5751	19.95776	21.39280969	0
281.004	1315.35	1092.55	21.959	3.2601	29.7143	8.9084	28.2491	11.5604	19.95776	21.57214081	0
281.504	1318.32	1095.83	22.491	3.4814	30.9011	7.8095	28.2784	11.5751	19.95776	21.80144342	0
282.011	1321.67	1098.99	23.15	3.7263	30.9158	7.8168	29.3333	10.6227	19.95776	21.98967384	0
282.504	1324.24	1102.11	23.15	3.8828	30.9011	7.8022	29.348	10.6227	19.95776	22.18064177	0
283.004	1327.17	1105.33	23.095	4.127	30.9597	7.8388	29.2894	10.6007	19.95776	22.36065962	0
283.51	1329.86	1108.46	23.296	4.462	30.8864	7.8095	29.3187	10.6081	19.95776	22.54889938	0
284.004	1332.86	1111.51	24.633	4.7474	31.9267	6.696	29.3333	10.63	19.95776	22.7953045	0



Time	FT	ST	dP	dH	CO in	CO2 in	CO out	CO2 out	k	Total Reduction	Drip mas
284.503	1335.32	1114.57	25.439	5.0763	31.9121	6.7033	30.359	9.7289	19.95776	23.0054351	0
285.01	1337.72	1118.01	24.597	5.5418	31.9267	6.696	30.3443	9.7289	19.95776	23.21487898	0
285.503	1340.63	1120.97	25.513	5.8669	31.8974	6.674	30.4029	9.7656	19.95776	23.43391354	0
286.01	1343.61	1124.25	26.135	6.2981	31.9267	6.6886	30.3443	9.7289	19.95776	23.64404881	0
286.503	1346.58	1127.54	26.52	6.6735	33.0549	5.5751	30.3443	9.7289	19.95776	23.90551498	0
287.01	1349.9	1130.56	27.143	7.0253	33.0403	5.6044	30.315	9.707	19.95776	24.16151078	0
287.504	1352.21	1133.55	27.839	7.4802	32.9963	5.5751	31.2967	8.9451	19.95776	24.39697515	0
288.003	1354.63	1136.78	28.15	8.0113	32.9963	5.5751	31.326	8.9597	19.95776	24.63517237	0
288.509	1356.5	1140.2	28.974	8.5348	33.0842	5.6044	31.3407	8.9377	19.95776	24.86515702	0
289.009	1359.27	1143.26	30.128	9.0759	33.011	5.5824	31.3114	8.9524	19.95776	25.10062139	0
289.509	1360.82	1146.36	30.311	9.5749	34.0659	4.4689	31.3114	8.9304	19.95776	25.38878542	0
290.009	1363.49	1149.55	31.392	10.0977	34.022	4.4542	32.3516	8.2198	19.95776	25.66257511	0
290.509	1366.02	1152.82	31.795	10.6433	34.1099	4.4835	32.3077	8.1832	19.95776	25.92405062	0
291.003	1367.83	1155.79	33.37	11.2225	34.0806	4.4762	32.3516	8.1905	19.95776	26.19030979	0
291.502	1370.04	1159.04	33.571	11.8544	34.1099	4.4835	32.3077	8.1905	19.95776	26.45246735	0
292.009	1372.01	1162.3	35.073	12.4855	35.2821	3.3407	32.381	8.1978	19.95776	26.77074413	0
292.503	1373.8	1165.09	36.135	13.1036	35.2821	3.3407	33.2894	7.4066	19.95776	27.05753473	0
293.009	1376.16	1168.14	37.985	13.8004	35.2527	3.3333	33.2747	7.4066	19.95776	27.34570342	0
293.509	1378.14	1171.51	38.718	14.4773	35.2821	3.3553	33.2601	7.3919	19.95776	27.62838773	0
294.002	1379.49	1174.67	40.604	15.1229	35.2821	3.3626	33.2308	7.3846	19.95776	27.90833919	0
294.502	1381.53	1177.7	42.747	15.8547	36.293	2.2051	33.2454	7.4505	19.95776	28.25605136	0
295.008	1383.9	1180.92	44.542	16.6613	36.2491	2.2198	34.2857	6.5714	19.95776	28.5709039	0
295.501	1385.57	1183.95	47.637	17.4237	36.2637	2.2125	34.2564	6.5641	19.95776	28.88370564	0
296.002	1387.02	1187.07	48.553	18.2936	36.293	2.2125	34.2564	6.5861	19.95776	29.19719409	0
296.508	1389.36	1190.41	46.685	19.0346	36.293	2.2418	34.2857	6.5641	19.95776	29.5072583	0
297.008	1390.32	1193.32	51.721	19.8726	37.4652	1.1282	34.2564	6.5714	19.95776	29.86592056	0
297.508	1392.56	1196.36	55.861	20.5807	37.4212	1.1062	34.2418	6.5568	19.95776	30.22664764	0
298.001	1394.14	1199.63	62.344	21.4385	37.4505	1.1136	35.1941	5.6923	19.95776	30.54903071	0
298.508	1395.67	1202.54	66.905	22.1917	37.4359	1.0989	35.1648	5.6703	19.95776	30.87004501	0
299.008	1397.11	1205.48	71.428	22.9083	37.4505	1.1062	35.2088	5.685	19.95776	31.19312414	0
299.501	1399.92	1208.91	78.132	23.6989	37.4652	1.1209	35.1502	5.6703	19.95776	31.51003216	0
300.008	1401.5	1211.51	82.674	24.359	38.4176	0.0293	35.1795	5.685	19.95776	31.88717971	0
300.501	1402.68	1214.61	89.34	25.0687	38.3736	0.022	35.8095	4.8352	19.95776	32.21709797	0
301.001	1404.32	1216.96	96.575	25.7357	38.5055	0.022	35.7802	4.8132	19.95776	32.53743023	0
301.507	1405.98	1220.19	105.11	26.4118	38.4762	0.0147	35.7949	4.8352	19.95776	32.8625555	0
302.001	1407.62	1223.47	114.395	27.0002	38.4615	0.0293	35.7949	4.8352	19.95776	33.18700338	0
302.5	1409.74	1226.1	124.285	27.6374	38.652	0.0293	35.7949	4.8278	19.95776	33.5018606	0
303	1411.02	1228.61	137.289	28.2097	38.6081	0.0293	36.5568	4.2418	19.95776	33.79961063	0
303.501	1412.93	1231.3	151.044	28.8782	38.652	0.0366	36.6007	4.2637	19.95776	34.09872475	0
304.007	1413.85	1234.1	164.835	29.4254	38.6227	0.0147	36.674	4.2564	19.95776	34.40399596	0
304.5	1415.6	1236.83	180.128	30.1091	38.6813	0.0366	36.5714	4.2637	19.95776	34.70037256	0
305	1417.61	1239.81	200.659	30.6029	38.5641	0.044	36.6007	4.2491	19.95776	35.00153749	0
305.5	1418.5	1242.12	217.93	31.1531	38.5788	0.0586	37.0842	3.7289	19.95776	35.27463579	0
306.006	1420.07	1244.98	239.707	31.717	38.6081	0.0073	37.1868	3.7289	19.95776	35.55595134	0
306.5	1421.93	1247.68	266.209	32.3085	38.6081	0.0513	37.1282	3.7216	19.95776	35.82973636	0
307.006	1422.48	1250.24	292.509	32.9571	38.5934	0.0073	37.1722	3.7582	19.95776	36.11379411	0
307.506	1423.98	1253.03	320.549	33.5264	38.652	0.0147	37.1575	3.7436	19.95776	36.39237213	0
308.013	1426.08	1255.41	349.835	34.0156	38.6227	0.0147	37.1282	3.7289	19.95776	36.66957672	0
308.513	1428.14	1258.34	378.626	34.446	38.6667	0	37.8168	3.2747	19.95776	36.93583122	0
309	1429.57	1260.68	407.564	34.9451	38.696	0.044	37.7436	3.2454	19.95776	37.19044891	0
309.506	1430.93	1262.86	442.161	35.393	38.652	0.022	37.7582	3.2601	19.95776	37.45123303	0
310.012	1431.99	1265.42	472.454	35.87	38.6667	0.0073	37.7436	3.2821	19.95776	37.71407731	0
310.506	1433.91	1268.13	505.458	36.3301	38.5495	0.0147	37.7582	3.2674	19.95776	37.98101385	0
311.006	1434.98	1270.74	541.3	36.7849	38.6227	0.044	38.3004	2.7106	19.95776	38.21510012	0
311.506	1436.62	1273.06	579.169	37.1436	38.5641	0.0147	38.3297	2.7326	19.95776	38.45808567	0
312.005	1437.75	1275.44	607.889	37.6183	38.5934	0.0513	38.3004	2.696	19.95776	38.69149456	0
312.505	1438.94	1277.77	642.689	37.9563	38.5788	0.022	38.3004	2.7106	19.95776	38.92968711	0
313.005	1440.1	1280.2	676.099	38.3745	38.6227	0.0147	38.3004	2.7033	19.95776	39.16582885	0
313.512	1442.05	1282.3	721.829	38.8767	38.6374	0	38.989	2.0806	19.95776	39.37664617	0
314.012	1443.73	1285.27	752.559	39.3246	38.652	0.044	38.989	2.0733	19.95776	39.58198844	0
314.505	1444.99	1287.63	785.289	39.7482	38.6227	0.0147	38.9744	2.0659	19.95776	39.79006356	0
315.005	1446.41	1289.66	822.359	40.2152	38.652	0.0366	38.989	2.0733	19.95776	39.99609722	0
315.511	1447.42	1291.97	857.909	40.5433	38.6667	0.0073	38.9011	2.0952	19.95776	40.20212154	0
316.005	1448.72	1294.5	905.859	41.0821	38.6667	0.022	39.6337	1.4799	19.95776	40.38350814	0
316.511	1450.1	1296.81	949.209	41.5133	38.6227	0.0147	39.5897	1.4725	19.95776	40.56488541	0
317.011	1451.4	1298.88	989.039	41.9437	38.6374	0.0073	39.5897	1.4505	19.95776	40.74421187	0
317.511	1453.24	1301.51	1032.599	42.4504	38.652	0.0147	39.5897	1.4652	19.95776	40.92353832	0
318.004	1454.96	1303.64	1083.179	43.0266	38.5934	0.022	39.6337	1.4799	19.95776	41.10834917	0
318.505	1455.4	1305.93	1121.959	43.7027	38.6081	0.0293	39.5897	1.4505	19.95776	41.28698891	0
319.011	1456.88	1307.94	1164.559	44.3796	38.5201	0.0293	40.2491	0.9377	19.95776	41.45263242	0
319.504	1457.77	1310.27	1183.989	45.0809	38.5641	0.0073	40.337	0.9524	19.95776	41.62375565	0



Time	FT	ST	dP	dH	CO in	CO2 in	CO out	CO2 out	k	Total Reduction	Drip mas
320.004	1459.61	1311.89	1201.019	45.7631	38.5348	0.0147	40.2784	0.9377	19.95776	41.7914453	0
320.504	1460.49	1313.84	1218.659	46.3202	38.5641	0.022	40.3077	0.967	19.95776	41.96119043	0
321.01	1462.02	1315.57	1229.519	47.0788	38.6227	0.0293	40.3077	0.9524	19.95776	42.1261519	0
321.505	1463.22	1317.16	1244.059	47.6526	38.6081	0.0366	41.0842	0.4982	19.95776	42.2849516	0
322.004	1463.97	1318.4	1252.759	48.3944	38.5641	0.0073	41.1136	0.5201	19.95776	42.45196387	0
322.51	1464.88	1319.55	1261.419	49.0301	38.5055	0	41.0842	0.5055	19.95776	42.61965819	0
323.01	1466.76	1321.07	1269.029	49.6482	38.4762	0.0073	41.0989	0.5128	19.95776	42.78940799	0
323.51	1467.29	1322.3	1279.059	50.3243	38.5641	0.0073	41.1575	0.5495	19.95776	42.96121794	0
324.01	1469.1	1323.23	1280.859	50.7456	38.5934	0.0147	43.5165	0.2711	19.95776	43.25432974	0
324.51	1469.72	1323.98	1281.939	51.3767	38.5641	0.0147	43.5018	0.2564	19.95776	43.46840718	0
325.01	1470.97	1324.67	1285.029	51.9231	38.5055	0.022	43.4286	0.2564	19.95776	43.72029202	0
325.503	1471.71	1325.49	1294.589	52.6381	38.5201	0	43.5604	0.293	19.95776	43.98312695	0
326.003	1473.29	1326.36	1295.219	53.1853	38.6227	0.022	43.5018	0.2711	19.95776	44.23432974	0
326.51	1475.04	1327.23	1293.019	53.8019	38.5934	0.022	45.8022	0.2344	19.95776	44.59093652	0
327.003	1475.04	1327.7	1292.539	54.3376	38.6813	0.044	45.7436	0.2051	19.95776	44.93590649	0
327.509	1476.69	1328.93	1288.419	54.9817	38.6081	0.0147	45.8168	0.2344	19.95776	45.29319064	0
328.009	1477.65	1329.52	1295.159	55.5868	38.6081	0	45.8462	0.2491	19.95776	45.6545951	0
328.503	1478.46	1330.17	1265.689	56.1638	38.5788	0.0293	45.7875	0.2198	19.95776	46.00915107	0
329.009	1479.26	1330.89	1251.389	56.8193	38.5934	0.0147	45.8168	0.2344	19.95776	46.36712194	0
329.509	1481.01	1331.16	1244.369	57.4023	38.5934	0.022	47.3114	0.2418	19.95776	46.79492301	0
330.002	1481.79	1331.27	1246.589	57.9296	38.6081	0.0073	47.3553	0.2637	19.95776	47.22750774	0
330.502	1482.92	1331.74	1250.729	58.534	38.5788	0.0073	47.3114	0.2418	19.95776	47.65736428	0
331.002	1483.78	1332.25	1246.659	59.0346	38.5788	0.0366	47.2527	0.2051	19.95776	48.0783122	0
331.502	1484.28	1332.64	1244.919	59.5963	38.5495	0.0366	47.2527	0.2051	19.95776	48.50062888	0
332.002	1485.26	1333.32	1243.289	60.1893	38.5641	0.0147	48.3663	0.2491	19.95776	48.98044289	0
332.508	1486.86	1333.71	1227.759	60.7196	38.5788	0.0147	48.3516	0.2564	19.95776	49.45956552	0
333.008	1486.91	1334.48	1222.649	61.4026	38.5934	0.0293	48.3077	0.2491	19.95776	49.93390915	0
333.502	1487.32	1334.57	1220.659	61.8468	38.5495	0.0073	48.3663	0.2418	19.95776	50.41441455	0
334.008	1488.91	1334.95	1202.139	62.3184	38.5348	0.0147	48.3516	0.2491	19.95776	50.89491061	0
334.508	1490.13	1335.93	1173.019	62.7137	38.5641	0.0147	49.0842	0.2857	19.95776	51.41168118	0
335.008	1491.14	1337.18	1148.269	63.3326	38.5201	0.022	49.0989	0.3004	19.95776	51.93188534	0
335.508	1492.36	1337.95	1128.529	64.0079	38.5201	0.044	49.0403	0.2637	19.95776	52.44386758	0
336.008	1493.02	1338.72	1111.749	64.5856	38.5495	0.0293	49.0842	0.2784	19.95776	52.95927407	0
336.501	1494.18	1339.08	1117.629	65.2183	38.5495	0.0293	49.0842	0.2784	19.95776	53.47468055	0
337.001	1494.52	1339.69	1122.649	65.8326	38.5348	0.0147	49.0989	0.2857	19.95776	53.9935066	0
337.501	1495.52	1340.8	1107.519	66.4675	38.5495	0.022	49.4799	0.3297	19.95776	54.53287342	0
338.002	1496.8	1341.82	1074.339	67.1612	38.5348	0.0293	49.4505	0.3297	19.95776	55.07087148	0
338.508	1497.48	1342.54	1071.409	67.6351	38.5201	0.0147	49.4799	0.3297	19.95776	55.61229378	0
339.001	1498.19	1342.35	1051.749	68.3631	38.5495	0	49.4945	0.359	19.95776	56.15713565	0
339.501	1498.41	1340.62	1071.529	68.9461	38.6081	0.022	49.4799	0.3297	19.95776	56.69376494	0
340.007	1500.55	1339.78	1076.529	69.6917	38.5788	0.0147	49.2161	0.4322	19.95776	57.22969818	0
340.507	1499.67	1337.17	1061.699	70.2946	38.5641	0.044	49.1722	0.4322	19.95776	57.7615298	0
341.007	1501.21	1336.55	1056.299	70.9096	38.5934	0.022	49.1722	0.4762	19.95776	58.2981591	0
341.5	1502.42	1335.58	1053.329	71.5858	38.5788	0.0147	49.2161	0.4542	19.95776	58.83614781	0
342.007	1502.84	1335.74	1050.529	72.1963	38.4762	0.022	49.2161	0.4469	19.95776	59.37756544	0
342.507	1504.56	1337.41	1044.999	72.7923	38.4908	0.0147	48.381	0.4908	19.95776	59.88407264	0
343.007	1505.2	1338.29	1037.739	73.3562	38.4615	0.0073	48.3956	0.4908	19.95776	60.39332203	0
343.5	1506.34	1339.83	1024.779	73.9072	38.5055	0.0293	48.3663	0.4762	19.95776	60.89572762	0
344	1507.42	1340.73	1007.029	74.4986	38.5055	0.0147	48.381	0.4908	19.95776	61.4015481	0
344.5	1508.36	1342.06	1004.899	75.0679	38.5201	0.0147	48.381	0.4982	19.95776	61.90737792	0
345	1508.74	1343.38	967.929	75.5868	38.5055	0.0147	49.4066	0.5495	19.95776	62.46659412	0
345.5	1509.26	1344.79	956.059	76.15	38.5348	0.0147	49.4066	0.5495	19.95776	63.02444156	0
346.006	1511.33	1345.81	951.769	76.8338	38.5201	0.022	49.4212	0.5568	19.95776	63.58365776	0
346.506	1511.48	1345.94	922.539	77.4534	38.5201	0.0293	49.4212	0.5421	19.95776	64.14081848	0
347.006	1513.08	1346.59	907.649	78.0762	38.5348	0.0147	49.4212	0.5495	19.95776	64.69934796	0
347.5	1513.16	1347.7	906.409	78.6661	38.5495	0.0293	49.4212	0.5421	19.95776	65.25513525	0
348.006	1513.31	1348.96	895.799	79.2933	38.5934	0	49.6703	0.6227	19.95776	65.83077659	0
348.512	1514.58	1350.24	888.809	79.868	38.5641	0.0147	49.5971	0.5861	19.95776	66.39957412	0
349.006	1515.13	1351.63	896.369	80.5151	38.4908	0.022	49.5971	0.5568	19.95776	66.96837632	0
349.506	1515.89	1351.12	889.029	80.9951	38.5348	0.0293	49.5971	0.5861	19.95776	67.53717852	0
350.012	1517.44	1351.97	886.849	81.5064	38.5055	0.022	49.5971	0.5861	19.95776	68.10803153	0
350.512	1517.64	1352.26	853.699	82.0406	38.5348	0.0147	49.0989	0.5421	19.95776	68.65081324	0
351.005	1518.21	1354.08	837.469	82.5214	38.4908	0.0147	49.0403	0.5421	19.95776	69.19291292	0
351.505	1518.89	1354.71	829.229	83.0136	38.4469	0.0293	49.011	0.5201	19.95776	69.73227506	0
352.012	1519.75	1355.7	795.509	83.5432	38.4908	0.0147	49.0403	0.5495	19.95776	70.27506612	0
352.512	1520.65	1356.75	765.729	84.2048	38.5641	0.0147	49.0696	0.5568	19.95776	70.81648375	0
353.005	1521.7	1358.02	738.619	84.7207	38.5641	0.0586	48.4542	0.4615	19.95776	71.31614714	0
353.512	1521.93	1357.54	707.009	85.3083	38.5641	0.0147	48.5128	0.4908	19.95776	71.82538719	0
354.011	1522.51	1358.29	701.989	85.8196	38.6374	0.022	48.5275	0.4835	19.95776	72.33052563	0
354.505	1523.7	1358.89	695.639	86.2447	38.5495	0.044	48.4249	0.4689	19.95776	72.83155778	0
355.011	1524.17	1359.61	713.049	86.9154	38.4908	0.0513	48.4689	0.4542	19.95776	73.33533212	0



Time	FT	ST	dP	dH	CO in	CO2 in	CO out	CO2 out	k	Total Reduction	Drip mas
355.504	1525.13	1358.49	724.669	87.3817	38.5201	0.022	47.7363	0.4469	19.95776	73.80556947	0
356.011	1525.57	1363.18	726.219	87.6465	38.5055	0.0073	47.7363	0.4469	19.95776	74.2778623	0
356.504	1526.1	1363.72	713.639	88.0624	38.4908	0.0147	47.7656	0.4615	19.95776	74.75288331	0
357.004	1526.81	1364.72	695.229	88.4921	38.5495	0.022	47.7363	0.4469	19.95776	75.22174723	0
357.511	1528.31	1364.11	673.929	88.8668	38.5641	0.0073	47.7509	0.4542	19.95776	75.69266663	0
358.011	1528.08	1363.35	642.339	89.246	38.5348	0.0293	47.7363	0.4469	19.95776	76.16153522	0
358.505	1529.52	1360.08	599.139	89.4124	38.5348	0.0147	47.2381	0.4249	19.95776	76.6064388	0
359.011	1529.55	1361.04	543.187	89.6741	38.5201	0.022	47.2381	0.4249	19.95776	77.05134705	0
359.51	1530.14	1358.18	501.685	89.755	38.5348	0.0366	47.2527	0.4322	19.95776	77.49556859	0
360.004	1531.04	1358.06	498.626	91.256	38.4908	0.0147	47.2527	0.4322	19.95776	77.94389174	0
360.511	1531.6	1358.93	530.494	91.399	38.4762	0	47.3114	0.4469	19.95776	78.398386	0
361.004	1532.31	1360.83	571.959	91.611	38.5641	0.022	46.9451	0.4396	19.95776	78.82892459	0
361.504	1533.49	1363.5	572.519	91.746	38.4615	0	46.9304	0.4103	19.95776	79.26288742	0
362.01	1534.55	1366.66	568.289	91.897	38.4908	0.0147	46.9451	0.4322	19.95776	79.69684091	0
362.504	1534.25	1369.92	556.899	92.113	38.5055	0.022	46.9158	0.4176	19.95776	80.12669279	0
363.003	1535.25	1373.14	554.059	92.251	38.5348	0.0147	46.9158	0.4322	19.95776	80.55722204	0
363.51	1536.05	1375.96	541.74	92.413	38.6227	0.022	45.4359	0.3297	19.95776	80.90425216	0
364.004	1536	1378.96	505.494	92.712	38.5201	0.044	45.4066	0.337	19.95776	81.25333308	0
364.51	1536.83	1382.02	487.82	93.128	38.5201	0	45.4652	0.3663	19.95776	81.61200001	0
365.003	1538.15	1384.73	465.311	93.325	38.5641	0.022	45.4652	0.359	19.95776	81.96587394	0
365.503	1538.58	1387.29	445.238	93.611	38.5201	0.0147	45.4799	0.3663	19.95776	82.32385415	0
366.009	1538.58	1390.49	433.974	93.865	38.5201	0.022	43.1062	0.2711	19.95776	82.56136933	0
366.503	1540.24	1393.17	410.476	94.23	38.5055	0.022	43.1355	0.2564	19.95776	82.79956188	0
367.009	1539.47	1395.74	387.784	94.461	38.4908	0.0073	43.0769	0.2564	19.95776	83.03707706	0
367.503	1541.12	1399.12	340.714	94.69	38.5055	0.0293	43.1062	0.2711	19.95776	83.27459223	0
368.009	1542.01	1401.62	326.611	94.99	38.5641	0.022	43.1062	0.2711	19.95776	83.51005193	0
368.502	1542.51	1403.03	335.622	95.459	38.5495	0.0293	43.1062	0.2711	19.95776	83.74551163	0
369.002	1543.89	1402.06	310.238	95.993	38.5495	0.022	41.7143	0.2491	19.95776	83.91457471	0
369.649	1544.08	1392.37	164.194	96.973	38.5201	0	41.685	0.2344	19.95776	84.08432451	105.1
370.009	1544.31	1389.75	149.102	97.345	38.5201	0	41.685	0.2271	19.95776	84.25339226	127.3
370.502	1545.01	1389.34	145.824	97.837	38.5201	0	41.6703	0.2271	19.95776	84.42177733	127.2
371.028	1546.12	1392.94	146.978	98.212	0.0293	0.0073	41.7436	0.2637	19.95776	86.39442973	168.8
371.502	1546.9	1396.7	151.593	98.689	0.0586	0.0073	14.8864	0.1245	19.95776	87.09806663	168.8
372.008	1546.37	1400.88	150.128	99.274	0.0733	0.022	14.9011	0.1172	19.95776	87.79964805	168.8
372.501	1548.18	1404.35	153.278	100.067	0.044	0.0147	14.8718	0.1172	19.95776	88.50191151	168.7
373.008	1548.3	1408.19	155.055	100.673	0.0147	0	14.8864	0.1099	19.95776	89.20691718	168.7
373.508	1548.88	1411.62	157.161	101.107	0.0586	0.022	14.9011	0.1172	19.95776	89.90918531	168.7
374.008	1549.42	1414.52	156.3	101.589	0	0	4.8205	0.044	19.95776	90.13848792	201
374.501	1549.3	1417.02	157.344	102.034	0	0	4.8205	0.044	19.95776	90.36779053	201
375.002	1550.75	1419.46	161.263	102.611	0.0293	0	4.8498	0.0659	19.95776	90.59913927	201
375.501	1551.11	1421.95	162.967	102.651	0.0147	0	4.8059	0.0586	19.95776	90.8284372	201
376.008	1552.23	1423.81	163.736	102.562	0	0	4.8059	0.044	19.95776	91.05705776	201
376.501	1552.18	1426.23	167.289	102.56	0.0733	0.0073	4.8791	0.0733	19.95776	91.28772913	201
377.001	1552.81	1427.97	166.044	102.677	0.1172	0.0293	1.7143	0.0073	19.95776	91.36028284	221.2
377.507	1553.68	1430.49	167.93	102.655	0.0147	0	1.7289	0.0293	19.95776	91.44309993	221.2
378.007	1554.1	1432.61	169.688	102.648	0.0293	0	1.7436	0.0293	19.95776	91.52592168	221.1
378.501	1553.76	1434.75	172.948	102.615	0	0	1.7143	0.0147	19.95776	91.60737935	226.1
379.007	1554.16	1437.62	174.34	102.678	0.0147	0	1.7729	0.0366	19.95776	91.69293396	264.6
379.5	1555.5	1439.6	177.069	102.615	0	0	1.4652	0.0293	19.95776	91.7641189	264.6
380	1556.12	1440.76	180.165	102.59	0	0	1.4212	0.022	19.95776	91.83256633	264.6
380.507	1556.5	1442.42	181.886	102.646	0	0	1.4359	0.0147	19.95776	91.90101842	264.6
381.007	1557.4	1444.14	181.318	102.692	0.0733	0	1.4212	0.0147	19.95776	91.96535956	264.5
381.5	1558.17	1445.72	182.674	102.703	0	0	1.4652	0.0366	19.95776	92.03722655	264.5
382.001	1558.42	1447.16	182.93	102.746	0	0	1.4799	0.0366	19.95776	92.10978026	264.5
382.507	1559.17	1448.57	183.974	102.712	0	0.0293	1.2747	0.022	19.95776	92.16864635	266.1
383	1560.09	1449.65	187.253	102.65	0.0147	0	1.3919	0.0513	19.95776	92.23777582	266.1
383.506	1560.68	1451.18	183.388	102.78	0	0	1.348	0.0293	19.95776	92.30348572	317.4
384.013	1561.01	1452.13	183.187	102.704	0	0.0073	1.3187	0.022	19.95776	92.36646277	317.4
384.506	1561.2	1453.43	184.505	102.668	0	0	1.2894	0	19.95776	92.42669763	317.3
385.006	1562.66	1455.16	186.52	102.676	0.0293	0	1.1136	0.0366	19.95776	92.48077072	317.3
385.506	1562.57	1456.2	187.509	102.629	0	0	1.0989	0.0293	19.95776	92.53484381	317.3
386.006	1563.44	1457.82	187.82	102.745	0	0.0073	1.0842	0.0147	19.95776	92.58618405	317.2
386.512	1563.87	1459.23	188.516	102.758	0	0	1.0842	0.022	19.95776	92.63888838	317.1
387.006	1564.74	1460.38	190.568	102.718	0	0.0147	1.0696	0.0147	19.95776	92.68885518	317.1
387.506	1564.65	1461.86	190.952	102.741	0	0	1.2015	0.044	19.95776	92.74909471	317
388.006	1565.34	1462.79	192.637	102.774	0	0	1.1136	0.022	19.95776	92.80317247	317
388.512	1565.42	1464.07	191.959	102.902	0	0.0073	1.1429	0.022	19.95776	92.85793695	317.5
389.005	1566.37	1465.03	194.872	102.725	0	0	1.1282	0.022	19.95776	92.91269676	317.8
389.505	1567.52	1466.11	194.707	102.758	0.0733	0	1.1429	0.044	19.95776	92.96677452	317.8
390.005	1568.12	1467.27	195.861	102.761	0	0	1.1282	0.022	19.95776	93.02153433	340.4
390.512	1568.47	1467.98	197.307	102.776	0	0	0.9524	0.0293	19.95776	93.06876361	340.7



Time	FT	ST	dP	dH	CO in	CO2 in	CO out	CO2 out	k	Total Reduction	Drip mas
391.012	1569.3	1469.11	198.681	102.716	0.0147	0	0.9231	0.022	19.95776	93.11325537	342.1
391.506	1570.21	1469.86	199.139	102.68	0.044	0.022	0.8645	0	19.95776	93.14952989	342
392.012	1569.64	1470.77	201.245	102.671	0	0	0.9231	0.0293	19.95776	93.19539041	341.9
392.505	1570.69	1471.81	202.802	102.717	0.0293	0	0.9231	0.0073	19.95776	93.23782669	352.2
393.005	1571.91	1473	205.311	102.798	0	0.0147	0.8645	0.0293	19.95776	93.27957626	352.1
393.511	1571.3	1473.92	206.611	102.696	0.0147	0	0.8645	0.0073	19.95776	93.31995706	352
394.005	1572.42	1474.89	208.571	102.755	0.044	0	0.9084	0.0293	19.95776	93.36307539	352.6
394.504	1573.42	1475.54	209.121	102.66	0.044	0	0.8498	0.0073	19.95776	93.40140071	352.5
395.004	1573.85	1476.59	211.117	102.751	0	0	0.8498	0.0147	19.95776	93.4424729	352.5
395.505	1573.71	1477.43	212.271	102.78	0	0	0.8645	0.0147	19.95776	93.48423181	357.4
396.011	1574.64	1478.32	213.663	102.682	0.0733	0.0073	0.7766	0.0147	19.95776	93.51777815	358.3
396.538	1575.8	1478.98	214.926	102.773	0	0	0.8205	0.022	19.95776	93.55816362	365.3
397.004	1575.93	1479.53	216.52	102.707	0.0293	0.0073	0.7912	0.0147	19.95776	93.59444749	365.3
397.511	1576.96	1480.14	217.344	102.719	0	0	0.7912	0.022	19.95776	93.6334642	365.2
398.004	1577	1481	219.011	102.759	0.0147	0	0.7912	0.0147	19.95776	93.67111215	365.1
398.504	1577.32	1481.7	221.227	102.786	0	0	0.7033	0.0147	19.95776	93.70534053	365.1
399.004	1578.93	1482.85	223.681	102.785	0.0586	0.0073	0.7619	0.0073	19.95776	93.73819548	365.4
399.51	1579.62	1483.26	225.403	102.681	0.0293	0	0.7033	0.0073	19.95776	93.77036372	365.3
400.003	1580.09	1483.94	228.187	102.755	0.044	0	0.7766	0.0073	19.95776	93.80526947	368.9
400.503	1580.25	1484.58	230.128	102.788	0	0	0.7033	0.0147	19.95776	93.83949786	369.2
401.003	1580.42	1484.87	230.531	102.691	0	0	0.8059	0.022	19.95776	93.87920129	369.1
401.503	1580.95	1485.92	234.267	102.826	0	0	0.674	0.0073	19.95776	93.91136952	369.1
402.003	1581.66	1487	235.366	102.806	0	0	0.7326	0	19.95776	93.94559323	369
402.504	1581.65	1487.57	237.344	102.774	0.0147	0	0.7033	0.044	19.95776	93.98187242	368.9
403.004	1582.53	1488.28	240.842	102.762	0	0	0.7473	0.0513	19.95776	94.02157585	369.2
403.503	1583.29	1489.22	242.839	102.79	0	0	0.6886	0.022	19.95776	94.05579956	369.1
404.003	1584.51	1489.97	243.956	102.778	0	0	0.7619	0.022	19.95776	94.09344752	369.2
404.509	1583.85	1490.42	245.696	102.731	0	0	0.7326	0.0073	19.95776	94.12835327	370.2
405.009	1585.2	1491.23	250.622	102.812	0	0	0.7473	0.0073	19.95776	94.16394575	370.9
405.502	1585.7	1491.91	250.311	102.757	0	0	0.7473	0.022	19.95776	94.20091165	371.5
406.009	1585.62	1492.45	253.754	102.807	0.044	0	0.7179	0.0073	19.95776	94.23307522	372.1
406.509	1586.92	1493.39	255.348	102.725	0.0147	0	0.7766	0.022	19.95776	94.27072317	372.8
407.009	1586.87	1493.97	258.315	102.817	0.0293	0	0.6886	0.0073	19.95776	94.30220468	373.5
407.509	1587.63	1494.67	259.89	102.771	0.1026	0.0147	0.674	0.0073	19.95776	94.32820648	374.2
408.002	1588.16	1495.38	263.095	102.879	0.0879	0	0.7179	0.0147	19.95776	94.35901063	374.5
408.509	1589.07	1495.68	264.304	102.712	0.0293	0	0.7033	0.022	19.95776	94.39255229	375.1
409.009	1589.06	1496.54	266.831	102.75	0	0	0.7033	0.0147	19.95776	94.42678068	375.5
409.502	1589.11	1497.08	269.945	102.84	0.0293	0	0.7619	0.0586	19.95776	94.46647944	375.8
410.008	1589.09	1497.72	271.959	102.815	0	0	0.6886	0.0073	19.95776	94.49932971	376.2
410.502	1590.11	1498.32	274.67	102.764	0.0147	0	0.7033	0.0147	19.95776	94.53287138	376.4
411.002	1590.54	1498.91	277.546	102.78	0	0	0.6593	0.0073	19.95776	94.5643529	376.7
411.501	1590.67	1499.4	280.238	102.71	0	0	0.7033	0.0147	19.95776	94.59858128	376.8
412.001	1591.46	1500.1	282.454	102.716	0	0	0.7033	0.0073	19.95776	94.63211828	377.1
412.501	1591.74	1500.73	284.047	102.753	0	0	0.7179	0.0073	19.95776	94.66633732	377.3
413.008	1592.04	1501.22	286.52	102.749	0	0.0073	0.7179	0.0293	19.95776	94.70192979	377.6
413.508	1593.34	1501.8	288.809	102.796	0	0	0.7619	0.0147	19.95776	94.7388957	377.9
414.008	1593.21	1502.54	289.56	102.761	0	0	0.7179	0.0147	19.95776	94.77380613	378.2
414.508	1593.85	1502.81	293.883	102.823	0	0	0.7179	0.0147	19.95776	94.80871655	378.5
415.001	1594.06	1503.47	296.154	102.815	0.0733	0.0073	0.6593	0.0147	19.95776	94.83678317	378.8
415.501	1594.05	1503.93	297.399	102.764	0	0.0366	0.5568	0	19.95776	94.85937475	379.1
416.001	1594.83	1504.62	300.183	102.885	0.0293	0.0073	0.674	0.022	19.95776	94.89086561	379.3
416.501	1595.08	1504.98	303.461	102.78	0	0	0.63	0.0147	19.95776	94.92166975	379.6
417.007	1595.66	1505.6	307.069	102.794	0	0.022	0.6007	0	19.95776	94.94767622	379.8
417.5	1596.65	1506.1	309.469	102.773	0	0	0.63	0.0147	19.95776	94.97848037	380
418	1596.43	1506.63	312.93	102.801	0.0293	0	0.6593	0.0147	19.95776	95.00928451	380
418.5	1596.75	1506.94	316.758	102.751	0	0	0.63	0	19.95776	95.03871522	380.3
419.007	1597.08	1507.73	317.784	102.789	0	0.022	0.5714	0	19.95776	95.06335293	380.6
419.5	1597.58	1508.19	321.154	102.864	0.044	0.022	0.5861	0	19.95776	95.08662188	380.8
420.007	1598.84	1508.62	325.97	102.775	0.0293	0.0147	0.6007	0	19.95776	95.11194163	381.1
420.5	1598.41	1509.02	328.351	102.774	0	0	0.6447	0.022	19.95776	95.14411454	381
421	1598.72	1509.48	330.531	102.83	0	0	0.6154	0.0073	19.95776	95.17354525	381.3
421.506	1598.89	1510.13	334.432	102.844	0	0	0.6447	0.022	19.95776	95.20571815	381.6
422	1599.61	1510.11	337.033	102.804	0	0.0073	0.6154	0	19.95776	95.23378477	381.8
422.506	1600.42	1510.53	339.194	102.894	0.0586	0	0.7033	0.0293	19.95776	95.26663972	381.8
423.007	1600.35	1510.22	341.025	102.866	0	0	0.5568	0	19.95776	95.29265086	382
423.5	1601.49	1510.79	344.652	102.862	0.0293	0	0.6447	0.044	19.95776	95.32551049	382.3
424.006	1601.33	1511.46	348.681	102.955	0	0	0.6007	0.0147	19.95776	95.35494587	382.3
424.506	1601.47	1511.39	351.19	102.838	0	0	0.5861	0.022	19.95776	95.38438125	382.5
425.006	1602.67	1511.75	355.604	102.962	0	0	0.5568	0.022	19.95776	95.41244787	382.5
425.506	1603.14	1512.71	355.97	102.942	0	0	0.6007	0.0147	19.95776	95.44188325	382.4
426.005	1602.85	1512.85	358.425	102.998	0	0	0.6154	0.022	19.95776	95.4726874	382.7



Time	FT	ST	dP	dH	CO in	CO2 in	CO out	CO2 out	k	Total Reduction	Drip mas
426.506	1603.45	1513.32	359.066	103.116	0	0	0.5568	0	19.95776	95.49869854	382.7
427.012	1603.21	1513.93	366.227	103.126	0.0147	0.0147	0.5568	0	19.95776	95.52264953	382.7
427.512	1604.14	1514.37	369.395	103.105	0.0147	0.0147	0.5275	0	19.95776	95.54523176	382.9
428.005	1604.78	1515.38	370.384	103.134	0.0293	0.0073	0.5714	0.0147	19.95776	95.57124757	382.9
428.512	1604.95	1515.7	373.608	103.099	0	0	0.5568	0.0073	19.95776	95.59794076	382.9
429.012	1605.2	1516.21	379.67	103.089	0.044	0	0.5568	0.0366	19.95776	95.62531599	383.1
429.512	1606.59	1516.52	381.447	103.053	0.0733	0	0.5568	0.0147	19.95776	95.64927633	383.1
430.006	1605.95	1516.9	381.557	103.237	0.0586	0	0.6447	0.0513	19.95776	95.68144923	383.1
430.512	1606.32	1516.49	383.535	103.125	0	0	0.5421	0.022	19.95776	95.70882914	383.1
431.005	1607.75	1517.43	387.637	103.153	0	0	0.5568	0.0147	19.95776	95.73621371	383.3
431.504	1607.01	1518.21	393.15	103.274	0.0147	0	0.5714	0.0147	19.95776	95.76359362	383.4
432.011	1607.46	1518.6	397.399	103.307	0	0	0.5861	0.022	19.95776	95.793029	383.4

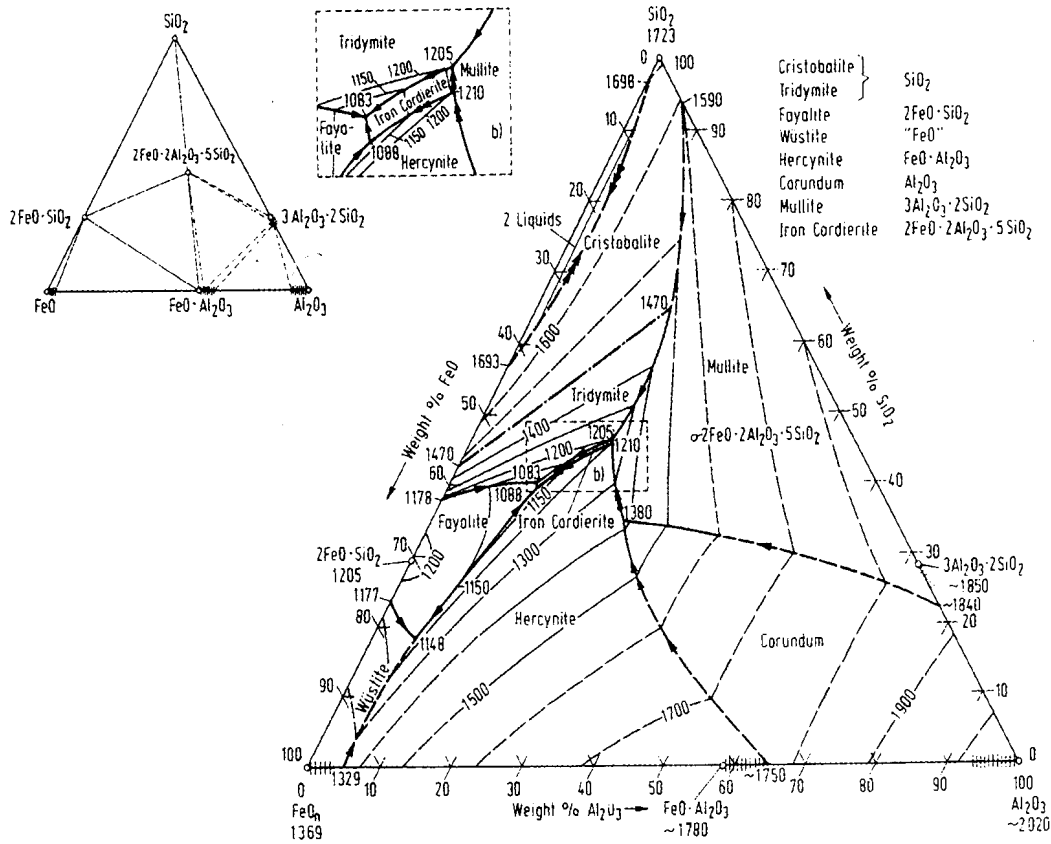


APPENDIX 3

FeO-SiO₂-Al₂O₃ – phase diagram



$Al_2O_3-FeO_x-SiO_2$





APPENDIX 4

MOLE PERCENTAGES OF THE DIFFERENT PHASES

The calculation proceeds on the basis that all the Na_2O and K_2O report to the alkali-rich liquid, that Al_2O_3 is present only in this liquid and as hercynite, that SiO_2 is present only in the alkali-rich liquid and the fayalite-based liquid, and that Fe can be present as metallic iron, wustite, or fayalite-based liquid. The calculation for test#2 is presented here as example.

Total composition
 (Mass percentage of total sample, including 740g of ore and 13g of coke ash):

Fe_2O_3	94.14
FeO	0.26
Fe	0.02
SiO_2	3.49
Al_2O_3	1.67
CaO	0.12
MgO	0.06
Na_2O	0.04
K_2O	0.13
P	0.04
S	0.04

Molar balance for 753g total mass:

In a 753g, there is 1.27g of alkalis (Na_2O and K_2O), which is 0.015 moles of ($\text{Na}_2\text{O}+\text{K}_2\text{O}$). According to the EDX analysis, 4.53% (molar basis) of the alkali-rich liquid phase is ($\text{Na}_2\text{O}+\text{K}_2\text{O}$); the analysed percentages of other species in this liquid, and the corresponding calculated molar amounts, are summarised in the table below.

Alkali-rich liquid composition:

	Mole %	Mole	Mass (g)
Al_2O_3	10.60	0.0355	3.62
FeO	48.37	0.162	11.64
SiO_2	36.50	0.122	7.32
$\text{Na}_2\text{O}+\text{K}_2\text{O}$	4.53	0.015	1.27

Given the amount of Al_2O_3 in the alkali-rich liquid, amount of hercynite can be calculated, since this takes up the balance of the Al_2O_3 :

$$\begin{aligned}
 \text{Total mass of } \text{Al}_2\text{O}_3 &= 12.6\text{g} \\
 \text{Mass of } \text{Al}_2\text{O}_3 \text{ in alkali-rich liquid phase} &= 3.62\text{g} \\
 \Rightarrow \text{Amount of } \text{Al}_2\text{O}_3 \text{ in hercynite} &= 9.0\text{g} = 0.088 \text{ moles}
 \end{aligned}$$

According to the stoichiometric hercynite composition ($\text{FeO}:\text{Al}_2\text{O}_3$), there is 0.088 mole of FeO in the hercynite phase.

Given the amount of SiO_2 in the alkali-rich liquid, the amount of fayalite-based liquid can be calculated, since this takes up the balance of the SiO_2 :



$$\begin{aligned}
 \text{Total mass of SiO}_2 &= 26.29\text{g} \\
 \text{Mass of SiO}_2 \text{ in alkali-rich liquid phase} &= 7.32\text{g} \\
 \Rightarrow \text{Amount of SiO}_2 \text{ in fayalite-based liquid} &= 18.97\text{g} = 0.316 \text{ moles}
 \end{aligned}$$

According to the stoichiometric fayalite composition ($2\text{FeO}:\text{SiO}_2$), there is 0.632 mole of FeO in the fayalite-based liquid.

Finally, the distribution of Fe can be calculated, given the amount of FeO in the alkali-rich liquid, hercynite, and the fayalite-based liquid, and knowing the degree of reduction. It is assumed that all the Fe which is not present in the alkali-rich liquid, hercynite, and the fayalite-based liquid, is present as Fe° and pure FeO.

The amount of metallic iron is calculated from the degree of reduction. Based on the gas composition, the percentage reduction at the end of test#2 is 35.4%. The amount of oxygen associated with iron in the original sample (based on the analysis given above) is 13.34 moles. Given 35.4% reduction, 8.62 moles of O hence remains in the sample as Fe_2O_3 and FeO (the latter may be present as pure FeO, in the alkali-rich liquid, the fayalite-based liquid, or hercynite). Based on the analysis of the original sample, the total amount of Fe present is 498 g = 8.92 mole.

With the amount of Fe present as FeO (in the phases as mentioned) being 8.62 moles, $8.92 - 8.62 = 0.30$ moles of Fe° is present, or 16.8 g.

The amount of pure FeO in the sample is then the balance of the iron, i.e. $8.53 - (0.162 + 0.088 + 0.632) = 7.648$ mole.

As this calculation shows, the composition of the alkali-rich liquid is one of the most important factors which affect the phase distribution. The measured compositions are summarised in the table below (mole percentages).

	% Al_2O_3	%FeO	% SiO_2	% $\text{Na}_2\text{O} + \% \text{K}_2\text{O}$
Test 1	17.1	25.1	53.4	4.4
Test 2	10.6	48.4	36.5	4.5
Test 3	10.7	34.5	48.5	6.3